Functional analysis of Prdm14 during *Xenopus* embryogenesis

Doctoral Thesis

Dissertation for the award of the degree
"Doctor rerum naturalium (Dr. rer. nat.)"
in the GGNB program "Genes and Development“
at the Georg August University Göttingen
Faculty of Biology

Submitted by
Rolf Patrick Berndt
born in Tokio, Japan

Göttingen, April 2015

Members of the Thesis Committee:

Dr. Kristine A. Henningfeld (Supervisor, Reviewer)
Institute of Developmental Biochemistry,
University of Göttingen

Prof. Dr. Gregor Bucher (Reviewer)
Department of Evolutionary Developmental Genetics,
University of Göttingen

Prof. Dr. Andreas Wodarz
Department of Microscopic Anatomy and Molecular Cell Biology,
University of Cologne

Affidavit

Herewith, I declare that I prepared the PhD thesis

"Functional analysis of Prdm14 during *Xenopus* embryogenesis"

on my own and with no other sources and aids than quoted.

Submission date
Göttingen, 30.04.2015

Rolf Patrick Berndt

Table of Contents

Acknowledgements

First of all, I would like to thank Dr. Kristine Henningfeld. I am very grateful for her supervision, help and patience over the last couple of years. She always supported me and gave advice and encouragement, not only in scientific matters.

I would also like to thank Prof. Dr. Pieler for his help, support and fruitful discussions during the years. Additionally, I thank him for being a member of my examination board on such short notice.

Furthermore, I thank Prof. Dr. Bucher and Prof. Dr. Wodarz for being part of my thesis committee and for their advices and suggestions. I also thank Prof. Dr. Wimmer and Prof. Dr. Mansouri for agreeing to be part of my examination board.

I thank all the members of the Department of Developmental Biochemistry for the great working atmosphere. Additionally, I thank the members of the TAL for their help with the RNA-sequencing. I would like to thank especially Katja Ditter for her technical assistance, Dr. Juliane Melchert, Dr. Marie Hedderich, Dr. Juliane Wellner, Ilona Wunderlich, Anita Smarandache, Maja Gere, Dr. Diana Bauermeister and Sven Richts. Their support and encouragement helped me a lot during the last weeks of finishing this thesis.

I would like to thank my family, and in particular my parents, for their unconditional love and support in everything I did throughout my life.

My special thanks go to my wife, Maren. Without her help, support and comfort during all these years, I would not have made it. She lifted me up, when I was down and was always there, when I needed her. I thank her for her love, her patience and for our son.

Abstract

Prdm14 is a member of the conserved family of Prdm proteins, which are emerging as crucial regulators of multiple early developmental processes and diseases. Members of the Prdm family are characterized by the presence of a single PR domain and a variable number of DNA-binding zinc fingers. Most members of the Prdm proteins directly influence transcription through intrinsic histone methyltransferase activity or recruitment of cofactors. In this thesis, a functional analysis of Prdm14 was undertaken to elucidate its role during early vertebrate development using the *X. laevis* model system.

Prdm14 is expressed during gastrulation in the prospective neuroectoderm. At late neural plate stages, the expression is restricted to the territories of primary neurogenesis. In tailbud stage embryos, expression of *prdm14* is detected in postmitotic neurons of the central nervous system and a subset of the cranial ganglia. *Prdm14* is regulated positively by the proneural bHLH gene *neurog2* and negatively by the Notch signaling pathway, which is strongly suggestive for a role during primary neurogenesis. Overexpression of *prdm14* in *X. laevis* embryos promotes the proliferation of neural progenitor cells, which results in the expansion of the neural plate and in a transient inhibition of neuronal differentiation. In tailbud stage embryos, *prdm14* overexpression induces the formation of ectopic neurons in the non-neural ectoderm that express markers indicative of a sensory glutamatergic neuronal cell fate. In pluripotent animal cap cells, *prdm14* overexpression is sufficient to induce a glutamatergic neuronal cell fate supporting the studies in embryos. The downstream transcriptional network induced by *prdm14* was studied through RNA-sequencing analysis of *prdm14*-injected animal caps at the equivalent of neural plate and tailbud stage. Predominant among the *prdm14*-upregulated genes were ligands and signaling components of the Wnt pathway and Wnt-regulated genes. Consistent with the RNA-sequencing analysis, *prdm14* overexpression in the embryo activated a canonical Wnt-signaling reporter. In addition, many of the upregulated genes have previously been shown to be involved in neural crest and sensory neuron specification, including the key neural plate border specifiers *pax3* and *zic1*. The activation of these genes may in part be attributed to the ability of *prdm14* to activate canonical

Wnt-signaling. Taken together, the results of this thesis provide evidence for multiple roles of Prdm14 during the development of the nervous system. During gastrulation Prdm14 promotes maintenance of the neural ectoderm and the specification of the neural plate border, which will give rise to neural crest and Rohon-Beard sensory neurons. Also suggested by the expression and regulation of *prdm14,* is a role during neuronal differentiation and maturation.

List of Figures

List of Tables

Abbreviations

A	Alanin
AP	alkaline phosphatase
aa	amino acid
BCIP	5-bromo-4-chloro-3-indolyl-phosphate
bHLH	basic-helix-loop-helix
BMB	Bohringer Mannheim blocking reagent
BMP	bone morphogenetic protein
bp	base pairs
BSA	bovine serum albumin
°C	degree Celsius
CC	control caps
cDNA	complementary DNA
CE	control embryos
CIAP	calf intestine alkaline phosphatase
CoMO	standard control morpholino oligo
Dex	dexamethasone
Dig	digoxigenin
DNA	desoxyribonucleic acid
DNAse	desoxyribonuclease
DTT	1,4-dithiothreitol
EDTA	ethylendiaminetetraacetic acid
EGTA	ethylenglycole-bis(2-aminoethylether)-N,N'- tetraacetate
et al.	*et alii*
EtOH	ethanol
FGF	fibroblast growth factor
Flu	fluorescein
GABA	gamma-aminobutyric acid
GR	glucocorticoid receptor
h	hour/hours
H4	histone 4
HA	hemagglutination
HCG	human chorionic gonadotropin

H_2O	water
is	injected side
k	kilo
kb	kilobase
l	liter
LB	Luria-Bertani
µ	micro
m	milli
M	molar
MAB	maleic acid buffer
MEM	MOPS-EGTA-$MgSO_4$ buffer
MEMFA	MOPS-EGTA-$MgSO_4$ formaldehyde buffer
MeOH	methanol
min	minutes
mRNA	messenger RNA
n	Nano, number
NaAC	sodium acetate
NBT	nitro-blue-tetrazolium
nm	nanometer
odc	*ornithine decarboxylase*
PAGE	polyacrylamide gel electrophoresis
PBS	phosphate buffered saline
PCR	polymerase chain reaction
pH	negative decade logarithm of hydrogen ion concentration
pH3	phosphorylated histone 3
%	percentage
Prdm	positive regulatory domain I-binding factor1 (PRD1-BF1/PRDM1) and retinoblastoma-interacting zinc finger protein 1 (RIZ1/PRDM2)
RNA	ribonucleic acid
RNase	ribonuclease
rpm	rounds per minute
RT	room temperature, reverse transcriptase
RT-PCR	reverse transcriptase PCR

SDS	sodium dodecyl sulfate
sec	second
SHH	Sonic Hedgehog
SpMO	splicing morpholino oligo
SSC	standard saline citrate buffer
st	stage
T_A	annealing temperature
Taq	*Thermus aquaticus*
T_m	melting temperature
U	units
V	voltage
Vol.	volume
wmish	whole mount *in situ* hybridization
X-Gal	5-bromo-4-chloro-3-indolyl-β-d-galactoside

1. Introduction

1.1 *Xenopus* neurogenesis

The African clawed frog *Xenopus* is an attractive model organism to elucidate the molecular mechanics of early vertebrate development. The two species mainly used are the allotetraploid *Xenopus laevis* (*X. laevis*), and the closely related *Xenopus tropicalis* (*X. tropicalis*), which has a diploid and sequenced genome (Amaya, 2005; Geach and Zimmerman, 2011; Grainger, 2012). One of the key advantages of the *Xenopus* model system is the external development of the embryos, which makes them readily accessible for chemical treatments and microinjections of DNA, mRNA or antisense morpholino oligonucleotides. More recently, the use of gene editing tools like TALENs or CRISPR/Cas have been successfully applied in the *Xenopus* model system (Lei *et al.,* 2012; Nakayama *et al.,* 2013; Guo *et al.,* 2014; Liu *et al.,* 2014). A relatively simple and yet powerful experimental method is the animal cap assay, in which prospective ectodermal cells of the animal pole are isolated from a blastula stage embryo. These cells are an attractive source for *in vitro* studies of differentiation since they are pluripotent and able to differentiate into many cell types upon overexpression of different mRNAs (Ariizumi *et al.,* 2009; Borchers and Pieler, 2010).

Xenopus is an important and compelling model organism in studies of early vertebrate neurogenesis, not only due to afore mentioned advantages, but also as the primary neurons are born during the first 24 hours of development (Hartenstein, 1989; Roberts, 2000). These neurons are termed primary neurons and arise in the posterior neural plate in three bilateral longitudinal domains (Chitnis *et al.,* 1995). With the exception of the trigeminal placodes, neuronal differentiation in the anterior neural plate is delayed until late neurula stages (Papalopulu and Kintner, 1996). The primary nervous system is required for touch responses and movements of the early tadpole (Roberts, 2000). Secondary neurogenesis occurs prior to metamorphosis and generates the mature nervous system required for the adult frog (Wullimann *et al.,* 2005).

1.2 Neural induction

One of the earliest events in the development of the vertebrate nervous system is the specification of the dorsal ectoderm into a neural lineage, which occurs through the process of neural induction (Pera *et al.,* 2014). The induced neuroectoderm forms the neural plate and is comprised of mitotically active neural precursor cells separated from the non-neural ectoderm by the neural plate border (Aruga and Mikoshiba, 2011) (Fig. 1.1). The neural plate is a bilayered epithelium with a superficial and a deeper sensorial layer (Hartenstein, 1989; Chalmers *et al.,* 2002). The primary neurons are born in the sensorial layer, while the cells in the superficial layer continue to proliferate and will later give rise to secondary neurons (Hartenstein, 1989; Chalmers *et al.,* 2002; Wullimann *et al.,* 2005). The neural plate will give rise to the brain, spinal cord and retina and derivatives of the neural plate border include the neural crest, neurogenic placodes, Rohon-Beard sensory neurons and the hatching gland (Kuroda et al., 2004; Rossi *et al*., 2009; Bae *et al.,* 2014).

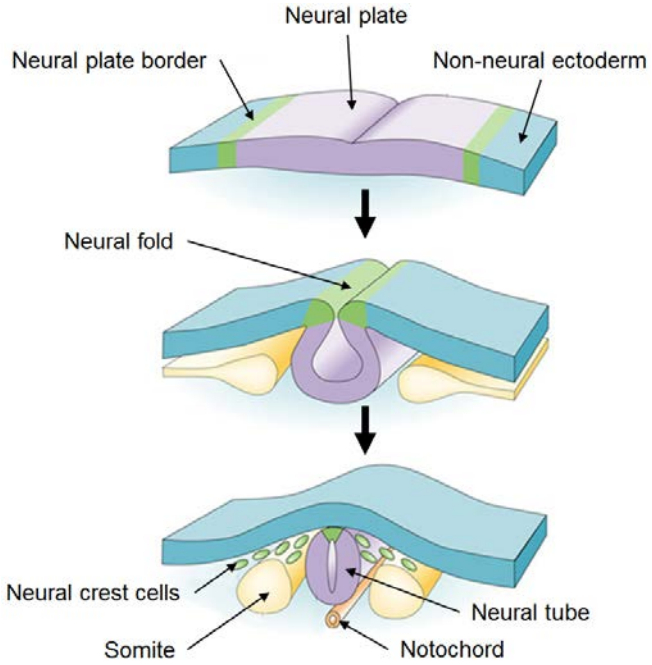

Fig. 1.1 Overview of the establishment of the central nervous system in *X. laevis.* After neural induction the dorsal ectoderm forms the neural plate. The non-neural ectoderm and the neural plate are separated by the neural plate border. After neurulation, the neurons differentiate into distinct subtypes, while the neural plate border contributes to the most dorsal aspect of the neural tube from where neural crest cells, Rohon-Beard sensory neurons and neurogenic placodes arise (Gammill and Bronner-Fraser, 2002; modified).

Many of the key experiments that essentially contributed to our understanding of vertebrate neural induction have been carried out in *X. laevis,* using transplantation and animal cap assay experiments (Linker and Stern, 2004). One crucial finding was the observation that intact animal cap explants, which normally give rise to atypical epidermis, differentiate into neural tissue upon dissociation (Wilson and Hemmati-Brivanlou, 1995) (Fig. 1.2). This suggested that a soluble inhibitor of the neural fate is present in the animal cap, but is diluted out upon dissociation (Grunz and Tacke, 1989; Sato and Sargent, 1989). This idea was further supported by the neuralization of animal caps upon overexpression of a dominant-negative activin receptor, and the inhibition of a neural fate when dissociated animal cap cells were cultured in the presence of BMP4 (Hemmati-Brivanlou and Melton, 1992; Hemmati-Brivanlou and Melton, 1994; Wilson and Hemmati-Brivanlou, 1995). The sum of these findings led to the postulation of the "default model" of neural induction. In this model, the default state of the ectoderm is thought to be neural and requires the inhibition of epidermal promoting BMP signaling (Hemmati-Brivanlou and Melton, 1997; Stern, 2005; Pera *et al.,* 2014).

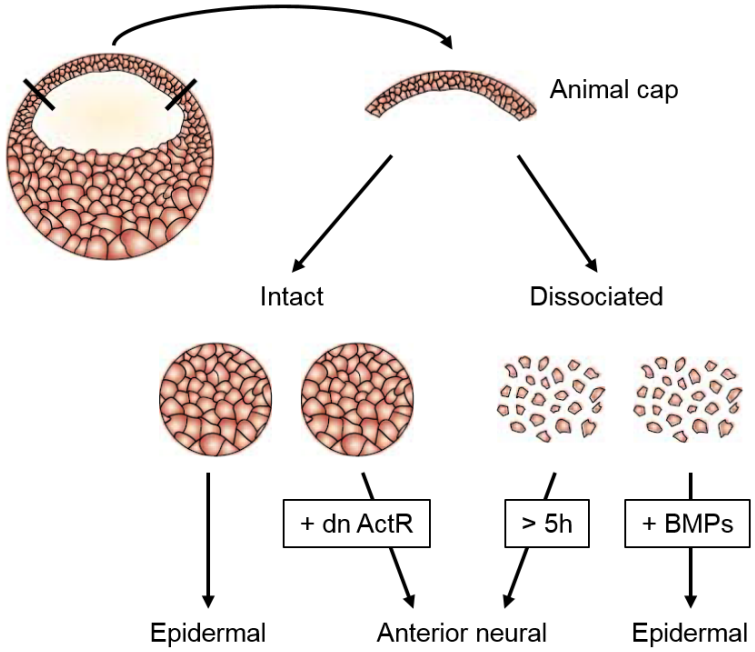

Fig. 1.2 Experimental evidence supporting the default model of neural induction in *X. laevis*. Intact ectodermal explants (animal caps), excised from the animal pole of a blastula stage embryo (stage 8-9) will give rise to atypical epidermis. If this tissue ectopically expresses a dominant-negative activin receptor (dn ActR) or is dissociated, these cells acquire an anterior neural fate. Addition of BMP to dissociated cells will restore epidermal fate (Muñoz-Sanjuán and Brivanlou, 2002; modified).

The inhibition of BMP signaling can occur on different levels, including extracellular inhibition by factors secreted from different signaling centers (Kuroda *et al.,* 2004; Ozair *et al.,* 2013) (Fig. 1.3). At blastula stages, Chordin (Piccolo *et al.,* 1996; Sasai *et al.,* 1994) and Noggin (Smith and Harland, 1992; Lamb *et al.,* 1993) are secreted from the blastula Chordin- and Noggin-expressing (BCNE) center, which is located in dorsal animal cells (Kuroda *et al.,* 2004). During gastrulation, Chordin, Noggin, Follistatin (Hemmati-Brivanlou *et al.,* 1994) and Cerberus (Bouwmeester *et al.,* 1996; Piccolo *et al.,* 1999) are expressed in the Spemann organizer, which involutes and secretes these BMP antagonists into the overlying prospective neuroectoderm (Aruga and Mikoshiba, 2011).

Despite the multiple lines of evidence supporting the “default model” of neural induction, numerous studies have convincingly challenged this model. In chick embryos, a requirement for FGF signaling prior to BMP antagonism has been demonstrated (Streit *et al*., 2000). Furthermore, the dissociation of *X. laevis* animal caps triggers the activation of the FGF pathway, while if FGF-signaling is blocked, neuralization of the dissociated animal caps is prevented (Kuroda *et al.,* 2005). Taken together, it is now accepted that inhibition of BMP signaling alone is not sufficient for neural induction but that FGF signaling is also required (Kengaku and Okamoto, 1995; Lamb and Harland, 1995; Streit *et al.,* 2000; Pera *et al.,* 2003; Linker and Stern, 2004, Delaune *et al.,* 2005) (Fig. 1.3). In addition, an involvement of Ca^{2+}-influx in the process of neural induction has also been demonstrated (Moreau *et al.,* 2008; Leclerc *et al.,* 2012).

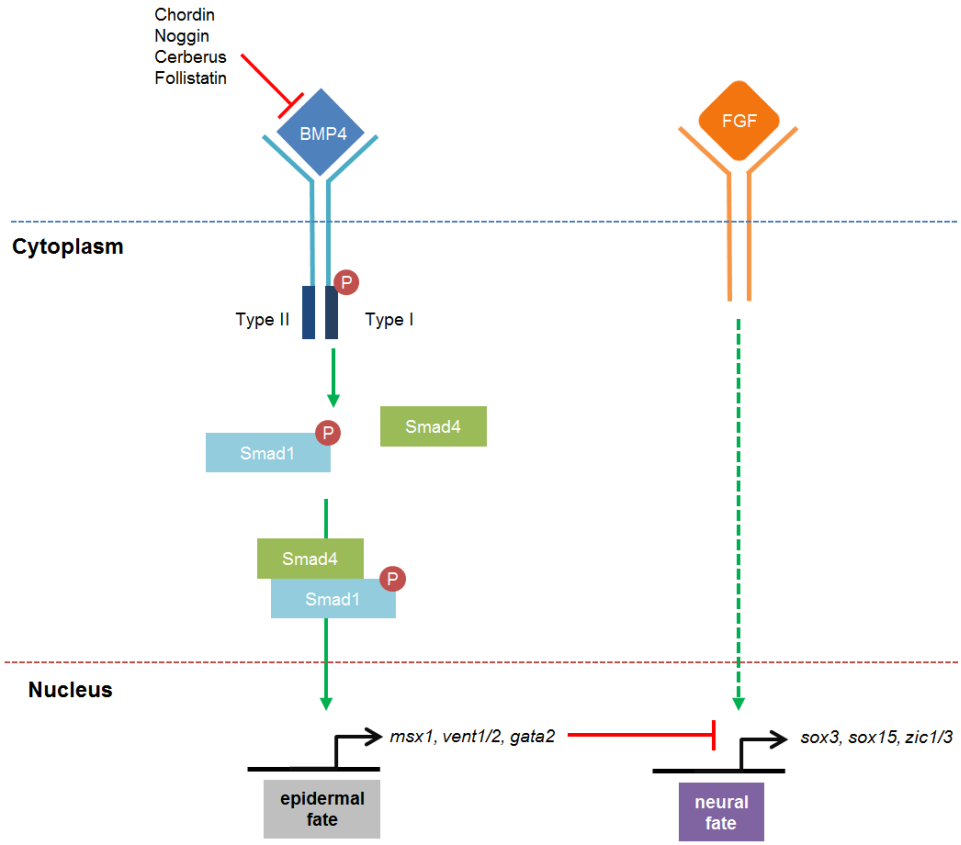

Fig. 1.3 Overview of the molecular mechanisms resulting in neural induction in *X. laevis*. BMP ligand binding triggers autophosphorylation and dimerization of the receptors, which in turn leads to the phosphorylation of SMAD1. SMAD1 and -4 form a complex and translocate to the nucleus where they activate the expression of epidermal genes such as *gata2*, *msx1* and *vent1/2*. This activation can be inhibited extracellularly by secreted BMP inhibitors (Chordin, Noggin, Cerberus and Follistatin). Active FGF signaling together with inhibition of BMP cause neuralization of the epidermis by expression of pan-neural genes such as *sox3, sox15* and *zic1/3.*

1.3 Stabilization of the neural fate

Neural induction results in the expression of several transcription factors within the neuroectoderm (Sasai, 1998; Moody and Je, 2002) including members of the Sry-related high-mobility group box (sox) family, which are expressed in the neural progenitor cells (Lefebvre *et al.,* 2007). *Sox2* and *sox3* are early pan-neural genes belonging to the SoxB1 subfamily, which maintain the neural progenitor state (Penzel *et al.,* 1997; Uchikawa *et al.,* 1999; Graham *et al.,* 2003; Pevny and Placzek, 2005). *Sox15* (also known as *soxd*) is also broadly expressed throughout the neural plate and is induced in response to BMP inhibition. Overexpression of *sox15* expands the neural plate and promotes a delayed neuronal differentiation (Mizuseki *et al.,* 1998b). Other transcription factors that maintain proliferating neural progenitors are the coiled-coiled protein Geminin (Kroll *et al.,* 1998; Seo and Kroll, 2006; Papanayotou *et*

al., 2008) and the forkhead/winged helix transcription factor FoxD5 (Solter *et al.,* 1999; Sullivan *et al.,* 2001).

Members of the *zic* family of zinc finger transcription factor genes are expressed throughout the neural plate border and are required in early neurogenesis and neural crest formation (Houtmeyers *et al.,* 2013). Overexpression of *zic1, 2* and *3* in *X. laevis* results in the expansion of the neural plate and promotes neural crest formation. In addition, *zic1* and *zic3* both promote neurogenesis upon overexpression (Nakata *et al.,* 1997; Mizuseki *et al.,* 1998a, Rogers *et al.,* 2009). In contrast, *zic2*, which is also expressed between the territories of primary neurogenesis, inhibits neuronal differentiation (Brewster *et al.,* 1998).

1.4 Neuronal differentiation

In *X. laevis* the primary neurons are born in three longitudinal bilateral domains in the sensorial layer of the posterior neural plate and the anteriorly located trigeminal placodes (Papalopulu and Kintner, 1996) (Fig. 1.4A). In these territories of primary neurogenesis, the first genes expressed are proneural basic helix-loop-helix (bHLH) transcription factor gene of the *neurogenin* family (Imayoshi and Kageyama, 2014). Members of this family are transcriptional activators that heterodimerize with more broadly expressed E proteins and bind within the regulatory domains of their target genes at E box motifs (CANNTG) (Bertrand *et al.,* 2002). These proneural genes trigger general neurogenesis and promote the differentiation of specific neuronal and/or glial cells, which suggest a common set of target genes for generic neurogenesis but an individual set of target genes for distinct neuronal subtypes (Powell and Jarman, 2008).

The *neurogenins* are orthologs of the *Drosophila* neuronal determination factor *atonal* (Ma *et al.,* 1996; Nieber *et al.,* 2009) and exhibit a proneural activity by inducing downstream proneural transcription factors and regulating cell-cycle exit (Ma *et al.,* 1996; Bertrand, 2002; Souopgui *et al.,* 2002; de la Calle-Mustienes *et al.,* 2002). The *neurogenins* are already expressed during early gastrulation, prefiguring the domains of primary neurons in the deep layer of the prospective neuroectoderm. The expression of *neurog1* and *neurog2* is

present in all three longitudinal stripes of primary neurogenesis with *neurog2* being expressed much broader (Ma *et al.,* 1996; Nieber *et al.,* 2009). *Neurog3* has a much more restricted expression domain that encompasses the medial domain (Nieber *et al.,* 2009).

Neurog2 is the best characterized proneural gene in *X. laevis* and its expression is induced by the pre-pattern genes *zic1*, *zic3* and the pan-neural gene *sox15,* whereas *zic2* represses the expression and function of *neurog1* and *neurog2* (Mizuseki *et al.,* 1998a; Mizuseki *et al.,* 1998b, Rogers *et al.,* 2009). Neurog2 induces the expression of several neuronal differentiation factor genes such as for the transcription factors *neurod1* (Ma *et al.,* 1996), *neurod4* (Perron *et al.,* 1999), *ebf2* (Dubois *et al.,* 1998), *ebf3* (Pozzoli *et al.* 2001), *myt1* (Bellefroid *et al.,* 1996), *mtgr1* (Koyano-Nakagawa and Kintner, 2005), *hes6* (Koyano-Nakagawa *et al.,* 2000), the RNA binding protein *seb4r* (Boy *et al.,* 2004), as well as the Notch ligands *dll1* and *dll4* (Chitnis *et al.,* 1995; Bray, 2006). Neurog2 additionally induces the expression of the cell cycle inhibitor genes *gadd45-γ* and *pak3*, which enables a proliferating cell to exit the cell cycle and start to differentiate (Souopgui *et al.,* 2002; de la Calle-Mustienes *et al.,* 2002). Surprisingly, the cdk inhibitor gene *cdknx* is required for neuronal differentiation by promoting the stabilization of Neurog2 (Vernon and Philpott, 2003; Nguyen *et al.,* 2006).

1.5 Neurulation and neuronal subtype specification

During neurulation, the neural plate folds and gives rise to the neural tube. The posterior neural tube forms the spinal chord, in which distinct neuronal subtypes are specified depending on their dorso-ventral position (Hartenstein, 1989; Roberts, 2000) (Fig. 1.4). In the closed neural tube, the neural precursor cells are located in the inner ventricular zone (Fig. 1.4B). As neural cells exit the cell cycle, they start to migrate outwards through the subventricular zone into the marginal zone where they differentiate into mature neurons (Taverna and Huttner, 2010; Spear and Erickson, 2012; Miyata *et al.,* 2014). The dorso-ventral patterning of the neurons is the consequence of two opposing morphogen gradients, BMP generated in the dorsal roof plate and sonic hedgehog (SHH) secreted from the ventral floor plate (Le Dreau and

Marti, 2012). This dorso-ventral morphogen gradient leads to the specification of distinct progenitor domains within the ventricular zone of the neural tube, which are defined by the expression of specific bHLH and homeodomain transcription factors (Jessell *et al.,* 2000; Alaynick *et al.,* 2011). The differentiating cells start to express a unique combinatorial code of transcription factors specific for its subtype and begin to migrate outwards through the subventricular zone into the marginal zone where the cells terminally differentiate into distinct populations of neurons (Ge *et al.,* 2006; Powell and Jarman, 2008; Alaynick *et al.,* 2011).

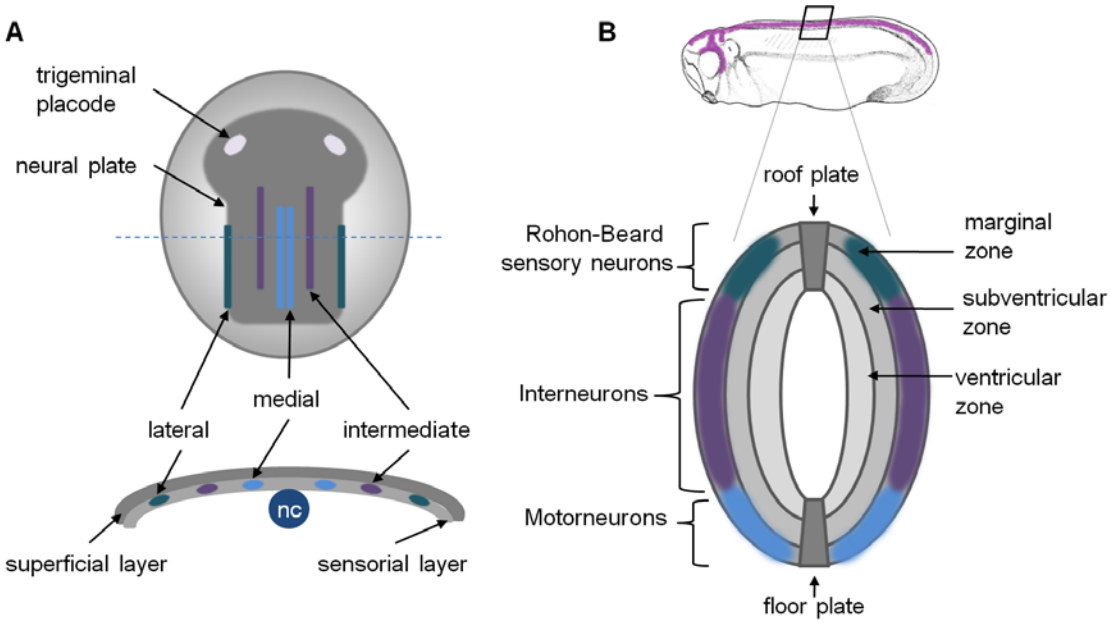

Fig. 1.4 Neuronal subtype specification in *X. laevis.* (A) In the open neural plate primary neurons are born in the sensorial layer of the neural plate bilaterally in three longitudinal stripes and in the trigeminal placodes. After neurulation, the primary neurons differentiate into specific neuronal subtypes depending on their position within the neural plate and subsequently on their dorso-ventral position within the closed neural tube. Dashed blue line indicates level of section. Nc, notochord **(B)** Neurons in the lateral stripes will give rise to Rohon-Beard sensory neurons, while neurons in the intermediate stripe differentiate into interneurons. Neurons that are located in the medial stripe will become motorneurons. In the closed neural tube, the neural progenitor cells are located in the ventricular zone where Notch signaling is high. Beginning with differentiation, the cells migrate through the subventricular zone into the marginal zone where they terminally differentiate and mature.

The first neurons are born at mid-gastrula stages and are the laterally located Rohon-Beard mechanosensory neurons (Lamborghini *et al.,* 1980; Rossi *et al.,* 2009) (Fig. 1.4A). These neurons are responsible for touch responses of *Xenopus* and zebrafish embryos and arise from the neural plate border, which is exposed to intermediate levels of BMP signaling and contributes to the most dorsal aspect of the neural tube (Rossi *et al.,* 2008;

Rossi *et al.,* 2009, Groves and LaBonne, 2014). With a slight delay, the ventrally located neurons differentiate into motorneurons and Kolmer-Agdhur cells. The latter are cells of unknown function but are speculated to be primitive sensory cells (Hartenstein, 1993; Djenoune *et al.,* 2014). The last neurons to differentiate are the interneurons, which can be subdivided into seven different subtypes (Hartenstein, 1993; Roberts *et al.,* 2012).

1.6 Lateral inhibition

The neural plate is comprised of a homogenous population of equipotent proliferating cells (Beatus and Lendahl, 1998). Through the activity of proneural factors such as Neurog2 and Ascl1, lateral inhibition is triggered. This leads to the inhibition of neuronal differentiation in neighbouring cells, resulting in a “salt-and-pepper” like pattern of postmitotic neurons (Chitnis *et al.,* 1995; Lewis, 1996; Vasconcelos and Castro, 2014) (Fig. 1.5A). The process of lateral inhibition is mediated by Notch signaling between two neighboring cells. In the signal sending cell that is destined to differentiate into a neuron, the proneural transcription factors induce the expression of transmembrane Notch ligands such as *dll1* and *4* as well as *jag1* in *X. laevis* (Kiyota and Kinoshita, 2002; Bray, 2006). The Notch ligands then bind to the Notch1-receptor on a neighboring signal receiving cell (Chitnis *et al.,* 1995; Bray, 2006), thereby inducing a series of proteolytic processes within the signal receiving cell that leads to the cleavage of the intracellular domain of the Notch receptor (NICD) (Schroeter *et al.,* 1998; Selkoe and Kopan, 2003). NICD translocates into the nucleus, where it displaces a co-repressor of Rbp-j and acts as a co-activator inducing the expression of genes of the *hairy and enhancer of split related* (*hes*) family (Wettstein *et al.,* 1997). These direct Notch target genes are bHLH transcription factor repressor proteins, which inhibit the expression and activity of proneural genes such as *neurog2* in the signal receiving cell (Dawson *et al.,* 1995; Wettstein *et al.,* 1997; Li and Baker, 2001; Schneider *et al.,* 2001; Cau *et al.,* 2002; Louvi and Artavanis-Tsakonas, 2006). Hence, the signal sending cell differentiates into a neuron, whereas the neighboring signal receiving cell is prevented from differentiating into a neuron and remains in a proliferating undifferentiated state to maintain a neural progenitor pool (Dawson *et al.,* 1995; Wang and Barres, 2000). Besides its role in lateral inhibition in the neural plate,

the Notch signaling pathway is also required for the maintenance of a progenitor pool of proliferating neurons in the ventricular zone of the neural tube (Lindsell *et al.,* 1996; Imayoshi and Kageyama, 2011).

The selection process that determines which cell from a pool of equipotent progenitors will differentiate into a neuron is not fully understood (Goodfellow *et al.,* 2014). It has been shown that Neurog2 activates the zinc finger transcription factor gene *myt1*, which enables a cell to escape lateral inhibition (Bellefroid *et al.,* 1996). Furthermore, the oscillating expression of proneural genes in neural progenitor cells, contributes to the determination of which cells differentiate into neurons (Hatakeyama and Kageyama, 2006; Nelson and Reh, 2008; Kageyama *et al.,* 2008, Goodfellow *et al.,* 2014). In mouse, the oscillating expression of *neurog2* and *dll1* is inverse to the Notch-mediated induction of *hes1,* which is an inhibitor of the proneural factors (Shimojo *et al.,* 2008) (Fig. 1.5B). Because of this oscillation, *neurog2* expression in a cell does not necessarily result in the differentiation of the cell into a neuron, but requires a certain threshold of *neurog2* to be reached and maintained (Kageyama *et al.,* 2008, Goodfellow *et al.,* 2014). The expression of *hes1* is regulated by autorepression as well as mRNA and protein instability (Hirata *et al.,* 2002; Momiji and Monk, 2009). The *hes1* mRNA is subject to degradation by miR-9, which itself is repressed by Hes1 (Bonev *et al.,* 2012). By this double-negative feedback loop, the expression of *hes1* oscillates (Bonev *et al.,* 2012). As the mature miR-9 is only slowly degraded, it accumulates in the cell, which leads to increased degradation of *hes1* mRNA. Thus, the proneural factors are released from repression and the cell differentiates into a neuron (Bonev *et al.,* 2012; Goodfellow *et al.,* 2014).

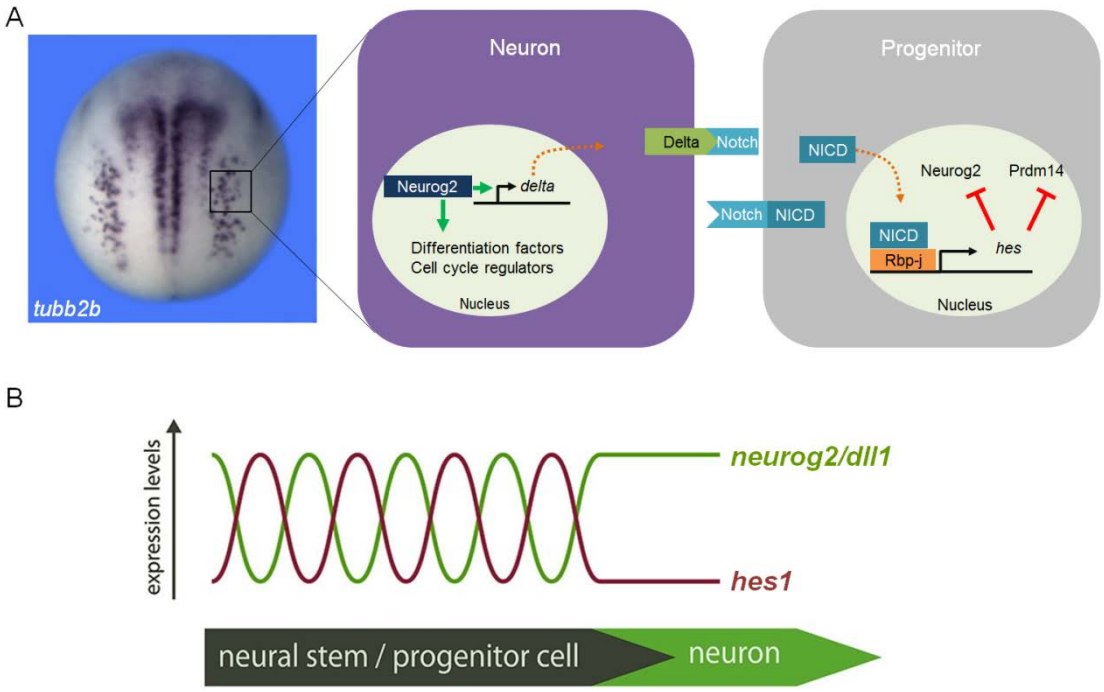

Fig. 1.5 Delta-Notch pathway mediated-lateral inhibition. (A) In the cell that is destined to differentiate into a neuron, Neurog2 activates the expression of *dll1*, which translocates to the membrane and interacts with the membrane bound Notch receptor on the signal receiving neighboring cell. In the signal receiving cell, the intracellular domain of Notch (NICD) is released by proteolytic cleavages and translocates to the nucleus. Together with the transcription factor Rbp-j, NICD activates the expression of transcription factors of the Hes-family, which inhibit the expression and function of proneural factors and therefore inhibit neurogenesis. **(B)** The expression of *hes1* and *neurog2* show an inverse oscillation. If *hes1* expression is extinguished, *neurog2* expression is sustained, which leads to the differentiation of neural progenitor cells into neurons in a “salt-and-pepper” like pattern (Vasconcelos and Castro, 2014; modified).

1.7 Neural crest

The neural crest is a multipotent population of cells that arises from the neural plate border and is unique to vertebrates (Gammil and Bronner-Fraser, 2003) (Fig. 1.6). It is characterized by its high migratory potential and the ability to give rise to multiple derivatives that derive from three different neural crest subpopulations, the cranial-, trunk- and vagal neural crest, which are located along the anterior-posterior axis (Simões-Costa and Bronner, 2015). The cranial neural crest cells contribute to the facial skeleton and neurons of the cranial sensory ganglia (Couly *et al.,* 1998), whereas the vagal neural crest cells form the outflow tract of the heart and enteric ganglia of the gut (Le Douarin and Teillet, 1973; Creazzo *et al.,* 1998). In the peripheral nervous system, the dorsal root and sympathetic ganglia are formed by the trunk neural crest (Le Douarin

and Smith, 1988). The melanocytes arise from neural crest cells of all three subpopulations (Le Dourain *et al.,* 2004). Upon neural tube closure, the trunk neural crest cells contribute to the most dorsal aspect of the neural tube before they start the process of migration and differentiation (Le Dourain *et al.,* 2004).

The formation of the neural crest occurs during gastrulation and is a multi-step process, which can be divided into neural plate border induction followed by neural crest specification, migration and differentiation (Pegoraro and Monsoro-Burq, 2012; Simões-Costa and Bronner, 2015) (Fig. 1.6A). The induction of the neural plate borders requires intermediate levels of BMP as well as Wnt, FGF and Notch signaling (Endo *et al.,* 2002; Monsoro-Burq *et al.,* 2003; Yardley and Garcia-Castro, 2012; Groves and La Bonne, 2014). The combinatory effects of these signaling pathways result in the expression of several genes within the neural plate border, which form a synexpression group that cross-regulates each other's expression (Nikitina *et al.,* 2008; Bhat *et al.,* 2013). Among these neural plate border specifiers are *tfap2, msx1, zic1, gbx2, pax3/7, dlx5/6, hairy2, c-myc, gata2/3* and *foxi1/2* (Bellmeyer *et al.,* 2003; Meulemans and Bronner-Fraser, 2004; Monsoro-Burq *et al.,* 2005; Nichane *et al.,* 2008; Khudyakov and Bronner-Fraser, 2009; de Croze *et al.,* 2011). *Pax3* together with *zic1* is sufficient, to promote the expression of the neural crest specifiers in animal cap cells (Milet *et al.,* 2013). In contrast, *pax3* alone promotes the formation of the hatching gland, while *zic1* alone induces a pre-placodal ectodermal fate (Hong and Saint-Jeannet, 2007; Bae *et al.,* 2014). The activity of the neural plate border specifiers results in the specification and migration of neural crest cells by inducing the expression of *foxd3, snai2* and *sox8/9/10* (Dottori *et al.,* 2001; Luo *et al.,* 2003; Cheung *et al.,* 2005; Monsoro-Burq *et al.,* 2005; Sato *et al.,* 2005; Nichane *et al.,* 2008; Coles *et al.,* 2007).

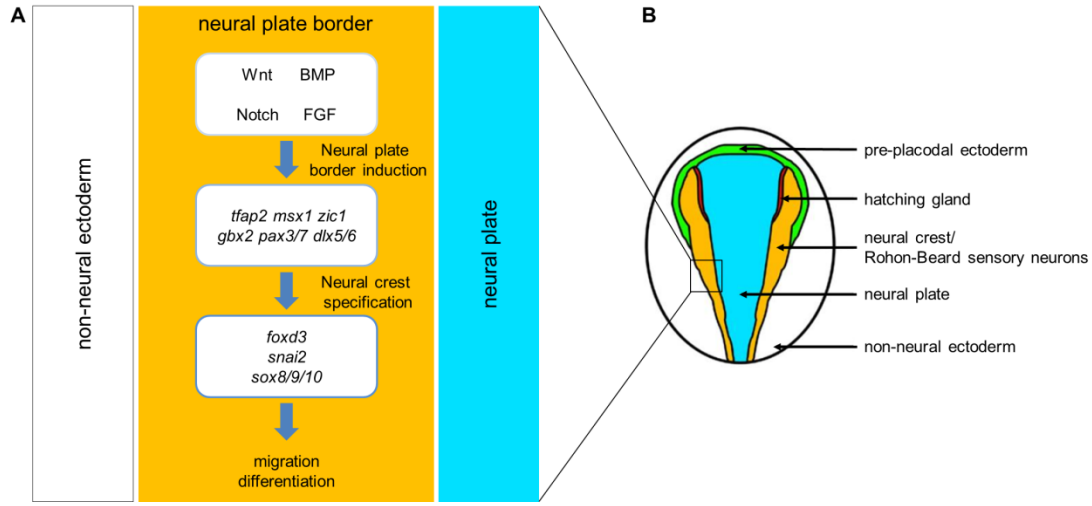

Fig. 1.6 Neural crest development in *X. laevis*. (A) Through the combinatory activity of Wnt, Notch, BMP and FGF signaling, the neural plate border inducing genes are activated. These genes mutually promote themselves and activate the neural crest specifying genes, that leads to the migration and differentiation of the neural crest cells (Pegoraro and Monsoro-Burq, 2012; modified). **(B)** Schematic illustration of a neurula stage embryo (dorsal view, anterior to top). Highlighted are the positions of the neural plate, and the neural plate border with its derivatives (pre-placodal ectoderm, hatching gland, neural crest, Rohon-Beard sensory neurons) (Hong and Saint-Jeannet, 2007; modified).

1.8 The Prdm protein family

Early vertebrate neurogenesis relies on multiple transcription factors and signaling pathways to ensure the proper establishment of the developing nervous system with its distinct neuronal and glial subtypes. In recent years, the Prdm proteins have emerged as critical players in neuronal subtype specification and neural crest formation (Hohenauer and Moore, 2012). Prdms belong to a highly conserved protein family whose members are involved in several cellular functions including the maintenance of stemness in embryonic stem cells and early developmental processes (Hohenauer and Moore, 2012). Deregulation of Prdms has also been implicated in several human diseases including cancer (Fog *et al.,* 2012).

1.8.1 Structural properties of Prdm proteins

Prdms are chromatin modifying proteins characterized by the presence of an N-terminally located PR-domain (Fog *et al*., 2012) (Fig. 1.7). The PR-domain is similar to the SET (Suppressor of variegation 3-9, Enhancer of zeste and trithorax) domain, found in several histone lysine methyltransferases (Huang,

2002). Correspondingly, several Prdm members have been shown to harbor intrinsic HMTase-activity (Fog *et al.,* 2012; Hohenauer and Moore, 2012). The methylation occurs on different lysine residues, which can result in transcriptionally silenced (Prdm2, 3, 6, 8, 16) as well as active (Prdm9) chromatin states (Table1.1) (Kim *et al*., 2003; Wu *et al.,* 2008; Eom *et al*., 2009; Hayashi *et al*., 2005; Bellefroid, unpublished; Hanotel *et al*., 2014; Pinheiro *et al*., 2012). However, a systematic analysis of the putative HMTase activity of other Prdms has not been carried out to date. Interestingly, the conserved motif, which is essential for the histone methylation on lysine by most SET proteins (H/RxxNHxC), is absent in the PR-domain (Rea *et al*.; 2000). While not all PRDMs show intrinsic HMTase-activity, several have been shown to recruit histone-modifying co-factors such as histone methyltransferases, deacetylases and acetyltransferases (Kouzarides, 2007; Fog *et al*., 2012; Hohenauer and Moore, 2012).

Gene	Intrinsic enzyme activity	References
Prdm2	H3K9me2	Kim *et al*., 2003
Prdm3	H3K9me1	Pinheiro *et al*., 2012
Prdm6	H4K20	Wu *et al*., 2008
Prdm8	H3K9me2	Eom *et al*., 2009
Prdm9	H3K4me3	Hayashi *et al*., 2005
Prdm12	Unknown	Bellefroid, unpublished
Prdm13	Unknown	Hanotel *et al*., 2014
Prdm16	H4K9me1	Pinheiro *et al*., 2012

Table 1.1 Prdms with known intrinsic HMTase activity. Histone modifications depicted in red promote heterochromatin formation, while histone modifications shown in green represent a transcriptionally active euchromatin state.

With the exception of Prdm11, all members feature a variable number of C2H2 zinc fingers in their C-terminus(Fog *et al*., 2012; Hohenauer and Moore, 2012) (Fig. 1.7). Through the zinc fingers, Prdms can bind to DNA and consensus binding sites that have been characterized for Prdm1, 3, 5, 9, 14 and 16 (Delwel *et al.,* 1993; Funabiki *et al.,* 1994; Kuo and Calame, 2004; Duan *et*

al., 2007; Seale *et al.,* 2007; Baudat *et al.,* 2010; Chia *et al.,* 2010; Ma *et al.,* 2011; Bard-Chapeau *et al.,* 2012).

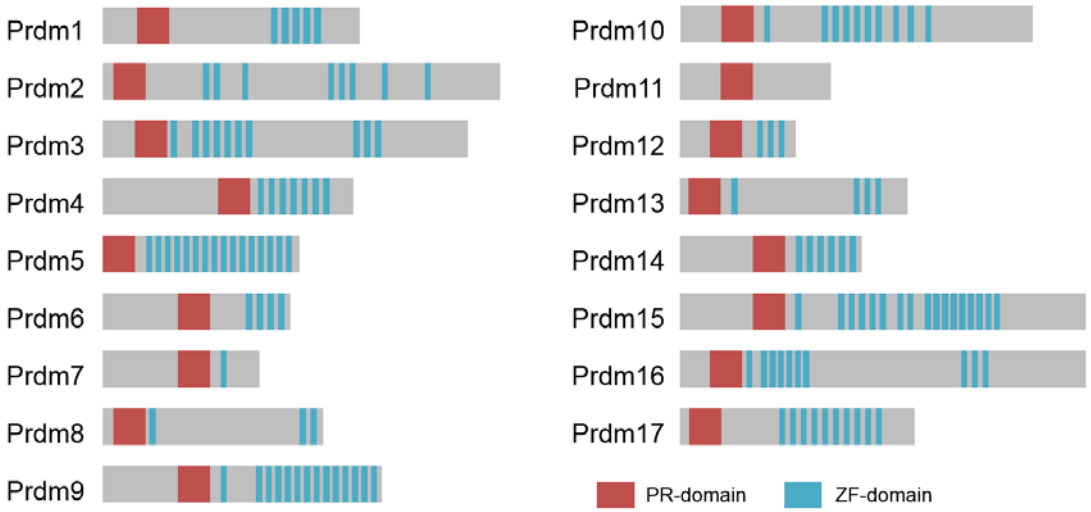

Fig. 1.7 Overview of the protein structure of members of the Prdm family. Shown is the longest isoform of each Prdm protein. The red box depicts the PR-domain and the blue bars represent zinc fingers. The structure is based on the mouse sequence.

1.8.2 The role of Prdms in early vertebrate neurogenesis and neural crest formation

Several members of the *prdm* family are expressed in the developing nervous system of vertebrates (Kinameri, *et al.,* 2008; Sun *et al.,* 2008; Liu *et al.,* 2012, Eguchi, *et al.,* 2015). Functional analyses of individual *prdms* have been carried out in various model systems and several have been shown to be involved in the specification of distinct neuronal subtypes and the specification of the neural crest (Hernandez-Lagunas *et al*., 2011; Ding *et al.,* 2013; Hanotel *et al.,* 2014).

1.8.2.1 Prdms in neural crest formation

In zebrafish as well as in *X. laevis, prdm1* is expressed at the neural plate border and essential for the migration of the trunk neural crest cells and the formation of Rohon-Beard sensory neurons (Hernandez-Lagunas *et al*., 2005; Rossi *et al*., 2008; Rossi *et al*., 2009; Olesnicky *et al.,* 2010; Hernandez-Lagunas *et al*., 2011; Powell *et al*., 2013). In zebrafish it has been shown that

prdm1a is coexpressed with the neural crest specifiers *foxd3* and *tfap2a,* which are directly regulated by Prdm1a (Powell *et al.,* 2013). Furthermore, Prdm1 regulates the expression of *sox10* and *islet1,* which are required for the specification of the neural crest and the formation of Rohon-Beard sensory neurons (Olesnicky *et al.,* 2010; Hernandez-Lagunas *et al*., 2011). The expression of *prdm1* in the neural plate border of the chick embryo was recently reported, suggesting a conservation of function (Zwane and Nikitina 2015).

1.8.2.2 Regulation of neuronal subtype specification by Prdms

Prdm12 has been shown to play a role in neuronal subtype specification in *X. laevis* and zebrafish. In the developing spinal cord, prdm12 promotes the formation of V1-interneurons at the expense of V0-neurons (Bellefroid, unpublished; Zannino *et al*., 2013). In addition, *X. laevis prdm12* is also required for the specification of sensory neurons as it regulates the expression of transcriptions required for sensory neuron formation such as *sncg*, *islet1* and *tlx3* (Nagy *et al.,* 2015).

In mouse and *X. laevis, prdm13* is a target of the Ptf1a-Rbp-J complex and responsible for the promotion of a GABAergic over a glutamatergic fate of neurons (Chang *et al*., 2013; Hanotel *et al*., 2014). Prdm13 promotes a GABAergic neural fate through the inhibition of the glutamatergic selector gene *tlx3* (Chang *et al.,* 2013; Hanotel *et al*., 2014).

1.8.2.3 Prdms in axon outgrowth

In the mouse spinal cord, *prdm8* is first expressed in the progenitor populations of ventral interneurons and motor neurons (Komai *et al.,* 2009). Together with the transcription factor Bhlhb5 (also known as Bhlhe22), Prdm8 forms a repressor complex to repress *cdh11,* whose downregulation is required for proper axon outgrowth of corticospinal motor neurons (Ross *et al*., 2012).

Prdm14 is required for proper motorneuron axon outgrowth in zebrafish. Loss of Prdm14 through mutation or injection of a splicing morpholino leads to shortened axons in caudal primary (CaP) motor neurons, which in turn results in defective embryonic movement. It has been shown that Prdm14 binds to the

promoter region of the transcription factor gene *islet2* and thus activates its expression, which is necessary for proper CaP axon outgrowth (Liu *et al.,* 2012).

1.8.3 Prdm14 is an epigenetic regulator and stemness factor

While in zebrafish a function for *prdm14* has been described for motorneuron axon outgrowth, *prdm14* in mice and humans is described in the context of primordial germ cell specification and stemness maintenance (Fog *et al.,* 2012; Liu *et al.,* 2012; Nakaki and Saitou, 2014). Prdm14 harbors a single PR-domain and six zinc finger domains that are highly conserved in vertebrates, while the N-terminus of the protein is more divergent (Nakaki and Saitou, 2014). Through its zinc finger domains, Prdm14 can bind and regulate its target genes (Ma *et al.,* 2011). Through ChIP-seq analysis in mouse and human ESC (hESC/mESC) the consensus binding sequence has been identified as 5'-GGTCTCTAA-3' (Yamaji *et al.,* 2013). Unlike other Prdms, no intrinsic HMTase activity has been demonstrated for Prdm14. However, in mammalian cell cultures it has been shown that Prdm14 regulates pluripotency and epigenetic reprogramming (Nakaki and Saitou, 2014). In mESCs Prdm14 interacts with the H3K27me3-ase PCR2, which leads to the repression of *fgfr1* and *fgfr2* and thereby to an inhibition of differentiation (Grabole *et al.,* 2013; Yamaji *et al.,* 2013). Furthermore, the Prdm14/PCR2 complex represses expression of the *de novo* methyltransferases *dnmt3a*, *dnmt3b* and *dnmt3l,* which leads to low levels of methylation in mESC (Grabole *et al.,* 2013). Through complexation with Ten-Eleven Translocation (TET) proteins, Prdm14 promotes the demethylation of germline specific promoters by oxidation of 5-methylcytosine (5mC) to 5-hydroxymethylcytosine (5hmC) (Hacket *et al.,* 2013; Okashita *et al.,* 2014).

Besides its repressing properties, Prdm14 is able to activate the expression of genes that are required to maintain pluripotency such as *sox2* or *klf5* and in a complex with PRMT4, Prdm14 activates its target genes in mESC through H3 arginine 26 dimethylation (Ma *et al.,* 2011; Burton *et al.,* 2013; Chan et al., 2013; Yamaji *et al.,* 2013; Nakaki and Saitou, 2014). Thus, regulation of Prdm14 target genes is context dependent and Prdm14 can act as an activator as well as a repressor (Ma *et al.,* 2011; Nakaki and Saitou, 2014).

It is suggested that Prdm14 is involved in the core pluripotency circuitry in hESC were it binds to the proximal enhancer of *oct4* and activates its expression (Chia *et al.,* 2010). Similar to mESCs, Prdm14 occupies several target genes together with Oct4, Sox2 and Nanog (Chia *et al.,* 2010). However, *prdm14* itself is also occupied by these three factors (Boyer *et al.,* 2005; Chia *et al.,* 2010).

Prdm14 is also required together with Prdm1 for the formation of primordial germ cells in mice (PGCs) by regulating three critical steps: repression of the somatic mesodermal program, reacquisition of potential pluripotency by *sox2* activation and epigenetic reprogramming through genome-wide DNA demethylation (Ohinata *et al.,* 2005; Yamaji *et al.,* 2008; Ohinata *et al.,* 2009).

1.9 Aims

In recent years, the Prdm proteins have emerged as critical transcriptional regulators involved in stemness maintenance, differentiation and epigenetic modification (Fog et al., 2011; Hohenauer and Moore, 2012). In addition, several members of the *prdm* family play crucial roles in the development of the neural crest and central nervous system (Hernandez-Lagunas *et al*., 2005; Rossi *et al*., 2008; Rossi *et al*., 2009; Olesnicky *et al.,* 2010; Hernandez-Lagunas *et al*., 2011; Powell *et al*., 2013, Liu *et al.,* 2012; Zannino *et al*., 2013; Hanotel *et al*., 2014; Nagy *et al.,* 2015). In a screen for target genes repressed by the Notch pathway effector protein Hes5.1, *prdm14* was identified in *X. laevis* (Klisch, 2006). Owing to the key role members of this family have during early development, a functional analysis of *prdm14* using the *X. laevis* model system was undertaken. Specifically, the developmental processes regulated by *prdm14* are to be investigated as well as the downstream gene regulatory network.

2. Material and Methods

2.1 Material

2.1.1 Model organism

During this study the South African clawed frog *Xenopus laevis* was used as a model system using animals obtained from Nasco (Ft. Atkinson, USA). The animals were kept according to the directive 2010/63/EU on the protection of animals used for scientific purposes. The developmental stages were determined according to Nieuwkoop and Faber (1967).

2.1.2 Bacteria

The chemical competent *Escherichia coli*-Strain XL1-Blue was used for transformations.
XL1-Blue: recA1, endA1, gyrA96, thi-1, hsdR17, supE44, relA1, lac[F'proAB, laclqZΔM15, Tn10(Tetr)] (Stratagene)

2.1.3 Antibiotics and Media

For culture medium 32 g Luria Bertani (LB) was dissolved in 1 liter dH_2O and autoclaved for 20 min at 121°C. After cooling down to 50°C the selective antibiotic was added. The agar plates were poured under a sterile bench and stored at 4°C in the dark. As selective antibiotic Ampicillin was used (stock: 100 mg/ml in dH_2O, working: 100 µg/ml, stored in the dark at -20°C).

2.1.4 Oligonucleotides

Oligonucleotides were purchased from Sigma-Aldrich and dissolved in HPLC-H_2O to a concentration of 100 µM or 500 µM. The following sequences of the oligonucleotides are written in 5' to 3' direction.

2.1.4.1 RT-PCR Oligonucleotides (Primer)

Gene	Sequence		T_A °C
	Forward	reverse	
neurog2	GCGCGTTAAAGCTAACAACC	GTTCAGGTGGAGCTCAGAGG	60
tubb2b	ACACGGCATTGATCCTACAG	AGCTCCTTCGGTGTAATGAC	57
tlx3	GCCAACAAGTACAAGTGCACAG	CAGGAGCCAGACTCACATTGAC	57
prdm14 a ex1-2	CAGGACAAGTCACCAGGGAG	CAACTGCAACGAGTCCCTG	60
prdm14 b ex1-2	CTATGGTAGCGACTCAAGGACCG	CAACTGCAACGAGTCCCTG	60
odc	GCCATTGTGAAGACTCTCTCCATTC	TTCGGGTGATTCCTTGCCAC	56

Table 2.1 Summary of RT-PCR oligonucleotides and their annealing temperatures

2.1.4.2 Sequencing oligonucleotides

Primer	Sequence	T_A °C
SP6	TTAGGTGACACTATAGAATAC	56
T7	TAATACGACTCACTATAGGGCGA	56
T7 (pCS2+)	TCTACGTAATACGACTCACTATAG	56
T3	AATTAACCCTCACTAAAGGG	56
GR7	ATCCTGCATATAACAACTTC	56

Table 2.2 Summary of sequencing oligonucleotides and their annealing temperatures

2.1.4.3 Morpholino oligonucleotides

The morpholino oligonucleotides (MO) used in this study were purchased from Gene Tools (Philomath, USA). The MOs were dissolved in RNase free H_2O to a concentration of 20 ng/nl and stored at 4°C. Before injection the MO were heated for 5 min at 65°C. The following sequences of the MO are depicted in 5' to 3' direction.

Morpholino Oligonucleotide	Sequence
Prdm14a SpMO	GTGTATAACATTTACCTGTAGAACT
Prdm14b SpMO	GTGTAACATTTACCTGTAGAAGTGC
Standard control MO	CCTCTTACCTCAGTTACAATTTATA

Table 2.3 Summary of morpholino oligonucleotides

2.1.5 Overexpression constructs

The following overexpression constructs used in this study have been described previously: **NICD-pCS2** (Coffman *et al*., 1993), **MT-Neurog2-pCS2+** (Ma *et al*., 1996), **MT-GFP-pCS2+** (Rubenstein *et al*., 1997), **MT-Wnt5a-pCS2+** (Damianitsch et al., 2009), **Wnt8a-MT-pSP64T** (Christian and Moon, 1993), **ATF2-luc-pGL** (van der Sanden *et al.,* 2004), **TOPFlash-luc-pGL3** (Korinek *et al.,* 1997), **Renilla-pRL-TK** (Promega)

Prdm14-pCS2+: This construct harbors the full open reading frame of *X. laevis prdm14*. The open reading frame was PCR amplified using following primers: Prdm14_for_EcoR1: 5'-CGG AAT TCG ATG GCT CTG TCT GT-3' and Prdm14_rev_Xho1: 5'-GGC TCG AGA TAG GAG GCT TGA AT-3' with Prdm14-pCS2p+ (National Institute for Basis Biology, Japan; clone XL280n24ex) as a template. *Prdm14* was subcloned into the pCS2+ expression vector using the EcoRI and XhoI restriction sites. For the transcription of sense mRNA, the construct was linearized with NotI and transcribed with the SP6 polymerase.

Prdm14-HA-pCS2+: This construct harbors the open reading frame of *X. laevis prdm14* without the stop codon and an HA tag at the C-terminus. The open reading frame was PCR amplified using following primers: P14-HA_EcoRI_ START: 5'-GAG AAT TCA TGG CTC TGT CTG TT-3' and P14-HA_XhoI_noSTOP2: 5'-TAC TCG AGG AGG CTG GAG TG-3' with Prdm14-pCS2p+ (National Institute for Basis Biology, Japan; clone XL280n24ex) as a template. *Prdm14* was subcloned into the pCS2+ HA vector (Damianitsch, 2009) using the EcoRI and XhoI restriction sites. This vector contains the human influenza hemaglutinin (HA) tag which allows the expression of HA-tagged proteins. For the transcription of sense mRNA, the construct was linearized with NotI and transcribed with the SP6 polymerase.

Prdm14-GR-pCS2+: This construct harbors the open reading frame of *X. laevis prdm14* without the stop codon. The *prdm14* open reading frame was excised from *prdm14*-pCS2+HA and ligated into GRpCS2+ using the EcoRI and XhoI restriction sites. This vector contains the human glucocorticoid ligand-binding

domain, which allows the induction of the translated protein by dexamethasone (Kolm and Sive, 1995). For the transcription of sense mRNA the construct was linearized with NotI and transcribed with the SP6 polymerase.

Prdm14-GR-HA-pCS2+: This construct harbors the open reading frame of *X. laevis* prdm14 without the stop codon. This vector contains the human glucocorticoid ligand-binding domain, which allows the induction of the translated protein by dexamethasone (Kolm and Sive, 1995). The GR-domain was PCR amplified using following primers: GR-tag_XhoI_for: ATC TCG AGA CCT CTG AAA ATC CT and GR-tag_+2_XbaI_noSTOP_rev: CGT CTA GAC ACT TTT GAT GAA ACA G using Prdm14-pCS2+GR as a template. The PCR product was cloned between the XhoI and XbaI sites of Prdm14-HA-pCS2+. For the transcription of sense mRNA the construct was linearized with NotI and transcribed with the SP6 polymerase.

2.1.6 antisense-RNA-constructs

Marker	Vector	RE	Poly-merase	Reference
n-tubulin/tubb2b	pBst KS	BamHI	T3	Chitnis *et al*., 1995
sox2	pBst SK	EcoRI	T7	Mizuseki *et al.,* 1998a
sox10	pCS2+	ClaI	T7	Aoki *et al.,* 2003
hox11L2/tlx3	BstEII	StuI	T3	Patterson & Krieg, 1999
neurog1	pCS2p+	EcoRI	T7	Nieber *et al*., 2009
neurog2	pBst II	BamH1	T3	Ma *et al.,* 1996
prdm14	pCS2p+	EcoRI	T7	Klisch, 2006
pax3	pCMV-Sport6	SalI	T7	Bang *et al.,* 1999
wnt8	pBst KS	BamHI	T3	-
zic1	pCS2p+	HindIII	T7	Mizuseki *et al.,* 1998a
zic2	pCS2p+	EcoRI	T7	Brewster *et al.,* 1998
zic3	pCS2p+	EcoRI	T7	Nakata *et al.,* 1997
vglut	pBst KS	NotI	T3	Gleason *et al.,* 2003
foxd3	pBst	EcoRI	T7	Pohl and Knöchel, 2001
hb9/mnx1	pBst KS	XbaI	T3	Saha *et al.,* 1997

Table 2.4 Summary of antisense RNA constructs

2.2 Methods

2.2.1 DNA-standard methods

2.2.1.1 Polymerase chain reaction (PCR)

2.2.1.1.1 Reverse transcription-PCR (RT-PCR)

For semi-quantitative RT-PCR 2.5 µl cDNA was used in a 12.5 µl reaction containing 1x Go Taq green reaction buffer (Promega), 0.2 mM of each primer and 0.5 units GoTaq DNA-polymerase (Promega). The amplification was carried out in a thermocycler (Biometra) with following conditions: 2 min 95°C, 45 sec 95°C, 30 sec T_A of primers -2 °C, 30 sec 72°C, 5 min 72°C. The number of cycles between step 2 and step 4 varied between the primer pairs and ranged between 25-35 cycles. The RT-PCR reaction were analyzed on a 2% agarose gel and documented in a Chemidoc chamber (Biorad) mounted with an Intas camera.

2.2.1.1.2 PCR Cloning

For molecular cloning the High Fidelity Enzyme Mix (Fermentas) was used. A PCR reaction contained 1x High Fidelity Buffer with 15 mM $MgCl_2$, 0.2 mM dNTP mix (Thermo Scientific), 0.75 µM of each primer, 0.1 ng/µl template DNA and 0.1 U/µl High Fidelity PCR enzyme mix. The amplification was carried out in a thermocycler (Biometra) with following conditions: 2 min 95°C, 45 sec 95°C, 45 sec T_A of primers -2 °C, 1 min/kb 72°C, 5 min 72°C. The number of cycles between step 2 and step 4 varied between the primer pairs and ranged between 30-40 cycles.

2.2.1.2 Agarose gel electrophoresis

TAE (Tris-acetate-EDTA): 40 mM Tris-acetate, 2 mM EDTA, pH 8.5

Restriction- and PCR-fragments were analyzed by agarose gel electrophoresis (Sharp *et al.,* 1973). Depending on the fragment size the percentage of the agarose gel was adapted (0.7-2%). Agarose powder was heated and dissolved in 1x TAE buffer. To visualize the DNA fragments ethidium bromide (0.5 µg/ml) was added to the liquid agarose gel. The

electrophoresis was performed in a horizontal electrophoresis chamber filled with 1x TAE at 100 V. For determination of the fragment sizes, standard DNA ladders (Fast Ruler DNA Ladder, Fermentas) were used. The documentation of the gel was carried out in a ChemiDoc (Bio-Rad) documentation chamber using an Intas camera and software.

2.2.1.3 Gel purification of PCR and restriction fragments

For isolation of DNA fragments from agarose gels, the agarose gel containing the desired fragment was excised and the DNA purified using the Fragment CleanUp Kit (Invitek) according to the manufacturer's instructions.

2.2.1.4 DNA restriction digestion

For restriction digestions of DNA restriction endonucleases were used from Fermentas Life Sciences according to manufacturer's instructions.

2.2.1.5 Ligation

For standard ligation reactions T4 DNA ligase (10 U/µl) (Fermentas Life Science) was used according to manufacturer's protocol. The ligation reaction was incubated overnight at 16°C.

2.2.1.6 Chemical transformation of bacterial cells

For chemical transformations the chemically competent *Escherichia coli*-strain XL1-Blue was used. Ligation or PCR reactions were added to 100-200 µl thawed cells and incubated on ice for 30 min. Afterwards the cells were heat shocked for 60-90 sec at 42°C and immediately cooled for 3 min on ice. LB medium (800 µl) was added to the cells which were then incubated for 30-45 min under constant shaking (300 rpm) at 37°C. After the incubation, the cells were centrifuged (30 sec, 10,000 rpm) and 800 µl of the overlying medium was discarded. The cells were resuspended in the remaining medium and seeded on LB agar plates containing selective antibiotic. The LB plates were incubated overnight at 37°C.

2.2.1.7 Plasmid preparation

The GeneJET Plasmid Miniprep kit (Fermentas) was used according to manufacturer's instructions to isolate DNA. For the isolation of DNA in preparative amounts (1 µg/µl) the NucleoBond Xtra Midi kit (Macherey-Nagel) was used following the manufacturer's protocol.
For DNA quantification the NanoDrop 2000c spectrophotometer (Thermo Scientific) was used.

2.2.1.8 DNA sequencing

For DNA sequencing, the chain termination method was used (Sanger *et al*., 1977). The sequencing was performed using the Big Dye Terminator Cycle Sequencing Kit (Applied Biosystems) according to manufacturer's instructions. The sequencing PCR mixture contained 200-400 ng DNA, 2 µl seq mix, 2 µl seq buffer and 1 pmol sequencing primer in a total of 10 µl reaction volume. The reaction was performed in a thermocycler using following program: 2 min 95°C, 30 sec 95°C, 30 sec 55°C, 4 min 72°C, with 26 cycles between step 2 and 4. For purification of the sequencing reaction, 1 µl NaAc (3 M), 1 µl EDTA (125 mM) and 50 µl 100% ethanol were added to the reaction mixture and incubated for 5 min at RT. After centrifugation for 15 min at 13,000 rpm, the DNA pellet was washed with 70% ethanol, air-dried and dissolved in 15 µl HiDi Buffer (Applied Biosystems). The automated sequencing was performed in the 3130 xl Genetic Analyzer (Applied Biosystems).

2.2.2 RNA standard methods

2.2.2.1 *In vitro* synthesis of capped sense mRNA

Capped sense mRNA was synthesized using the SP6 or T7 mMessage mMachine Kits (Ambion) according to manufacturer's protocol. A reaction of 20 µl contained 1 µg of linearized plasmid and was incubated at 37°C for 2 hours. After DNase digestion using 5 U of Turbo DNase I, the synthesized mRNA was purified using the Illustra RNAspin Mini kit (GE Healthcare) and eluted in 30 µl RNase free water at 80°C. RNA concentration was measured using the NanoDrop 2000c spectrophotometer (Thermo Scientific) and the quality was

checked on a 1% agarose gel. The RNA was aliquoted (2-4 µl) and stored at –80°C.

2.2.2.2 *In vitro* synthesis of antisense RNA

For the detection of *in vivo* transcripts antisense RNA was used in whole mount *in situ* hybridizations (WMISH).
A standard reaction of 25 µl contained 1 ng linearized plasmid, 1x Transcriptionbuffer (Fermentas), 1 mM rATP, rGTP, rCTP (Boehringer), 0.64 mM rUTP (Boehringer), 0.36 mM Digoxygenin-rUTP (Boehringer), 0.03 µM DTT, 1.6 U/µl Ribolock RNase inhibitor (Fermentas), 1.2 U/µl T3, T7 or SP6 RNA-Polymerase, add RNase-free water. The reaction was incubated for three hours at 37°C, followed by template digestion with 0.2 U/µl Turbo DNaseI (Ambion) for 30 min at 37°C. The RNeasy Mini kit (Qiagen) was used to purify the synthesized antisense RNA according to manufacturer's instructions. The RNA was eluted twice with 50 µl RNase-free water at 80°C. The quality was checked on a 1% agarose gel. The antisense RNA was stored at -20°C in 1 ml hybridization mix (see whole mount *in situ* hybridization).

2.2.2.3 Total RNA isolation from ectodermal explants and whole embryos

For the isolation of total RNA three embryos or 50-100 ectodermal explants were fixed in liquid nitrogen and lysated in 400 µl peqGOLD TriFast reagent (Peqlab) using a 29-gauge syringe and afterwards vortexed for 30 sec. After addition of 80 µl chloroform (Roth) and vortexing for 30 sec, the samples were centrifuged for 10 min at 13,000 rpm and 4°C. The supernatant (200 µl) was transferred into a new eppendorf tube. 200 µl chloroform were added and the sample vortexed for 30 sec and centrifuged for 5 min at 13,000 rpm at 4°C. The supernatant (180 µl) was transferred into a new eppendorf tube and 180 µl isopropanol were added. After vortexing, the samples were kept overnight at -20°C for precipitation. After precipitation the samples were centrifuged for 30 min at 13,000 rpm at 4°C and the pellet was washed with 400 µl 70% ethanol. After air drying the pellet was dissolved in 12.5 µl RNase-free water and DNase digestion was carried out using DNaseI (1 U/µl) (Thermo Scientific) for 30 min at 37°C. The DNaseI was denatured by incubation at 70°C for 10 minutes and the

RNA concentration measured on the NanoDrop 2000c spectrophotometer (Thermo Scientific). The quality of the RNA was analyzed with the 2100 Bioanalyzer (Agilent). To check for genomic DNA contamination, a control PCR with H4 or ODC was performed.

2.2.2.4 Reverse transcription

For the synthesis of 10 µl cDNA, 50-75 ng RNA was used in a standard reaction mix containing 1x Go Taq flexi buffer, 5 mM $MgCl_2$ (Fermentas), 2.5 mM random hexamer (Invitrogen), 1 mM dNTP mix (Thermo Scientific), 0.8 U/µl Ribolock RNase inhibitor (Thermo Scientific), 2 U/µl MulV reverse transcriptase (Roche). The reaction was carried out in a thermocycler. After an initial incubation for 20 min at 20°C the reaction was incubated for 1 hour at 42°C and terminated at 95°C for 5 min.

2.2.2.5 RNA-sequencing

2.2.2.5.1 Total RNA isolation from ectodermal explants

For the isolation of total RNA for RNA-sequencing 70-100 ectodermal explants were fixed in liquid nitrogen and lysates prepared in 360 µl peqGOLD TriFast reagent (Peqlab) using a 29-gauge syringe and afterwards incubated for 10 min at RT. After addition of 72 µl chloroform the solution was incubated at RT for 5 min and centrifuged for 20 min with 13,000 rpm at 4°C. The upper phase was transferred into a new Eppendorf tube to which 200 µl chloroform was added. The solution was centrifuged for 10 min at 4°C and the upper phase transferred into a new Eppendorf tube. After adding 180 µl isopropanol the RNA was precipitated overnight at -20°C. The next day, the solution was centrifuged for 30 min at 4°C. The pellet was washed with 70% ethanol and centrifuged for 5 min at 4°C. The pellet was air dried, and resuspended in 43.5 µl RNase-free water. For the digestion of genomic DNA, the RNA was incubated for 1 h at 37°C in a 50 µl reaction containing 1x DNaseI reaction buffer (Thermo Scientific), 1 µl DNaseI (Thermo Scientific) and 0.5 µl RNase inhibitor (Thermo Scientific). To stop the DNase treatment, 150 µl RNase free water and 200 µl phenol/chloroform/isoamylalcohol (25/24/1, Roth) was added to the RNA. After centrifugation for 10 min at 4°C the upper phase was transferred to a new

Eppendorf tube, 1 vol. of chloroform/isoamylalcohol (24/1) was added. Afterwards the RNA was centrifuged for 10 min at 4°C. The supernatant was transferred to a new Eppendorf tube to which 1/10 vol. of 5 M ammonium acetate and 1 vol. of isopropanol was added. The solution was incubated overnight at -20°C. The following day the RNA was centrifuged for 30 min at 4°C and the pellet washed twice with 70% ethanol and centrifuged for 5 min at 4°C. The pellet was air dried and resuspended in 20 µl RNase free water. The quality of the RNA was analyzed with the 2100 Bioanalyzer (Agilent). To check for genomic DNA contamination, a control PCR with H4 or ODC was performed.

2.2.2.5.2 Sample preparation and sequencing

LIbrary preparation and sequencing was performed by the DNA Microarray and Deep-Sequencing Facility Göttingen (UMG) - Transkriptomanalyselabor (TAL). Before sequencing, the RNA-libraries were prepared with the "TruSeq RNA Sample Prep Kit v2" (Illumina) following the manufacturer's protocol. The single read (50 bp) sequencing was performed using the HiSeq 2000 (Illumina). Three independent biological replicates were used for each sequencing reaction. The quality of the sequencing was controlled using the FastQ software (http://www.bioinformatics.babraham.ac.uk/projects/fastqc/).

2.2.2.5.3 Sequencing alignment (performed by TAL)

The sequence reads were aligned to the genome reference sequence of *X. tropicalis* (Joint Genome Institute assembly v4.2) using the STAR alignment software version 2.3.0e (Dobin *et al.,* 2012). For the alignment, 5 mismatches were allowed within 50 bases.

2.2.2.5.4 Statistical analysis (performed by TAL)

For normalization and identification of differentially expressed genes the R/Bioconductor environment (www.bioconductor.org) with the DESeq2 package version 1.2.10 (Anders and Huber, 2010) was used. Genes showing at least a 2-fold change and a FDR-corrected p-value < 0.05 were considered as candidate genes.

2.2.3 *X. laevis* embryo culture and micromanipulations

For detailed descriptions refer to Sive *et al.,* 2010.

10x MBS: 880 mM NaCl, 10 mM KCl, 10 mM $MgSO_4$, 25 mM $NaHCO_3$, 50 mM HEPES, pH 7.8
1x MBS: 1x MBS, 0.7 mM $CaCl_2$
5x MBS AC: 880 mM NaCl, 10 mM KCl, 10 mM $MgSO_4$, 25 mM $NaHCO_3$, 50 mM HEPES, 2.1 mM $CaCl_2$, 1.7 mM $Ca(NO_3)$, pH 7.8
Dejelly solution: 2% (w/v) L-cysteine hydrochloride in 0.1x MBS, pH8
Injection buffer: 1% ficoll in 1x MBS
Nile Blue staining solution: 0.01 (w/v) nile blue chloride, 89.6 mM Na_2HPO_4, 10.4 mM NaH_2PO_4, pH 7.8
Agarose dishes: 60 mm petri-dishes coated with 1% agarose made with 0.8x MBS AC

2.2.3.1 Stimulation of eggs

To induce the *X. laevis* female frogs to lay eggs, 1000 U of human chorionic gonadotropin (HCG, Sigma Aldrich) was injected subcutaneous into the dorsal lymph sac the evening before desired egg laying. The frogs were kept at 16°C and started egg-laying 12-24 hours after HCG injection.

2.2.3.2 Preparation of *X. laevis* testis

For *in vitro* fertilization of the laid eggs, a male *X. laevis* was sacrificed by submersion in 0.05% benzocaine for 30 min at RT. The testis was removed and stored at 4°C in 1x MBS for approximately one week.

2.2.3.3 *In vitro* fertilization

Egg-laying was stimulated by massaging the abdomen and sides of the frogs. The layed eggs were fertilized by addition of ¼ Vol. macerated testis in 1x MBS which was diluted with ¾ Vol. of H_2O. To prevent dehydration the fertilized eggs were covered in 1x MBS.

2.2.3.4 Microinjections

The jelly coat of the embryos was removed by treatment with dejelly solution and washing 3-4 times with 0.1 x MBS. The microinjections were performed in injection buffer on a cooling plate set to 12.5°C using a borosilicate glass capillary (Harvard Apparatus), which was pulled with a needle puller (PN-30, Scientific Products GmbH). The needles were back-loaded with the injection solution using microloaders (Eppendorf) and placed into a mechanical micromanipulator (M1, H. Sauer Laborbedarf) that was attached to a microinjector (PV 820, H. Sauer Laborbedarf). Depending on the experimental setup, 4 nl of the injection solution was injected animally into either one or two blastomeres of two-cell stage embryos, or into one dorsal blastomere of a four-cell stage embryos. After injection, the embryos were kept for at least one hour in injection buffer and were then transferred into 0.1x MBS and cultured at different temperatures (12.5-18°C) until the desired developmental stages were reached. The developmental stages were determined according to Nieuwkoop and Faber (1967).

2.2.3.5 *X. laevis* ectodermal explants (“animal caps”)

Ectodermal explants were excised at blastula stage (stage 8-9) in 0.8x MBS on an agarose coated petri-dishes on a cooling plate set at 12.5°C. The vitelline membrane was removed with forceps and the ectodermal explant was excised from the animal hemisphere using a Gastromaster (Xenotek Engineering, Bellville, USA) set to “yellow high” with a yellow tip. The explants were cultivated in 0.8x MBS until control sibling embryos reached the desired stage. Explants were snap frozen in liquid nitrogen and stored at -80°C until RNA isolation.

2.2.3.6 Dexamethasone treatment

To control the time point of protein activity, the coding sequence of the gene of interest was fused to the ligand binding domain of the human glucocorticoid receptor (Kolm and Sive, 1995). To induce protein activity, the fusion construct injected embryos or animal caps were cultivated in 0.1x or 0.8x

MBS containing 10 µM dexamethasone in the dark until the desired stage was reached.

2.2.3.7 β-Gal staining

10x MEM: 1 M Mops, 20 mM EGTA, 10 mM $MgSO_4$, pH 7.4 sterile filtered and stored in the dark
10x PBS: 1.8 M NaCl, 1 M KCl, 65 mM Na_2HPO_4, 18 mM KH_2PO_4, pH 7.4
Dent´s solution: 20% (v/v) DMSO in methanol
$K_3Fe(CN)_6$: 0.5 M in H_2O, stored in the dark
$K_4Fe(CN)_6$: 0.5 M in H_2O, stored in the dark
MEMFA: 4% (v/v) formaldehyde (37%) in 1x MEM
X-Gal: 40 mg/ml 5-bromo-4-chloro-3-indolyl-s-D-galactopyranoside in formamide, stored at -20°C in the dark.
X-Gal staining solution: 1 mg/ml X-Gal, 5 mM $K_3Fe(CN)_6$, 5 mM $K_4Fe(CN)_6$, 2 mM $MgCl_2$ in 1x PBS

To distinguish the uninjected from the injected side of an embryo *lacz* mRNA (*β-Gal*) was co-injected as a lineage tracer (Hardcastle *et al.,* 2000). The embryos were fixed at the desired stages for 20 min in MEMFA, washed three times for (10 min each) in 1X PBS and transferred to X-Gal staining solution. Staining took place in the dark until sufficient staining was observed (20-30 min). The reaction was stopped by washing three times (10 min each) with 1x PBS followed by fixation for 25 min in MEMFA. Finally, the embryos were dehydrated by washing several times in absolute ethanol and stored at -20°C. For pH3 staining and fluorescent immunostaining, the embryos were dehydrated in absolute methanol, fixed in Dent's fix for at least 24 hours at -20°C and stored in absolute methanol at
-20°C.

2.2.4 Whole mount *in situ*-hybridization (WMISH)

10X PBS: 1.8 M NaCl, 1 M KCl, 65 mM Na_2HPO_4, 18 mM KH_2PO_4, pH 7.4
20X SSC: 3 M NaCl, 0.3 M NaCitrate, pH 7.2 - 7.4
5X MAB: 500 mM maleic acid, 750 mM NaCl, pH 7.5

Antibody solution: 2% Boehringer Mannheim Blocking reagent (BMB), 20% heat treated horse serum (Gibco), 1:2000 dilution of anti-digoxigenin or anti-fluorescein antibody coupled to alkaline phosphatase (Roche) in 1X MAB
APB: 100 mM Tris-HCl, pH 9.0, 50 mM $MgCl_2$, 100 mM NaCl,
0.1% TWEEN-20
BCIP: 50 mg/mL in 100% dimethylformamide; stored at -20°C
Bleaching solution: 50% formamide, 1-2% H_2O_2 in 5x SSC
Color reaction solution: 80 µg/ml NBT, 175 µg/ml BCIP in APB
EtOH series: 100%, 75%, 50% ethanol in H_2O, 25% ethanol in PTw
Hybridization Mix (Hyb Mix): 50% formamide, 1 mg/ml, Torula-RNA, 10 µg/ml Heparin, 1X Denhardt's, 0.1% Tween-20, 0.1% CHAPS, 10 mM EDTA in 5X SSC
MeOH series: 100%, 75%, 50%, 25% methanol in H_2O
MAB/BMB: 2% BMB in 1X MAB
MAB/BMB/HS: 2% BMB, 20% heat-treated horse serum in 1X MAB
NBT: 100 mg/mL in 70% dimethylformamide; stored at -20°C
PTw: 0.1% Tween-20 in 1X PBS
PTw/FA: 4% (v/v) formaldehyde in PTw
Proteinase K: 5 µg/ml proteinase K (Merck) in 0.1X PBS
RNAse Solution: 10 µg/ml RNAse A, 0.01 U/ml RNAse T1 in 2X SSC
Triethanolamine: 0.93 triethanolamine in H_2O, pH 7.5

To visualize temporal and spatial gene expression, WMISH was performed as previously described (Harland, 1991; Hollemann and Pieler, 1999) using digoxigenin-UTP or fluorescin-UTP labelled antisense RNA. All steps were performed with mild shaking at room temperature, if not otherwise noted.

The embryos were rehydrated in an ethanol series (75%, 50%, and 25%) and washed four times for 5 min in PTw. To make the surface of the embryo penetrable for the antisense RNA probe, they were treated with PTw/proteinase K solution (10 µg proteinase K/ml PTw). Stage 14 embryos were treated for 6 min while Stage 27-28 embryos were treated for 17 minutes. To stop the proteinase K treatment the embryos were washed twice for 5 min with triethanolamine. To prevent unspecific binding of the antisense RNA probe, free amino-acid ends were blocked by addition of 25 µl acetic anhydride to the

triethanolamine. After incubation for 5 min, an additional 25 µl acetic anhydrite was added to the triethanolamine. Following acetylation, the embryos were washed two times for 5 min in PTw, refixed for 20 min in PTw/FA and finally washed 5 times for 5 min in PTw. For pre-hybridization, the embryos were incubated with Hyb Mix for 5 h at 65°C. After pre-hybridization the embryos were incubated overnight at 65°C in Hyb Mix containing the antisense RNA probe.

The following day, the antisense RNA probe containing Hyb Mix was exchanged with fresh Hyb Mix for 10 min at 65°C followed by washing three times for 15 min each at 65°C with 2x SSC. To remove remaining non-hybridized antisense RNA probe, the embryos were treated with RNase solution at 37°C and afterwards washed once in 2x SSC for 5 min at RT, twice in 0.2x SSC at 65°C and two times for 15 min at RT in 1x MAB. To avoid unspecific binding of the antibody, the embryos were blocked for 15 min in MAB/BMB and afterwards for 40 min in MAB/BMB/HS. The embryos where then incubated overnight at 4°C in the antibody solution.

The next day, the embryos were washed at least 5 times for 10 min in 1x MAB. For the color reaction, the embryos were first washed twice for 5 min at 4°C in fresh APB and then transferred to the color reaction solution. The reaction took place at 4°C, in the dark, until staining was sufficient. To stop the color reaction and remove background staining, the embryos were dehydrated in 100% methanol until no background color leached out of the embryos. For rehydration the embryos were incubated in sequentially in 100%, 75%, 50% and 25% methanol and afterwards fixed in MEMFA for 15 min. The embryos were stored indefinitely in MEMFA. To remove the pigmentation, the embryos were incubated in bleaching solution until pigmentation was gone and afterwards washed two times in 5x SSC followed by fixation and storage in MEMFA.

2.2.5 Phosphorylated Histone 3 (pH3) staining

10X PBS: 1.8 M NaCl, 1 M KCl, 65 mM Na_2HPO_4, 18 mM KH_2PO_4, pH 7.4
1° AB solution: 20% horse serum, 5% DMSO, 1/270 dilution rabbit anti-pH3 antibody (Biomol)
2° AB solution: 20% horse serum, 5% DMSO, 1/750 dilution goat anti-rabbit IgG horseradish peroxidase-coupled secondary antibody (Sigma)

APB: 100 mM Tris-HCl, pH 9.0, 50 mM $MgCl_2$, 100 mM NaCl,
0.1% tween-20
Color reaction solution: 80 µg/ml NBT, 175 µg/ml BCIP in APB
MeOH series: 100%, 75%, 50%, in H2O and 25% methanol in 1xPBS
PBS-TB: 0.05% Tween-20, 0.2% BMB in 1x PBS
PBS-TBN: 0.3 M NaCl in PBS-TB
Proteinase K: 5 µg/ml Proteinase K (Merck) in 0.1X PBS

To mark mitotically active cells in whole embryos, phosphohistone H3 staining was performed as previously described (Dent *et al*., 1989). Embryos were fixed in Dent's fix after β-gal staining and rehydrated in a MeOH series to PBS. After Proteinase K treatment for 10 min, the embryos were washed two times in PBS-TB for 10 min at RT. For the first antibody reaction, the embryos were pre-incubated in PBS with 20% horse serum. After 2 h at RT the embryos were transferred to the 1° AB solution and incubated overnight at 4°C. The next day, the embryos were washed twice with PBS-TB for 2 h at RT and afterwards with PBS-TB overnight at 4°C. The following day, the embryos were washed for 2 h with PBS-TBN, 5 min with PBS-TB and overnight at 4°C in 2° AB solution. The next day, the embryos were washed twice in PBS-TB for 30 min, once for 30 min in PBS-TBN, once in PBS-TB for 5 min and then washed overnight in PBS-TB at 4°C. For the color reaction the embryos were first washed with PBS-TB for 10 min, twice in fresh APB for 5 min at 4°C and afterwards transferred to the color reaction solution. When the desired staining was reached, the embryos were dehydrated and stored in 100% methanol at -20°C.

2.2.6 Fluorescent immunostaining

Blocking solution:
Murray's clear: benzyl benzoate/benzyl alcohol, 2/1
TBS: 50mM Tris-HCl, 150 mM NaCl, pH 7.6
TBST: 0.05 % Tween-20 in TBS

Fluorescent immunostaining was performed to detect acetylated tubulin, which marks the axons of neurons (Friedmann *et al.,* 2012). After β-gal staining, embryos were fixed overnight in Dent's fix and dehydrated for at least 24 h in

100% methanol. For rehydration the embryos were subjected to a MeOH series to TBS. To prevent nonspecific antibody binding, the embryos were blocked for 30 min in blocking solution at RT. The primary antibody was added directly to the blocking solution (anti-acetylated tubulin, 1/200, Sigma-Aldrich) and incubated overnight at 4°C. The following day, the embryos were washed at RT for 3 h in TBST that was exchanged every 30 min. For the second antibody reaction, the embryos were blocked in blocking solution for 15 at RT. The secondary antibody (goat anti-mouse Alexa 488, 1/300, Invitrogen) was added directly to the blocking solution and incubated overnight at 4°C. The next day, the embryos were washed at RT for 3 h in TBST that was exchanged every 30 min. The embryos were dehydrated in 100% methanol and cleared in Murray's clear for confocal imaging on a LSM780 (Zeiss).

2.2.7 Luciferase reporter assay

For luciferase reporter assay two cell stage embryos were injected animally into both blastomeres with 100 pg Atf2-Firefly-luciferase reporter (van der Sanden *et al.,* 2004) or 200 pg TOPFlash-Firefly-luciferase reporter (Fujimi *et al.,* 2011) together with 10 pg Renilla luciferase reporter (Promega) for normalization. The reporters were injected alone or co-injected with either 500 pg MT-*wnt5b*, 100 pg *wnt8a*-MT or 500 pg *prdm14*-GR respectively. At least six injected embryos at stage 14 were collected per sample and two samples were tested for one condition. For measurement of the Firefly and Renilla luciferase activity the Dual Luciferase Reporter Kit (Promega) and a Centro LB960 luminometer (Berthold Technologies) were used according to manufacturer's protocols.

2.2.8 Vibratome sectioning

Gelatin/Albumin: 4.9 mg/ml gelatin albumin was heat dissolved in PBS at 60°C, followed by the addition of 0.3 g/ml bovine serum albumin and 0.2 mg/ml sucrose. The solution was sterile filtered using 0.45 µm filter (Sartorius) and stored at -20°C.

Mowiol: 5 g Mowiol was dissolved in 20 ml PBS and stirred overnight. Afterwards 10 ml glycerol was added and the solution again stirred overnight. After centrifugation for 30 min at 20,000 g, the undissolved Mowiol was

collected and removed and the supernatant was set to pH 7. The solution was aliquoted and stored at -20°C.

For sectioning the embryos were mounted in gelatin/albumin, which was solidified by addition of glutaraldehyde. Sections of 30 µm were cut using a Leica VT1000M vibratome and mounted on a glass slide in Mowiol.

2.2.9 Protein standard methods

2.2.9.1 SDS-polyacrylamide gelelectrophoresis (SDS-PAGE)

10x Laemmli buffer: 250mM Tris, 2.5 M glycine, 0.1% SDS
2x SDS loading buffer: 100 mM Tris-HCl pH 6.8, 4% (w/v) SDS, 0.2% (w/v) bromophenol blue, 20% (v/v) glycerol, 200 mM β-mercaptoethanol

Proteins were separated according to their molecular weight by SDS-polyacrylamide gel electrophoresis (Laemmli, 1970). For denaturing of the proteins, samples were diluted with 2x loading buffer and boiled for 3 min at 95°C. For separation of the proteins, a 10% SDS gel was prepared according to standard protocols (Sambrook and Russel, 2001). The gel electrophoresis was performed in 1 x Laemmli buffer and was started with a voltage of 80 V. As soon the samples entered the separating gel the voltage was turned up to 200 V. To determine the molecular weight of the proteins, a standard protein marker was used (Page Ruler Plus Prestained Protein Ladder, Fermentas).

2.2.9.2 Western blotting

Blocking solution: 5% (w/v) dry, non-fat milk powder in TBST
TBS: 50 mM Tris, 150 mM NaCl, pH 7.6
TBST: 0.05 % Tween-20 in TBS

After separation of the proteins by SDS-PAGE, the proteins were transferred to a nitrocellulose membrane by semi-dry blotting for 1 h in transfer buffer at 13-15 V (Sambrook and Russel, 2001; Towbin *et al*., 1979). After the transfer of the proteins the membrane was blocked in blocking solution for 1 h at RT. Incubation with the primary antibody was carried out overnight at 4°C in

blocking solution. The following day, the membrane was washed 3 times for 10 min in blocking solution. The secondary antibody, which was coupled to a fluorescent IRdye (LI-COR), was applied to the blocking solution and the membrane was incubated for 1 hour at RT and afterwards washed twice for 10 min with blocking solution and once for 10 min with TBST at RT. To detect the fluorescent signals the LI-COR Odyssey Infrared Imaging system was used.

Name	Company	Host	Type	Clonality	dilution
anti-HA	Convance	mouse	primary	monoclonal	1:1000
anti-GR	Santa Cruz	rabbit	primary	polyclonal	1:200
anti-GAPDH	Abcam/Biozol	rabbit	primary	polyclonal	1:2500
anti-mouse 800 CW IRdye	LI-COR	goat	secondary	polyclonal	1:15000
anti-rabbit 680 RD IRdye	LI-COR	goat	secondary	polyclonal	1:15000

Table 2.5 Summary of antibodies for western blot analysis

3. Results

3.1 Temporal and spatial expression analysis of *X. laevis prdm14*

To gain insight into the function of *prdm14* during early *X. laevis* embryogenesis, a detailed expression analysis was performed. The temporal expression of *prdm14* was evaluated by semi-quantitative RT-PCR analysis using total RNA from staged embryos. As shown in Figure 3.1A, *prdm14* transcripts are maternally provided and are maintained at high levels throughout tadpole stages.

The spatial expression of *prdm14* was then determined by whole mount *in situ* hybridization. *Prdm14* transcripts are detected in the animal hemisphere from early cleavage stages (stage 5, Fig. 3.1B) to blastula stages (stage 8, Fig. 3.1C). At early mid-gastrula stages (stage 10.5, Fig. 3.1D), *prdm14* expression is confined to the dorsal ectoderm, which marks the prospective neuroectoderm. As shown in the sagittal section, *prdm14* transcripts are restricted to the deep layer of the ectoderm (Fig. 3.1D'). At the end of gastrulation (stage 11.5, Fig. 3.1E), *prdm14* is broadly expressed throughout the dorsal ectoderm with enrichment in the lateral domains, which most likely corresponds to the prospective neural plate border. At stage 12.5, *prdm14* transcripts are present throughout the anterior neural plate (Fig. 3.1F). Posteriorly, the expression becomes refined to three longitudinal domains on both sides of the midline, which prefigures the territories of primary neurogenesis. Strong expression is observed in the intermediate and lateral domains, while the expression in the medial domain is weak (Fig. 3.1F). From stage 13 to 15, *prdm14* expression in the posterior neural plate is maintained and becomes stronger in the medial stripe (Fig. 3.1G-I). As seen in transversal section of a stage 15 embryo (Fig. 3.1I'), the expression of *prdm14* is restricted to the deep layer of the neuroectoderm, where the primary neurons arise (Hartenstein, 1989). At stage 13, the expression becomes restricted to the anterior neural plate border, the trigeminal-profundal placode and to a horseshoe shaped domain, which will give rise to the ventral midbrain (Eagleson and Harris, 1990) (Fig. 3.1G).

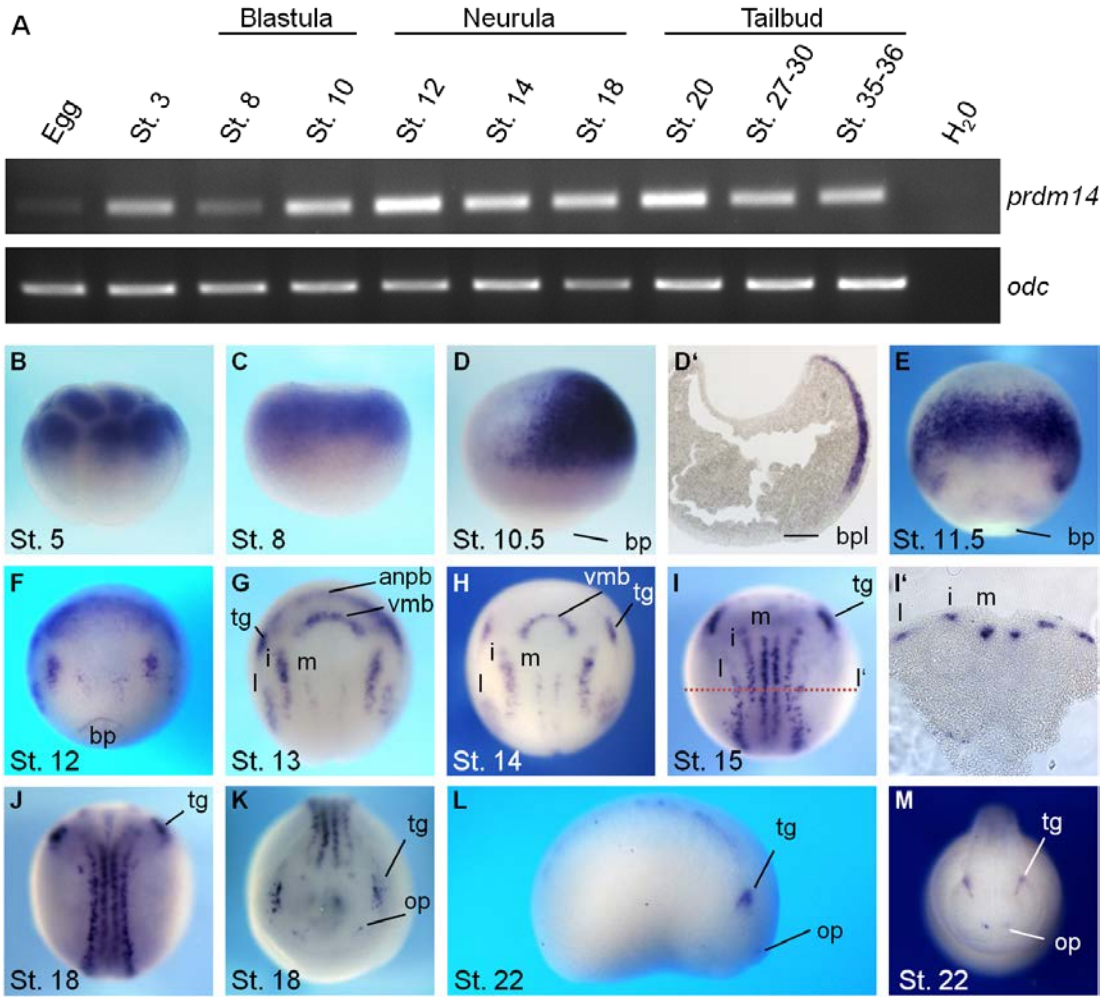

Fig. 3.1 Temporal and spatial expression analysis of *prdm14* in *X. laevis* embryos. (A) Prdm14 is maternally expressed. Temporal *prdm14* expression analysis by semi-quantitative RT-PCR at indicated stages. Expression levels were shown by *odc* expression. **(B-M)** *Prdm14* is expressed throughout the developing nervous system. Spatial expression analysis of *prdm14* in *X. laevis* embryos by whole mount *in situ* hybridization. **(B-D)** Lateral view of the embryos, animal up. **(D')** Sagittal section of embryo shown in D. **(E-J)** Dorsal view of embryos, anterior up. **(I')** Transverse section at indicated level of embryo shown in I. **(K, M)** Anterior view of embryo, dorsal up. **(L)** Lateral view of embryo, anterior right, dorsal up. anpb, anterior neural plate border; bp, blastoporus; bpl, blastoporus lip; i, intermediate; l, lateral; m, medial; op, otic placode; tg, trigeminal-profundal placode; vmb, ventral midbrain

During neurulation, the expression of *prdm14* is maintained in the posterior primary neurons, the trigeminal-profundal placode and olfactory placodes (Fig. 3.1J-M). At stage 26, *prdm14* transcripts are detected in the trigeminal placodes, otic vesicles, olfactory placodes and throughout the spinal cord (Fig 3.2A). Transverse sections show that *prdm14* transcripts are present in the inner segment of the otic vesicle and in the marginal zone of the neural tube where postmitotic neurons reside (Fig. 3.2A'-A''') (Bellefroid *et al.,* 1996). In the anterior neural tube, *prdm14* expression is restricted to two distinct domains (Fig. 3.2A''), while more posteriorly the expression spans the entire marginal zone of the neural tube (Fig. 3.2A'''). Double whole mount *in situ* hybridization

for *prdm14* and *tubb2b* shows that the expression domains for both genes overlap in the marginal zone throughout the neural tube, confirming that *prdm14* indeed is expressed in postmitotic neurons (Fig. 3.2B-B'').

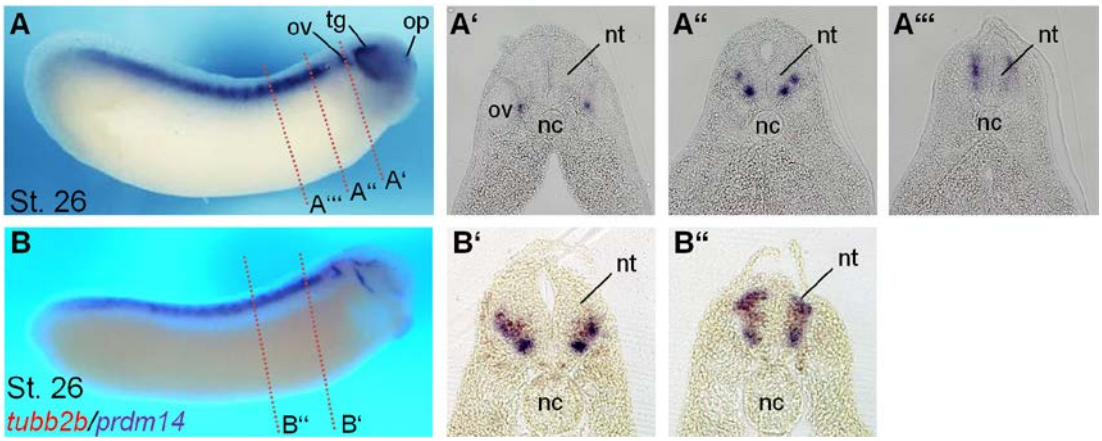

Fig. 3.2 *Prdm14* is expressed in the marginal zone of the neural tube. (A-B'') Spatial expression analysis of *prdm14* in *X. laevis* stage 26 embryos by whole mount *in situ* hybridization. **(A, B)** Lateral view of embryo (anterior right). **(A'-A''')** Transverse sections at indicated levels of embryo shown in A. **(B-B'')** Double whole mount *in situ* hybridization of stage 26 embryos for *tubb2b* (red) and *prdm14* (purple). **(B'-B'')** Transverse sections at indicated levels of embryo shown in B. nc, notochord; nt, neural tube; op, olfactory placode; ov, otic vesicle; tg, trigeminal profundal placode

Taken together, the expression of *prdm14* is strongly indicative for a role during the early development of the nervous system. While *prdm14* is clearly present in the post-mitotic neurons of the neural tube, it is also expressed in the neural plate when the proneural genes specify the primary neurons. To further clarify the timing of *prdm14* expression in relationship to the proneural genes *neurog1* and *neurog2*, to which *prm14* is most similar, a comparative expression analysis was performed. Both *prdm14* and *neurog2* are expressed throughout the prospective neuroectoderm at the onset of gastrulation (stage 10), with the expression of *neurog2* being weaker and located closer to the blastopore (Fig. 3.3). At the end of gastrulation (stage 12), transcripts of *neurog1* and *neurog2* are detectable in the posterior neural plate in three distinct domains prefiguring the territories of primary neurogenesis. At this stage *prdm14* transcripts are only present in the medial and lateral stripes of primary neurogenesis and the anterior neural plate. At stage 14, *prdm14, neurog1* and *neurog2* are all expressed in the trigeminal-profundal placodes as well as in the three bilateral longitudinal domains of primary neurogenesis. However, the expression of *prdm14* and *neurog1* are strikingly similar. They are both expressed in the future ventral midbrain, and compared to *neurog2*, their

expression in the longitudinal domains is more refined and extends more anteriorly. During neurulation (stage 18) all transcripts are present in the neural fold and in the trigeminal-profundal placodes.

In summary, *prdm14* differs from the analyzed proneural genes as it is expressed early and strongly in the anterior neural plate. In the territories of primary neurogenesis of the posterior neural plate, the expression of *neurog2* prefigures that of *prdm14*.

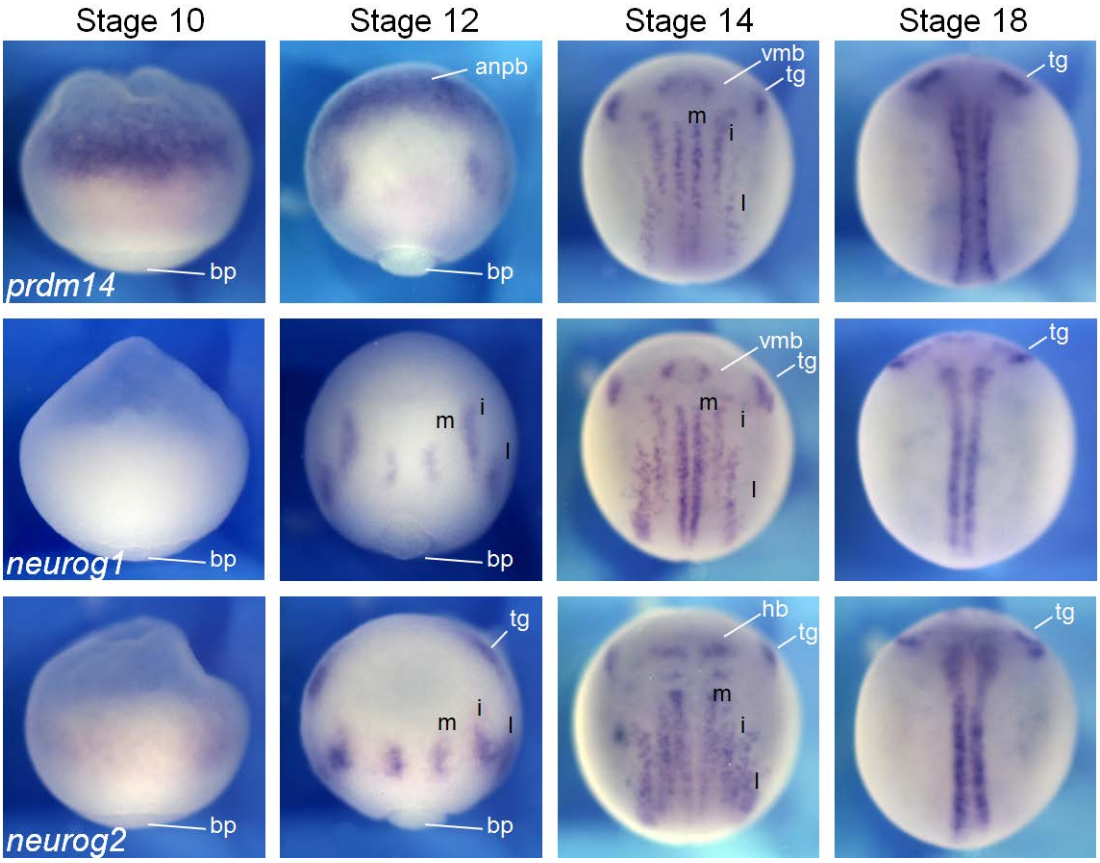

Fig. 3.3 *Prdm14*, *neurog1* and *neurog2* are co expressed in territories of primary neurogenesis. Comparative expression analysis of stage matched embryos. Stage 10: lateral view, animal up; Stage 12-18: dorsal view, anterior up. anpb, anterior neural plate border; bp, blastoporus; hb, hindbrain; i, intermediate; l, lateral; m, medial; tg, trigeminal-profundal placode; vmb, ventral midbrain

The temporal expression of *prdm14* in the neural plate and in the outer mantel layer of the neural tube suggests a function for Prdm14 downstream of Neurog2. Therefore, the regulation of *prdm14* by the proneural transcription factor Neurog2 was analyzed (Ma *et al.,* 1996). *Neurog2* mRNA was injected together with *β-gal* mRNA to indicate the cells that have received the injected material, into one blastomere of two-cell stage embryos. The embryos were analyzed by whole mount *in situ* hybridization at neural plate stage (Fig. 3.4A).

As anticipated, microinjection of *neurog2* mRNA strongly induces expression of the postmitotic neuronal marker *tubb2b* (also known as *n-tubulin*) in the deep layer of the ectoderm (n= 13, 100% ectopic expression) (Fig. 3.4 B-B') (Ma *et al.,* 1996, Chalmers *et al.,* 2002). Strong ectopic expression was similarly observed for *prdm14* (n= 28, 100% ectopic expression) (Fig. 3.4D-D').

Prdm14 was identified as a putative target gene of the repressor protein Hes5.1, which itself is a target of the Notch pathway (Klisch, 2006, Kiyota *et al.,* 2001). Therefore, the influence of Notch signaling on *prdm14* expression was also analyzed. mRNA encoding for the Notch intracellular domain (*NICD*), which is the constitutively active version of the Notch receptor, was injected into one blastomere of two-cell stage embryos. Consistent with the known activity as a negative regulator of primary neurogenesis (Chitnis and Kintner, 1996), *NICD* mRNA injection resulted in the inhibition of *tubb2b* on the injected side of the embryo (n= 19, 100% downregulated). *NICD* also strongly inhibited the expression of *prdm14* (n= 31, 90% downregulated) (Fig. 3.4C-E). Taken together, the expression and regulation of *prdm14* suggests a role for *prdm14* in primary neurogenesis in *X. laevis.*

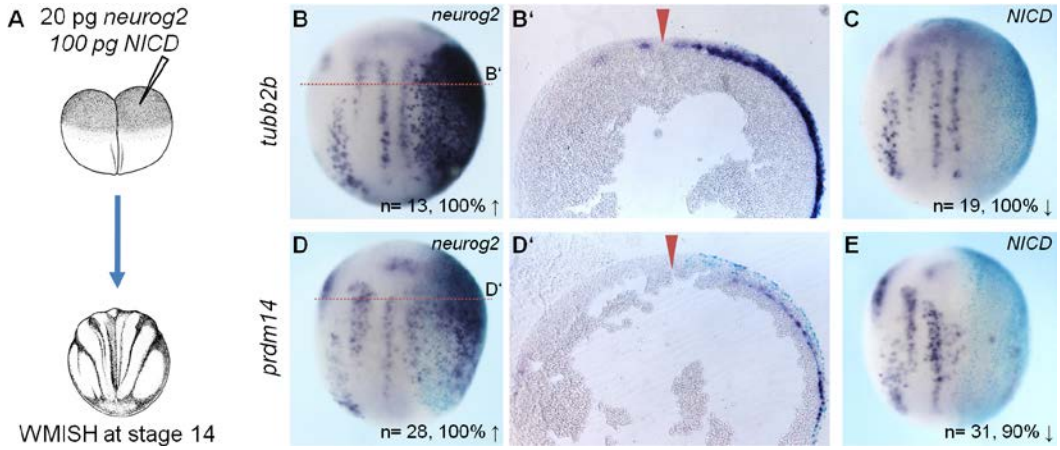

Fig. 3.4 *Prdm14* expression is regulated by key regulators of neurogenesis. (A) *Neurog2* (20 pg) or *NICD* (100 pg) mRNA together with *β-Gal* (75 pg) mRNA (light blue staining) were injected into one blastomere of a two-cell stage embryo. **(B-E)** Gene expression was analyzed by whole mount *in situ* hybridization using markers indicated on the left side. The injected side is on the right, dorsal view, anterior up. **(B', D')** Transverse sections at indicated levels of embryo shown in B and D, respectively. Red arrows indicate the midline.

3.2 *Prdm14* gain of function

To gain further support for a role of *prdm14* during *X. laevis* primary neurogenesis, a gain of function approach was performed. mRNA encoding a HA-tagged version of *prdm14* (500 pg) was microinjected into one of two blastomeres and the influence on neuronal differentiation evaluated by whole mount *in situ* hybridization. At neural plate stage, the expression of *tubb2b* was inhibited on the *prdm14* mRNA injected side of the embryo (n= 36, 64% downregulated) (Fig. 3.5B). To ensure that the observed phenotype was not due to an unspecific effect, *gfp* mRNA was injected at the same concentration as *prdm14*-HA. Microinjection of *gfp* mRNA did not affect *tubb2b* expression, which suggested that any observed phenotypes could be attributed to the injected *prdm14* mRNA (Fig. 3.5A).

The inhibition of neuronal differentiation by *prdm14* was only transient, as in the neural tube of tailbud stage embryos the expression of *tubb2b* was recovered (Fig. 3.5C-D'). Since the transient inhibition may be due to low protein stability, a GR-tagged version of *prdm14* was generated, as GR-fusion proteins often exhibit an increased effectiveness due to higher protein stability (Kolm and Sive, 1995). The mRNA encoding for *prdm14*-GR was injected into one blastomere of two-cell stage embryos and the activity of the fusion protein was induced by addition of dexamethasone (dex) at the four-cell stage (stage 3). Embryos that were injected with *prdm14*-GR mRNA and treated with dex showed an inhibition of *tubb2b* at the neural plate stage. Inhibition of *tubb2b* was not observed in injected and untreated embryos, demonstrating that Prdm14-GR is indeed hormone inducible (Fig. 3.5E). The phenotype induced by *prdm14-GR* mRNA is similar to that of *prdm14-HA* mRNA injected embryos (n= 39, 64% downregulated). However, the inhibition of neuronal differentiation was observed at a higher frequency (n= 17, 100% downregulated) (Fig. 3.5F). Moreover, Prdm14-GR induced ectopic *tubb2b* expression in the non-neural ectoderm of tailbud stage embryos (n= 23, 83% ectopic expression) (Fig. 3.5G-H', red arrows). In the transverse section, *tubb2b* expression was strongly increased and the entire dorsal region of the neural tube was enlarged compared to the uninjected side (Fig. 3.5H'). The strongest expansion was observed in the dorsal half of the neural tube. Interestingly, a thickening of mesenchymal tissue on the injected side of tailbud stage embryos was also

observed, which was more prominent in the *prdm14*-GR injected embryos than in the *prdm14*-HA injected ones (Fig. 3.5D', H', black brackets).

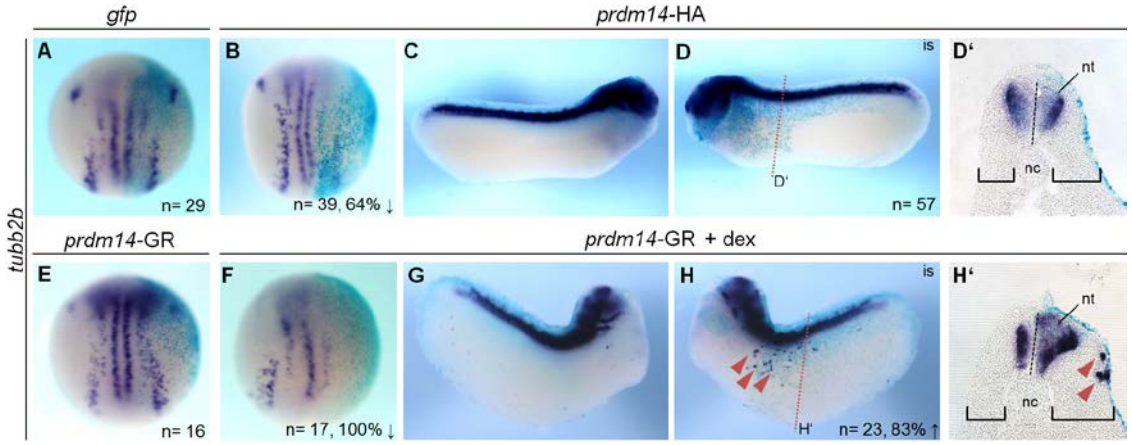

Fig. 3.5 *Prdm14*-GR overexpression induces stronger phenotypes. (A-H') ** Indicated mRNA was injected together with *β-Gal* (75 pg) mRNA (light blue staining) into one blastomere of a two-cell stage embryo. *tubb2b* expression was analyzed by whole mount *in situ* hybridization. Injected side is always to the right. **(A, B, E, F) Neural plate stage, dorsal view, anterior up; **(C, D, G, H)** tailbud stage, lateral view, dorsal up; **(A)** 500 pg MT-*gfp* mRNA; **(B-D')** 500 pg *prdm14*-HA; **(E)** 500 pg *prdm14*-GR; **(F-H')** 500 pg *prdm14*-GR, embryos were treated from four-cell stage on with dex; **(D', H')** Transverse sections at indicated levels of embryo shown in D and H respectively. Black brackets indicate width of mesenchymal tissue at the level of the notochord. Dashed line indicates midline of the neural tube.is, injected side; nt, neural tube; nc, notochord

3.3. Prdm14 promotes proliferation and the expansion of neural progenitors

Prdm14 overexpression at neural plate stage inhibited the expression of the postmitotic neuron marker *tubb2b* (Fig. 3.5B, F) and at tailbud stages resulted in an enlarged neural tube and ectopic neuronal differentiation (Fig. 3.5H'). To analyze if these effects were caused by the expansion of progenitor cells, the effect of *prdm14*-GR overexpression on the neural plate marker *sox2* was evaluated, as it is a definitive marker of neural progenitors (Graham *et al.,* 2003; Ellis *et al.,* 2004) (Fig. 3.6A). Microinjection of *prdm14*-GR results in the expansion of the *sox2* expression domain on the injected side of the embryo (n= 20; 75% increased) (Fig. 3.6B).

To determine if the expansion of *sox2* expression by *prdm14-GR* is the result of increased proliferation, the number of mitotically active cells in the dorsal ectoderm was quantified by staining for phosphorylated histone 3 (pH3) (Dent et al., 1989) (Fig. 3.6C). To quantify the number of mitotically active cells, three embryos were sectioned and the pH3 positive cells were counted in the dorsal halves of 15 consecutive sections. The number of mitotically active cells

in the neuroectoderm was increased almost two-fold on the *prdm14*-GR injected side compared to the uninjected side (Fig. 3.6C'-D). These results suggest that *prdm14* promotes the proliferation of progenitor cells, resulting in the inhibition of neuronal differentiation at neural plate stage and in an enlarged neural tube in later stages.

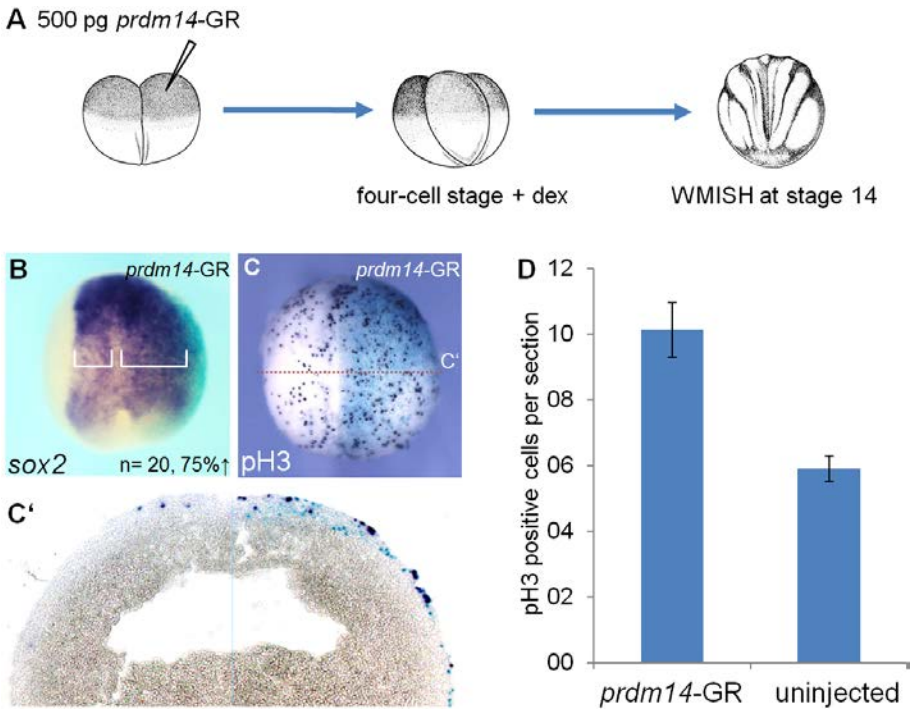

Fig. 3.6 *Prdm14*-GR overexpression promotes proliferation. (A) *Prdm14-GR* (500 pg) mRNA together with *β-Gal* (75 pg) mRNA (light blue staining) were injected into one blastomere of a two-cell stage embryo. Embryos were treated from four-cell stage on with dex. **(B-C)** Gene expression was analyzed at stage 14 by whole mount *in situ* hybridization using markers indicated on the bottom left side. The injected side is on the right, dorsal view, anterior up. **(B)** The white brackets indicate width of expression domain. **(C')** Transverse section at indicated levels of embryo shown in C. **(D)** The graph shows the statistical evaluation of 15 consecutive sections of three embryos based on the number of pH3 positive cells in the dorsal half on the injected and uninjected site as indicated in the cross-section C'. Error bars represent the standard error of the mean of two independent experiments (+/-SEM).

3.4 Prdm14 promotes ectopic sensory neuron formation

Prdm14-GR induces ectopic neurons in the non-neural ectoderm of tailbud stage embryos (Fig. 3.5G-H') raising the question as to which neuronal subtype they belong to. As the dorsal neural tube, which arises from the neural plate border (NPB), was strongly expanded, the expression of *tlx3* was analyzed, which is expressed in the NPB and the dorsally located glutamatergic Rohon-Beard sensory neurons (Patterson and Krieg, 1999; Rossi *et al*., 2009). Whole mount *in situ* hybridizations of embryos overexpressing *prdm14*-GR showed ectopic expression of *tlx3* in the non-neural ectoderm (n= 22; 76% ectopic staining) (Fig. 3.7C, red arrows) and an increased expression in the dorsal neural tube (Fig. 3.7C', red arrows). The glutamatergic neurotransmitter identity of these neurons was further supported by the ectopic expression of the vesicular glutamate transporter 1 *slc17a7* (*vglut1*) (n= 25; 80% ectopic staining) (Fig 3.7D-E'). To determine if other ectopic neuronal subtypes are induced by Prdm14-GR, the expression of *mnx1* (also known as *hb9*) was analyzed, which is expressed in cholinergic motor neurons in the most ventral aspect of the neural tube (Saha et al., 1997). Ectopic *mnx1* expression was never observed in the non-neural ectoderm. Nonetheless, an expansion of the endogenous expression domain was observed, which may be the result of an overall enlargement of the neural tube caused by *prdm14*-GR overexpression (Fig. 3.7F-G').

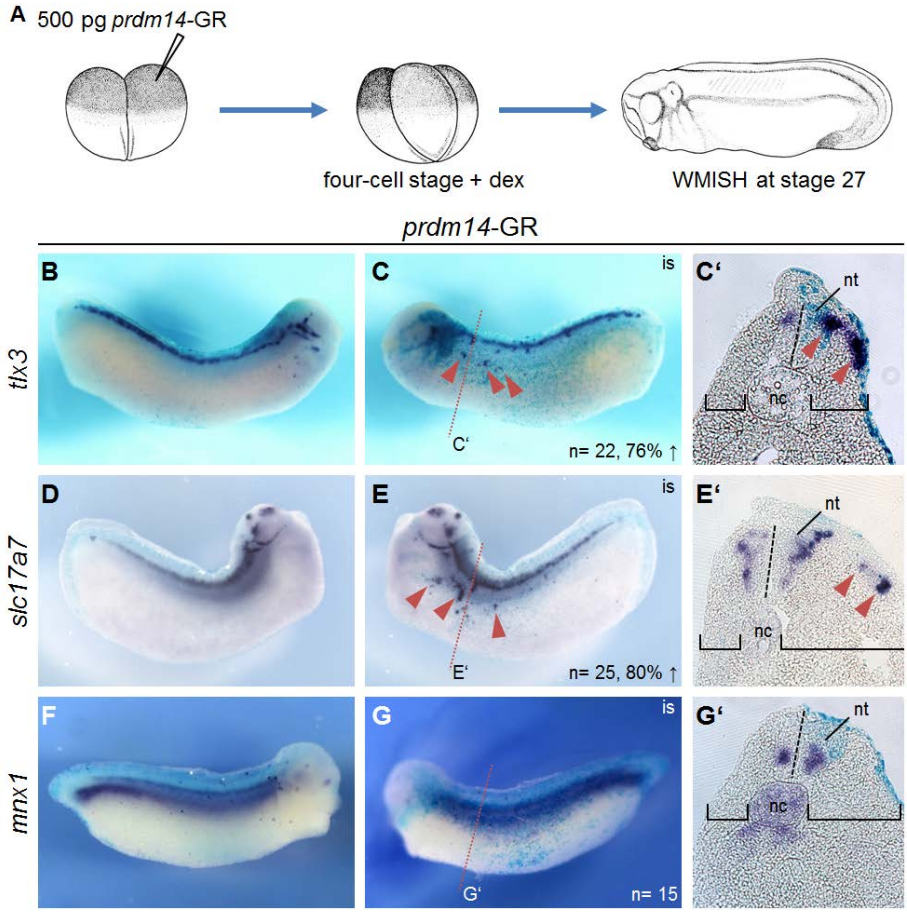

Fig. 3.7 *Prdm14*-GR overexpression promotes sensory neurons in tailbud stage embryos. **(A)** *Prdm14*-GR (500 pg) mRNA together with *β-Gal* (75 pg) mRNA (light blue staining) were injected into one blastomere of a two-cell stage embryo. Embryos were treated from four-cell stage on with dex. **(B-G')** Gene expression was analyzed at stage 27 by whole mount *in situ* hybridization using markers indicated on the left. The injected side is on the right, lateral view. is, injected side **(C', E', G')** Transverse sections at indicated levels of embryo shown in C, E, G respectively. Black brackets indicate width of mesenchymal tissue at the level of the notochord. Dashed line indicates midline of the neural tube. nt, neural tube; nc, notochord

To determine if *prdm14* overexpression is sufficient to induce glutamatergic sensory neurons in pluripotent cells, the animal cap assay was used. Control and *prdm14*-GR mRNA-injected embryos were treated with dex at stage 3 and animal caps were isolated from blastula stage embryos (Fig. 3.8A). At the equivalent of neural plate stage (stage 14) and tailbud stage (stage 27) total RNA was isolated and analyzed by RT-PCR. Similar to the phenotype in embryos, at the equivalent of tailbud stages, *tubb2b* as well as *tlx3* were induced. These markers were not observed in *prdm14*-GR mRNA-injected animal caps not treated with dex, or control uninjected caps treated with dex. To elucidate if *prdm14* directly promotes neural differentiation or requires the activity of proneural genes, the expression of *neurog2* was analyzed. At the equivalent of stage 14, *neurog2* is induced in caps expressing Prdm14-GR. The

absence of *tubb2b* at the equivalent of neural plate stage is similar to the transient inhibition of neurogenesis observed in the embryos. The regulation of *neurog2* by Prdm14-GR is unexpected as *neurog2* strongly promotes *prdm14* (Fig. 3.4B), suggesting a positive feedback loop between these two factors. Hence, active Prdm14-GR is able to promote neuronal differentiation in whole embryos as well as animal caps.

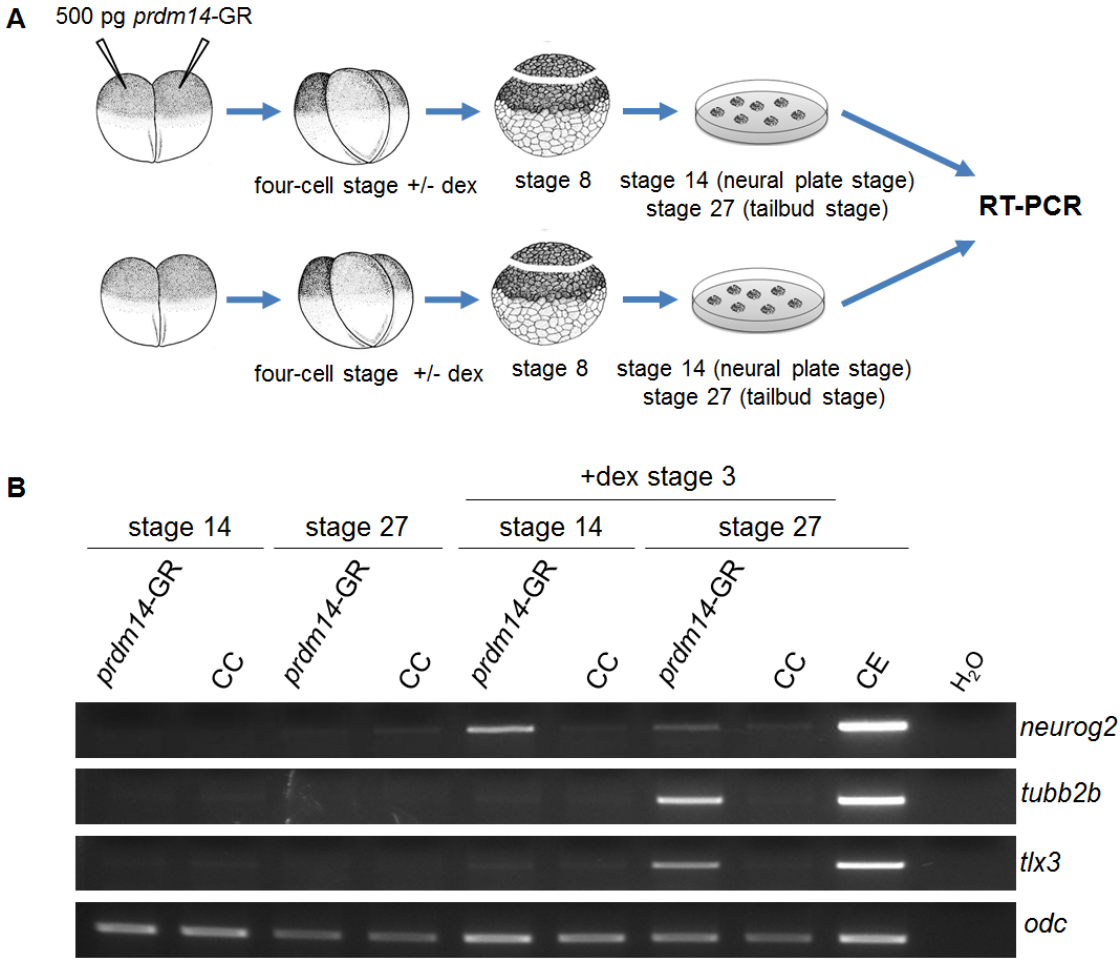

Fig. 3.8 *Prdm14*-GR overexpression activates sensory neuron marker *tlx3* in animal caps. **(A-B)** *Prdm14*-GR (500 pg) mRNA was injected into both blastomeres of a two-cell stage embryo. Control and *prdm14*-GR mRNA-injected embryos were treated with dex from four-cell stage on and animal caps were isolated from blastula stage embryos. At the equivalent of neural plate stage (stage 14) and tailbud stage (stage 27) total RNA was isolated and analyzed by RT-PCR using markers indicated on the right. Expression levels were shown by *odc* expression.

3.5 Knock down of Prdm14

To further analyze the role of Prdm14 in the regulation of neuronal differentiation, loss of function studies were performed. Antisense morpholino oligonucleotides were proven as an effective tool in *X. laevis* for the inhibition of gene function (Heasman *et al.,* 2000; Nutt *et al.,* 2001; Heasman, 2002). However, their use in *X. laevis* is complicated by the fact that *X. laevis* is allotetraploid and therefore redundancies might exist. For *prdm14* two sequence-related paralogs in *X. laevis* exists, *prdm14a* and *prdm14b*. In order to efficiently knock down the expression of *prdm14*, two splicing morpholinos (SpMO) were simultaneously used to disrupt the splicing of *prdm14a* and *prdm14b.* Both SpMOs target the exon1-intron1 boundary to prevent the splicing of intron1 (Fig. 3.9A-B). If intron1 is retained, only a truncated protein should be translated, as the intron1 contains a stop codon. The resulting truncated Prdm14 proteins would have 208 amino acids (Prdm14a) and 210 amino acids (Prdm14b), and would not contain the PR and Zn finger domains (Fig. 3.9C).

To test the specificity and function of the SpMOs, they were injected alone or together at increasing concentrations (5, 10, 25 ng) into both blastomeres of a two-cell stage embryo. The embryos were collected at stage 14 and RT-PCR analysis was performed using primers which bind within exon1 and exon2 of *prdm14a* and *prdm14b*. Knock down of *prdm14* by both SpMOs led to a concentration-dependent upward shift of the amplicon bands indicating a larger size (Fig. 3.9D). As verified by sequencing analysis of these amplicons, the increase in size was due to the impaired splicing resulting in intron 1 retention. While Prdm14a SpMO was specific for *prdm14a,* the Prdm14b SpMO impaired the splicing of both *prdm14a*, and *prdm14b*. However, *Prdm14b* was more effective on inhibiting *prdm14b* splicing. Analysis of tailbud stage embryos injected with both SpMOs demonstrated that splicing is efficiently inhibited at later stages of development. Hence, the Prdm14 SpMOs are an effective tool to knockdown Prdm14.

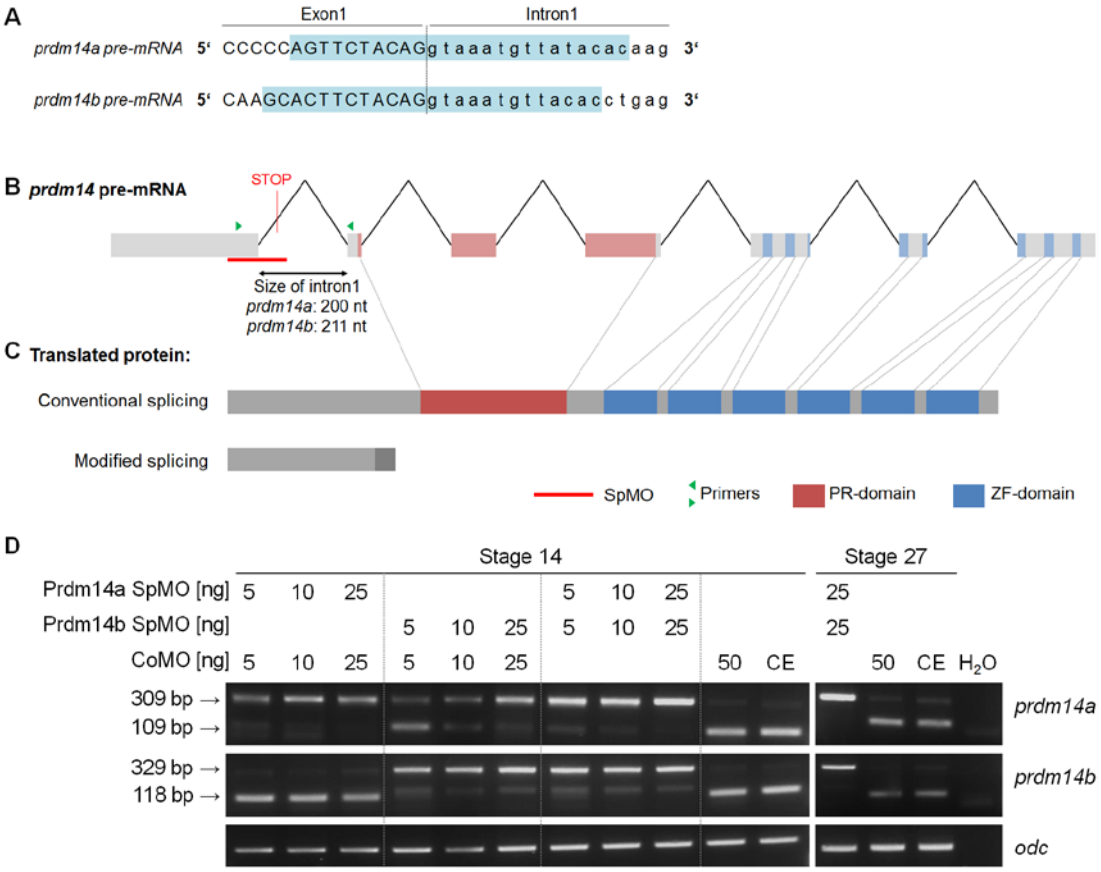

Fig. 3.9 Injection of Prdm14 splicing morpholinos causes intron1 retention. (A) Nucleotide sequence of *prdm14a* and *prdm14b* exon1/intron1 boundary. SpMO binding sites are highlighted in blue. **(B)** Schematic representation of *prdm14* pre-mRNA. **(C)** Schematic representation of the translated protein after conventional splicing and intron1 retention. **(D)** Morpholino oligonucleotides were injected in indicated combinations into both blastomeres of two-cell stage embryos. At the equivalent of neural plate stage (stage 14) and tailbud stage (stage 27) total RNA was isolated and analyzed by RT-PCR using markers indicated on the right. Expression levels were shown by *odc* expression. Expected amplicon sizes are indicated on the left.

To determine how *prdm14* loss of function would affect neuronal differentiation at tailbud stage, Prdm14 was knocked down by SpMOs in one dorsal blastomere of four-cell stage embryos (Fig. 3.10A). As shown by whole mount *in situ* hybridization, the loss of Prdm14 had no influence on the expression of *tubb2b* and *tlx3* (Fig. 3.10B-E'). Next, the influence of Prdm14 knock down on motor neuron axonal outgrowth in the spinal cord was analyzed, since impairments thereof have been reported in zebrafish Prdm14 morphants (Liu et al., 2012). Therefore, both morpholinos where injected into both dorsal blastomeres of 4-cell stage embryos to specifically target the SpMOs to the neural tube (Fig. 3.10F). As shown by immunofluorescence staining against acetylated Tubulin, the motor neuron axon outgrowth is not impaired by the control morpholino (Fig. 3.10G) or Prdm14 knock down (Fig. 3.10H). In

summary, while overexpression of *prdm14* leads to the ectopic formation of neurons of a specifically glutamatergic character, the knock down of Prdm14 has no effect on the specification of sensory neurons and neuronal differentiation.

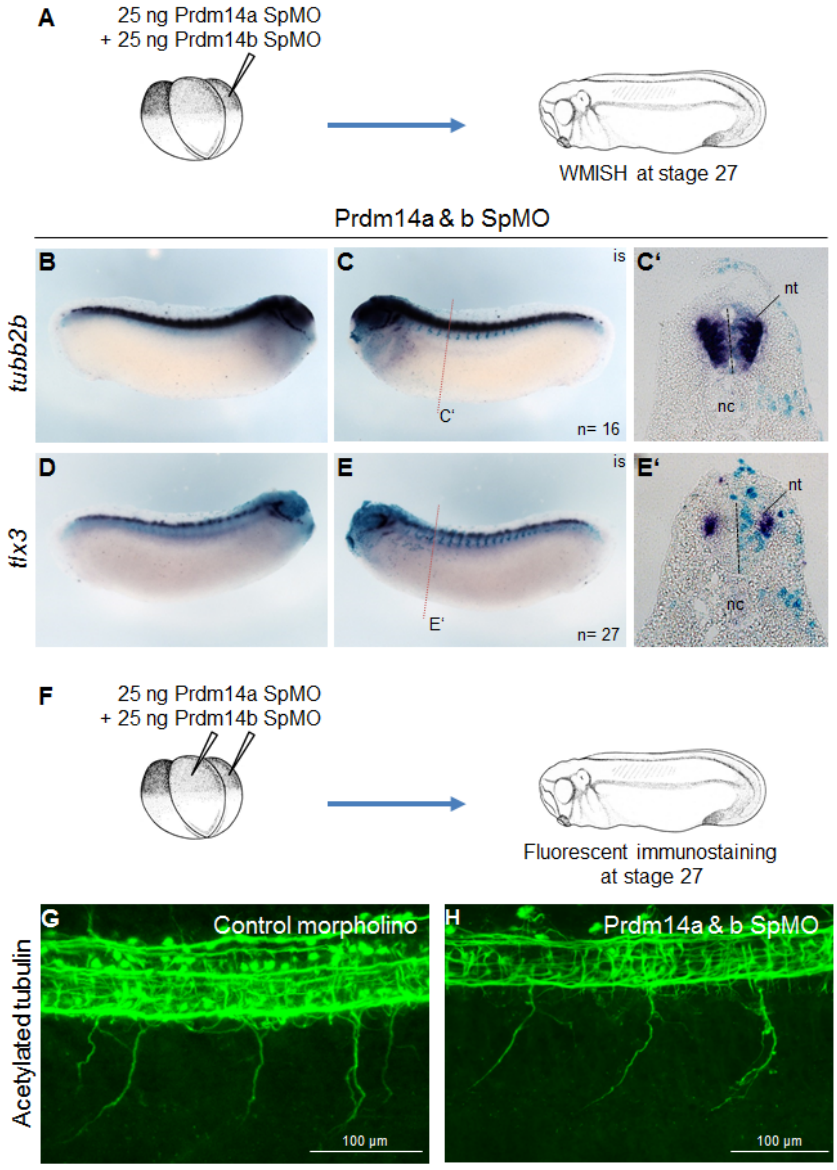

Fig. 3.10 Knock down of Prdm14 does not influence neuronal differentiation and axon outgrowth of motor neurons. (A) Prdm14a SpMO and Prdm14b SpMO (25 pg each) together with *β-Gal* (75 pg) mRNA (light blue staining) were injected into one dorsal blastomere of four-cell stage embryos. **(B-E')** Gene expression was analyzed at stage 27 by whole mount *in situ* hybridization using markers indicated on the left. The injected side is on the right, lateral view. is, injected side **(C', E')** Transverse sections at indicated levels of embryos shown in C and E, respectively. Dashed line indicates the midline of the neural tube. nt, neural tube; nc, notochord **(F)** Prdm14a SpMO and Prdm14b SpMO (25 pg each) or control morpholino (50 ng) were injected into both dorsal blastomeres of four-cell stage embryos. **(G-H)** Axon outgrowth of motor neurons was visualized by fluorescent immunostaining against acetylated tubulin at stage 27.

3.6 Identification of Prdm14 downstream targets

To further investigate the function of Prdm14 during early development, gain of function approaches were employed. Overexpression of *prdm14*-GR was sufficient to induce glutamatergic neurons in pluripotent animal cap cells. Hence, we decided to use this system to identify the global regulatory gene network induced by Prdm14 through RNA-sequencing analysis (Fig. 3.11A). Control and *prdm14*-GR mRNA-injected embryos were treated with dex at four-cell stage and animal caps were isolated from blastula stage embryos. At the equivalent of neural plate stage (stage 14) and tailbud stage (stage 27) total RNA was isolated and reverse transcribed into cDNA, which was subjected to single read (50 bp) sequencing. The sequence reads were aligned to the genome reference sequence of *X. tropicalis* (Joint Genome Institute assembly v4.2) using the STAR alignment software (Dobin *et al.,* 2012), allowing 5 mismatches within 50 bases. Using this approach in total 86-89% of the reads could be annotated. Genes were considered as candidates if they showed at least a 2-fold change (log2FC>1) over control caps and a FDR-corrected p-value <0.05.

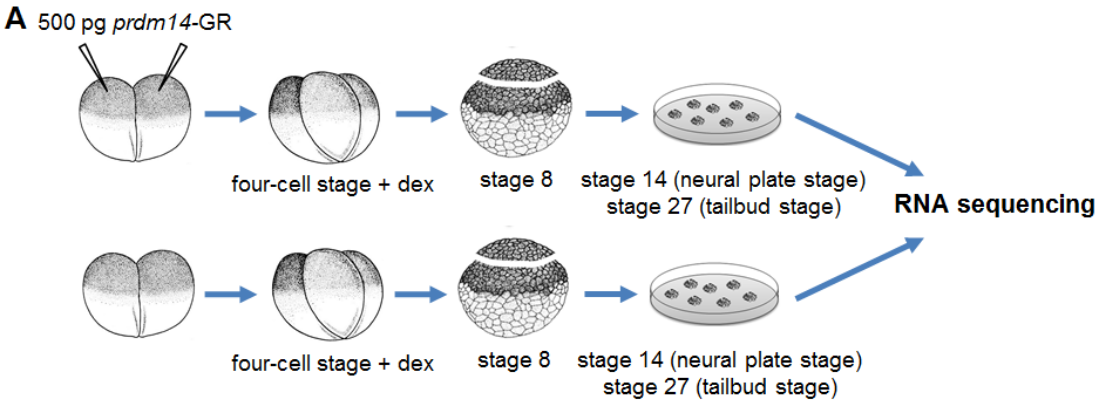

C

log2 fold change	*prdm14*-GR vs. CC	
	Stage 14	Stage 27
↑ > 5	18	46
↑ > 3	68	208
↑ > 2	140	296
↑ > 1	**338**	**356**

log2 fold change	*prdm14*-GR vs. CC	
	Stage 14	Stage 27
↓ > 5	0	0
↓ > 3	3	0
↓ > 2	48	4
↓ > 1	**571**	**41**

Fig. 3.11 RNA-sequencing analysis of *prdm14*-GR overexpression in animal caps. (A-B) *Prdm14*-GR (500 pg) mRNA was injected into both blastomeres of two-cell stage embryos. Control and *prdm14*-GR mRNA-injected embryos were treated with dex from four-cell stage on and animal caps were isolated from blastula stage embryos. At the equivalent of neural plate stage (stage 14) and tailbud stage (stage 27) total RNA was isolated and analyzed by RNA-sequencing. **(B)** Venn diagrams show the number of unique and shared target genes at stage 14 and 27, respectively. **(C)** Summary of identified putative target genes of Prdm14 after application of different fold-change categories. Given is the number of target genes with a log2 fold change higher than 1, 2, 3 or 5 compared to uninjected control caps (CC).

Applying these parameters, Prdm14 induced 338 genes at stage 14 and 356 genes at stage 27, respectively. From these a total of 65 genes were upregulated at both stages (Fig. 3.11B). Conversely, 571 and 41 genes were downregulated at stage 14 and 27, with only 11 genes shared between both stages. In a more stringent analysis using a minimum log2 fold change of three, *prdm14*-GR induced 68 and 208 genes at stage 14 and 27, respectively. In contrast the number of downregulated candidate genes dropped to three and zero at stage 14 and stage 27, respectively. For this reason, the further analysis

was focused on the candidate genes upregulated by *prdm14*-GR overexpression.

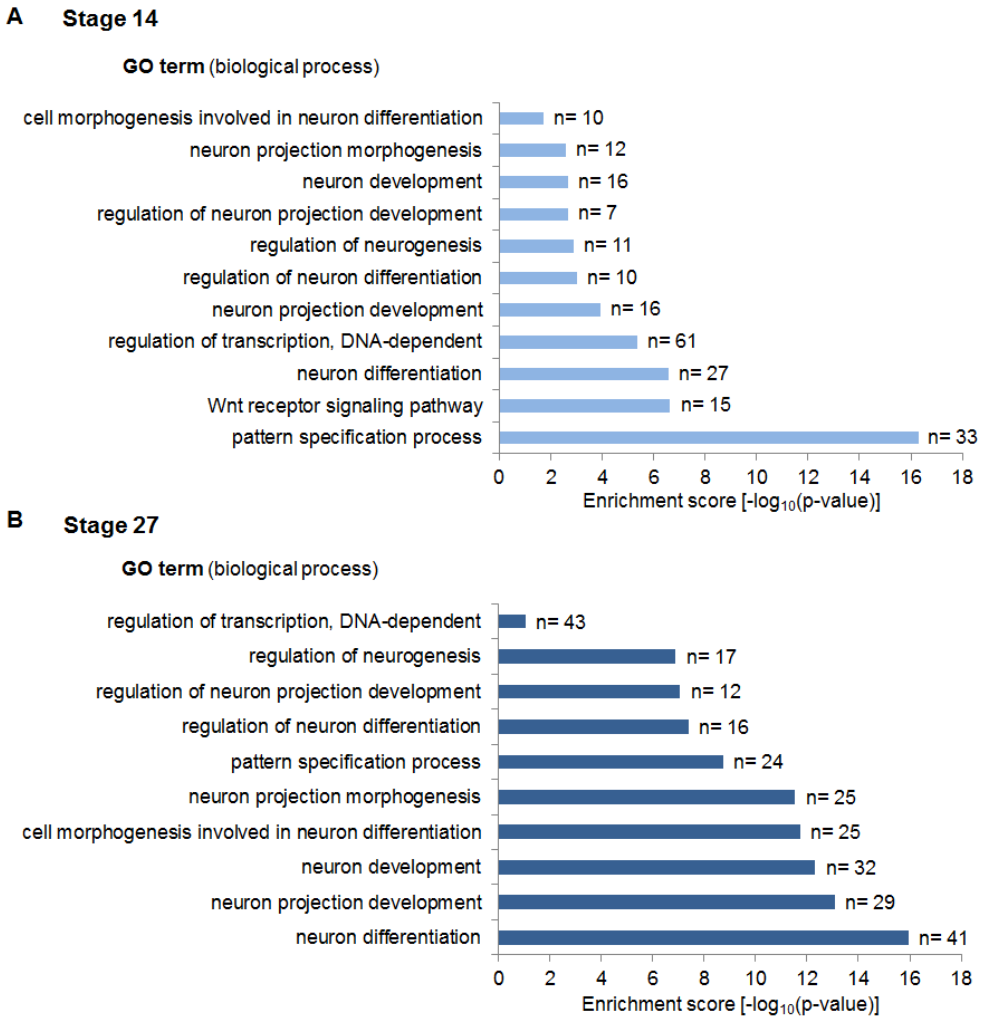

Fig. 3.12 Genes of biological processes involved in neural development are enriched in *prdm14*-GR overexpressing animal caps. Gene Ontology (GO) analysis was performed using DAVID (http://david.abcc.ncifcrf.gov) (Dennis *et al.* 2003). The number of genes in each category is shown as well as the -$\log_{10}$ P value at false discovery rate.

Consistent with the previous results in embryos and in animal caps, the RNA-sequencing analysis revealed a delayed neuronal differentiation induced by *prdm14*-GR, with the expression of *tubb2b, tlx3* and *slc17a7* all induced at the equivalent of stage 27 (Table 3.1). To gain insight into the pathways and processes of the Prdm14-induced genes, gene ontology (GO) analysis was performed (Appendix 6.2, Fig 3.12). *Prdm14*-GR upregulated genes at stage 14 were highly enriched in the category of pattern specification process, of which many were *hox*-transcription factors *(hoxc6, hoxc8, hoxc9, hoxa5, hoxa7, hoxc5, hoxa10, hoxa9, hoxb4, hoxb7, hoxb8, hoxb6)* (Fig. 3.12A). In addition,

genes involved in the Wnt receptor signaling pathway, including multiple ligands, co-receptors and intracellular components *(wnt8a, wnt10a, wnt10b, wnt5b, ryk, ror2, fzd7, fzd10)* were also upregulated. Several processes, which are related to neural development, were upregulated at neural plate as well as tailbud stage, such as neuron differentiation, neuron projection development, morphogenesis or regulation of neurogenesis (Fig. 3.12B). Interestingly, among the strongly upregulated *prdm14*-GR genes were those involved in the process of neural crest formation such as *wnt8*, *cdx1/2/4*, *pax3* and *zic1* (Table 3.1).

function	Gene	log2 fold change	
		Stage 14	Stage 27
neural pre-patterning	*zic3*	8.23	
proneural	*neurog1*	6.52	
	ebf2	4.27	4.96
glutamatergic selector gene	*tlx3*	2.17	5.91
glutamate transporter	*slc17a7*		5.78
postmitotic neurons	*tubb2b*		1.98
Wnt signaling	*wnt5b*	1.48	
	wnt8a	7.13	
	wnt10a	5.39	
	axin2	4.05	
	ror2	4.55	
Neural crest induction	*fgf3*	5.17	
	cdx1	8.98	
	cdx2	5.57	2.30
	cdx4	8.14	2.18
	sp5	7.21	2.06
Neural plate border specification	*pax3*	5.51	4.82
	zic1	2.54	
Neural crest specification	*snai2*		1.92
	tfap2b	2.81	2.57
	foxd3		6.34
	sox9	2.09	
	sox10		7.92
	prdm1a	1.83	

Table 3.1 List of selected candidate genes upregulated in *prdm14*-GR overexpressing animal caps. Overview of selected candidate genes with their log2 fold changes at stage 14 and 27 respectively.

3.7 Prdm14 activates canonical Wnt-signaling

Many components of the Wnt-signaling pathway were identified to be upregulated by *prdm14-GR* in the RNA-sequencing analysis. As the Wnt pathway is upstream of many of the genes that were also induced, the activation of the Wnt pathway was subject to further verification.

Ligands associated with both the non-canonical and canonical Wnt-pathways were induced. Therefore, luciferase reporter assays were performed to measure the activation of these two different pathways. *Atf2*-luc and TOPflash served as reporters for non-canonical and canonical signaling, respectively (Korinek et al., 1997; Ohkawara and Niehrs, 2011). The reporters were injected together with *prdm14*-GR, *wnt5a* or *wnt8a,* which served as positive controls for the non-canonical and canonical reporters (Fig. 3.13A). At stage 14 embryonic lysates were prepared and luciferase activity quantified. Consistent with previous reports (Ohkawara and Niehrs, 2011), the *atf2*-luc reporter was strongly (12-fold) activated upon injection of *wnt5a* but not of *wnt8a* mRNA. Conversely, the TOPFlash reporter was induced (2-fold) by *wnt8a* but not by *wnt5a mRNA* injection. Upon overexpression of *prdm14*-GR the non-canonical *atf2-luc* reporter was only sligthly activated compared to *wnt5a* (Fig. 3.13B). However, *prdm14*-GR induced the canonical TOPflash reporter to similar levels as those observed for *wnt8a*. The difference in the activation level of the non-canonical and canonical Wnt-pathways by Prdm14 is also reflected in the data obtained from the RNA-sequencing. There Prdm14-GR activates *wnt8a* (log2FC, 7.1) to a much higher extent than *wnt5b* (log2FC, 1.5). Consistent with the results from the RNA-sequencing, Prdm14-GR activates *wnt8* expression in whole embryos at stage 14 (n= 27; 78% increase) (Fig. 3.13D, red arrows). The activation of the TOPFlash reporter by Prdm14-GR further supports the notion that Prdm14 activates canonical Wnt-signaling in embryos at neural plate stage.

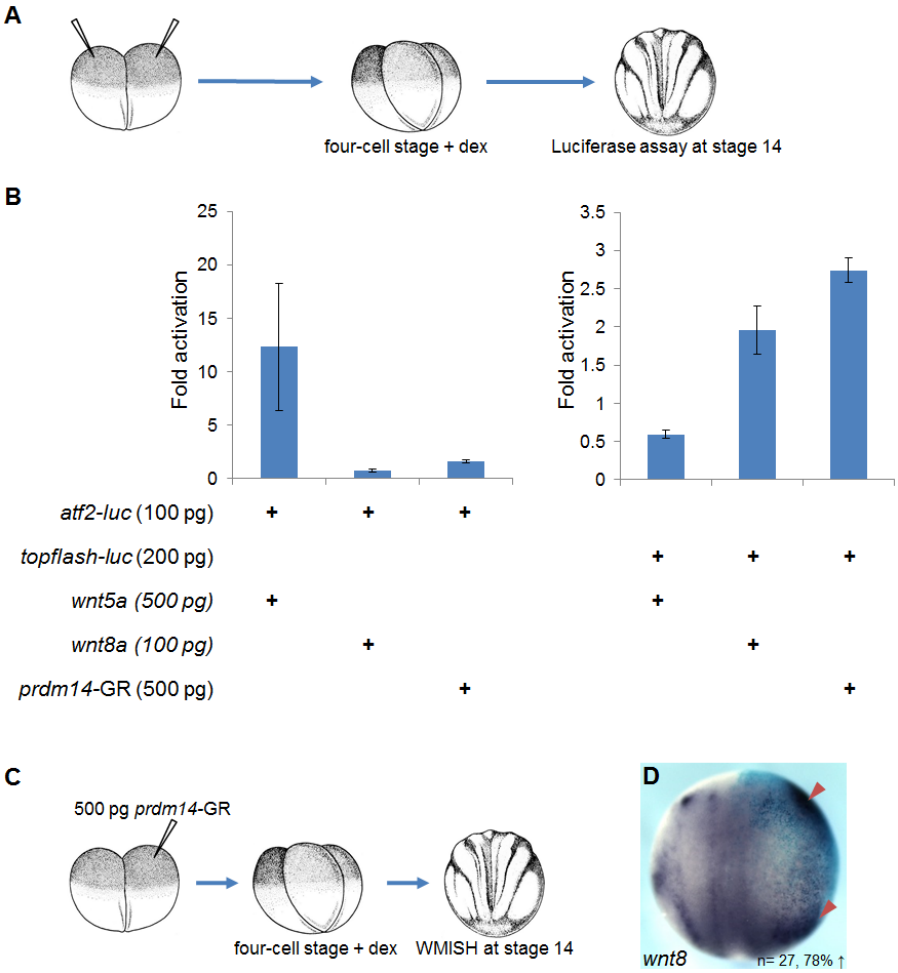

Fig. 3.13 *Prdm14*-GR overexpression activates canonical Wnt-signaling. (A) *Atf2-luc* and *topflash-luc* reporter were injected together with indicated mRNA into both blastomeres of two-cell stage embryos. Embryos were cultivated until open neural plate stage and luciferase activity was measured and normalized to renilla luciferase. **(B)** Shown is a summary of three independent luciferase experiments. Six embryos per injection were collected in duplicates for each experiment. Error bars represent the standard error of the mean (+/-SEM). Note the different scales in each diagram. **(C)** *Prdm14*-GR (500 pg) mRNA together with *β-Gal* (75 pg) mRNA (light blue staining) were injected into one blastomere of a two-cell stage embryo. Embryos were treated from four-cell stage on with dex. **(D)** *Wnt8* expression was analyzed at stage 14 by whole mount *in situ* hybridization. The injected side is on the right, dorsal view, anterior up.

3.8 Comparative expression analysis of *prdm14* with neural plate border specifiers

In addition to Wnt signaling components, the RNA-sequencing analysis suggests that *prdm14*-GR is sufficient to induce the expression of several genes involved in the gene regulatory network of neural crest formation. These include the upstream neural plate border specifiers *pax3* and *zic1* (Hong and Saint-Jeannet, 2007). To determine if *prdm14* is present at the correct time and place to regulate *pax3* and *zic1*, a comparative expression analysis was performed

(Fig. 3.14). At stage 10.5 a broad expression of *prdm14* in the dorsal ectoderm is observed, while at stage 11.5 the first strong and specific expression of *pax3* and *zic1* occurs. *Pax3*, *zic1* and *prdm14* are all expressed in the lateral neural plate border and the expression of *zic1* and *prdm14* extends into the anterior neural plate border until stage 13. At stage 14 *zic1* is still expressed throughout the anterior neural plate border while anterior *prdm14* expression is maintained in the trigeminal-profundal placode. During all developmental stages *pax3* expression is restricted to the lateral neural plate border. Taken together, the observation that *prdm14* expression precedes and also co-localizes with *pax3* and *zic1* expression, at the neural plate border, suggests an early function of *prdm14* in the regulation of *pax3* and *zic1*.

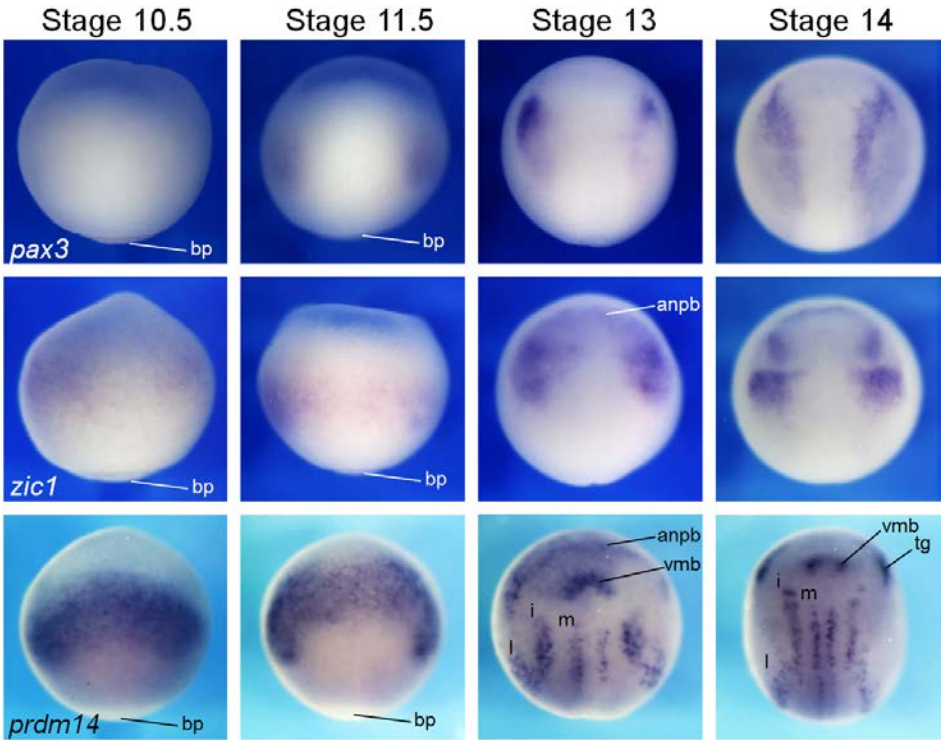

Fig. 3.14 *Prdm14* is co-expressed with *pax3* and *zic1* in regions of the neural plate border. Comparative expression analysis of stage matched embryos by whole mount *in situ* hybridization using markers indicated on the bottom left. Stage 10.5-14: dorsal view, anterior up. anpb, anterior neural plate border; bp, blastoporus; i, intermediate; l, lateral; m, medial; tg, trigeminal-profundal placode; vmb, ventral midbrain

3.9 Knock down of Prdm14 has no influence on candidate gene expression

To determine whether Prdm14 is required for the induction of selected *prdm14*-GR candidate genes (Table 3.1), their expression was evaluated under knock-down conditions. The specificity and efficiency of the SpMOs has been previously confirmed (Fig. 3.9). Therefore, both Prdm14 SpMOs were injected into one blastomere of two-cell stage embryos and marker gene expression was analyzed by whole mount *in situ* hybridization at stage 14 (Fig. 3.15A). While *prdm14*-GR overexpression results in an inhibition of *tubb2b* (Fig. 3.6B, F), Prdm14 loss of function showed no effect on *tubb2b* expression at neural plate stage (Fig. 3.15B'). The candidate genes *wnt8,* the neural plate border genes *pax3*, *zic1*, *zic2* and *zic3* as well as the neural crest specifying genes *sox10* showed also no alteration in expression on the injected site (Fig. 3.15C-G, J). This was also the case for *neurog1* and the Rohon-Beard sensory neuron marker *tlx3* (Fig. 3.15H-I). The fact that knock down of Prdm14 had no influence on the expression of the tested marker genes suggests that Prdm14 might not be necessary for their regulation. However, it cannot be excluded that residual Prdm14 is sufficient for its downstream activity or that redundancies exist with other Prdms.

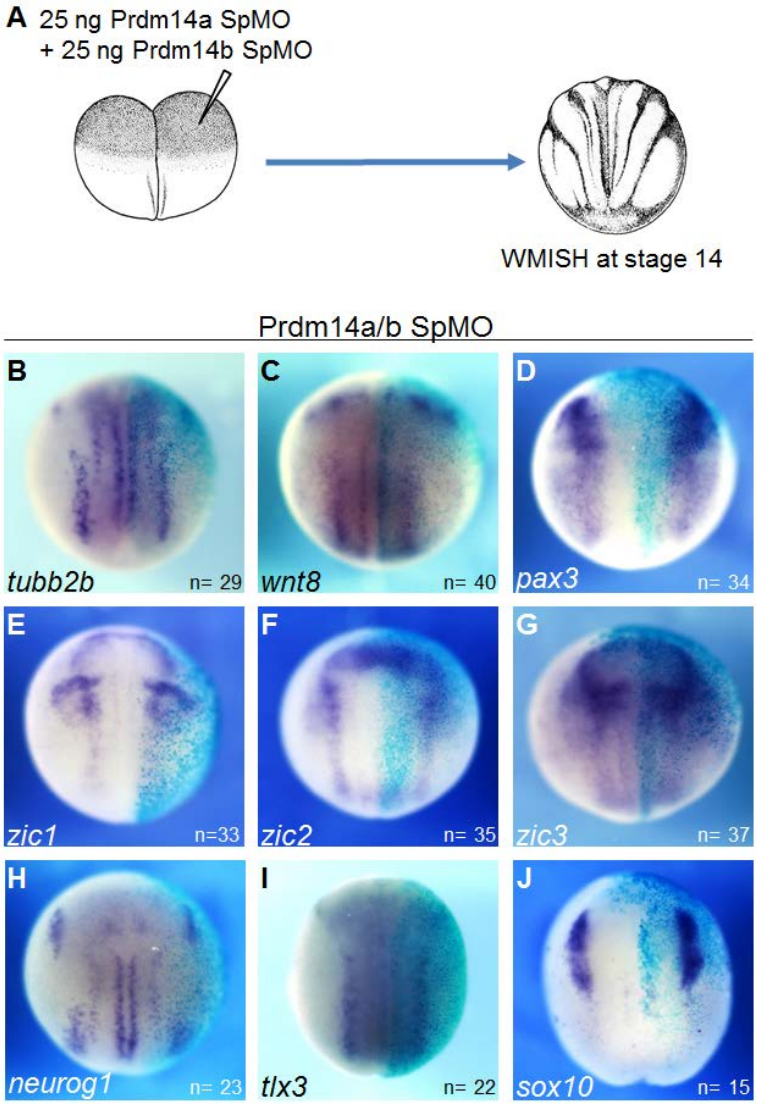

Fig. 3.15 Prdm14 knock down does not influence the expression of selected candidate genes in whole embryos. (A) Prdm14a SpMO and Prdm14b SpMO (25 pg each) together with *β-Gal* (75 pg) mRNA (light blue staining) were injected into one blastomere of a two-cell stage embryo. **(B-J)** Gene expression was analyzed at stage 14 by whole mount *in situ* hybridization using markers indicated on the bottom left. The injected side is on the right, dorsal view, anterior up.

3.10 *Prdm14* gain of function activates neural crest genes in whole embryos

As the knock down of Prdm14 showed no effect on the expression of candidate genes, a gain of function analysis was performed to verify their regulation by Prdm14. *Prdm14*-GR mRNA was injected into one blastomere of two-cell stage embryos, which were treated with dexamethasone at the four-cell stage (Fig. 3.16A).

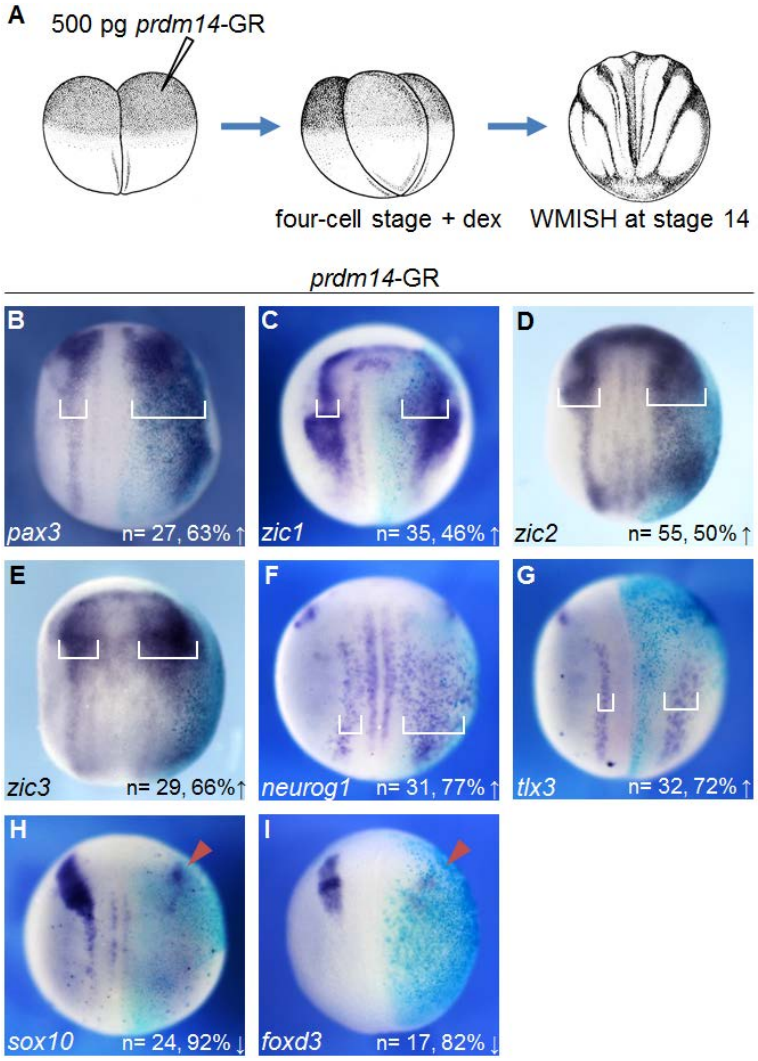

Fig. 3.16 *Prdm14*-GR overexpression promotes the expression of selected candidate genes in whole embryos. (A) *Prdm14*-GR (500 pg) mRNA together with *β-Gal* (75 pg) mRNA (light blue staining) were injected into one blastomere of two-cell stage embryos. Embryos were treated from four-cell stage on with dex. **(B-I)** Gene expression was analyzed at stage 14 by whole mount *in situ* hybridization using markers indicated on the bottom left. The injected side is on the right, dorsal view, anterior up. White brackets indicate width of expression domain.

As *prdm14*-GR overexpression activates a number of genes involved in the gene regulatory network of neural crest formation, the expression of the neural plate border specifiers *pax3* and *zic1* were analyzed (Fig. 3.16B-C). *Prdm14*-GR overexpression leads to the expansion of *pax3* (n= 27; 63% increased) as well as *zic1* (n= 35; 46% increased) expression, although the effect on *zic1* is much weaker (Fig. 3.16C). This observation is consistent with the RNA-sequencing data, which indicate a stronger activation of *pax3* than of *zic1* (Table 3.1). Interestingly, the neural plate border appeared enlarged on the injected side of the embryos. To verify this result, the expression of other neural plate border specific genes, which are members of the *zic* family namely *zic2*

and *zic3* was analyzed (Houtmeyers *et al.,* 2013). These were also shown to be upregulated in the *prdm14*-GR overexpressing animal caps (Table 3.1). In agreement with previous observations, the expression of *zic2* (n= 55; 50% increased) and *zic3* (n= 29; 66% increased) was likewise expanded (Fig. 3.16D-E). Beside genes involved in neural crest formation, the proneural transcription factor *neurog1* was also highly upregulated in the *prdm14*-GR overexpressing animal caps (Table 3.1). Consistently, an expansion of *neurog1* expression could be shown (n= 31; 77% increased), whereas the expression in the trigeminal placode was alleviated (Fig. 3.16F).

The RNA-sequencing data revealed not only a strong activation of the glutamatergic sensory marker *tlx3* at the tailbud stage, but also a weak activation at neural plate stage (Table 3.1). This led to the question, wether *prdm14* promotes the earliest step of Rohon-Beard sensory neuron differentiation at the neural plate stage. Indeed, on the injected side *tlx3* expression was expanded in the neural plate border (n= 32; 72% increased), but inhibited in the trigeminal placode (Fig. 3.16G).

In addition, the RNA-sequencing data revealed a strong upregulation of the neural crest specifiers *sox10* and *foxd3* at tailbud stage (Table 3.1). These genes are already active at the neural plate stage (Pohl and Knöchel, 2001; Aoki *et al.,* 2003), therefore the potential role of Prdm14-GR in the regulation of their expression was analyzed. Interestingly, these marker genes were inhibited at neural plate stage upon *prdm14*-GR overexpression (*sox10*: n= 24; 92% downregulated, red arrow; *foxd3*: n= 17; 82% downregulated, red arrow) (Fig. 3.16 H-I).

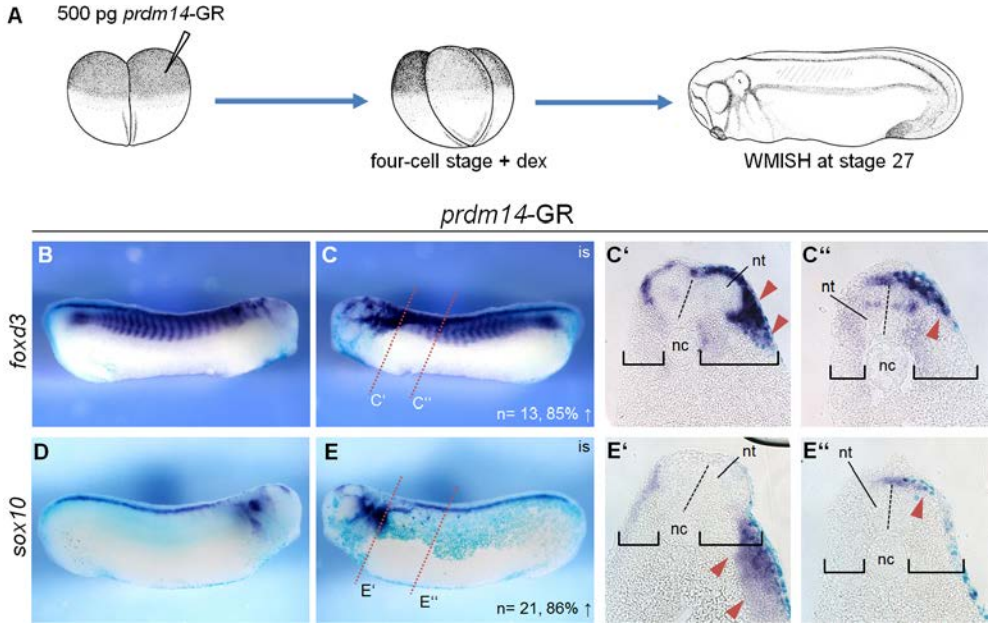

Fig. 3.17 *Prdm14*-GR overexpression promotes the neural crest formation in whole embryos. (A) *Prdm14*-GR (500 pg) mRNA together with *β-Gal* (75 pg) mRNA (light blue staining) were injected into one blastomere of two-cell stage embryos. Embryos were treated from four-cell stage on with dex. **(B-E'')** Gene expression was analyzed at stage 27 by whole mount *in situ* hybridization using markers indicated on the left. The injected side is on the right, lateral view. is, injected side **(C', C'', E', E'')** Transverse sections at indicated levels of embryo shown in C and E, respectively. Black brackets indicate width of mesenchymal tissue on the level of the notochord. Dashed line indicates midline of the neural tube. nt, neural tube; nc, notochord

However, consistent with the RNA-sequencing data, *prdm14-GR* microinjection led to an ectopic expression of *sox10* and *foxd3* in tailbud stage embryos (Fig. 3.17B-E'). In cranial neural crest cells, *foxd3* and *sox10* expression was increased (Fig. 3.17C', D'), whereas the trunk neural crest was expanded laterally. In all *prdm14*-GR injected embryos thickening of the mesenchymal tissue on the injected side could be observed (Fig. 3.17C', E'; black bracket). Consequently, these findings suggests that *prdm14*-GR leads to the expansion and activation of the expression of neural plate border genes, which subsequently might lead to the induction of downstream genes involved in neural crest specification such as *sox10* and *foxd3*.

In summary this study demonstrated that *prdm14* is expressed during gastrulation in the prospective neuroectoderm and later during development in the territories of primary neurogenesis. Consistently, overexpression of the proneural transcription factor Neurog2 ectopically activates *prdm14* expression. At neural plate stage *prdm14* promotes and maintains the proliferation of neural precursors and therefore delays differentiation at neural plate stage.

Overexpression of *prdm14* activates canonical Wnt-signaling, expands the neural plate border and promotes the expression of neural plate border genes. Consequently this might lead to the ectopic differentiation of neural plate border derivatives such as Rohon-Beard sensory neurons and neural crest cells.

4. Discussion

Regionalized specification and differentiation of the ectoderm is under the control of multiple intrinsic and extrinsic factors. The prospective epidermal cells are characterized by high BMP signaling, while neural fate differentiation within the dorsal ectoderm requires low BMP signaling and the presence of FGF signaling (Rogers *et al.,* 2009; Pera *et al.,* 2014). In contrast, Wnt-signaling is required for posterior fates but must be inhibited for anterior neural fates (McGrew *et al.,* 1997). The neural plate border separates the neural plate from the non-neural ectoderm and is established through the interaction of Wnt- and FGF-signaling, as well as intermediate levels of BMP signaling, and will give rise to the neural crest, the neurogenic placodes and Rohon-beard sensory neurons (Simoes-Costa and Bronner, 2015). In this thesis, the role of Prdm14, a member of the PR domain family of transcriptional regulators, in the context of ectodermal differentiation is described.

The expression of *prdm14* in the prospective neuroectoderm is suggestive for a role in the establishment of the neural progenitor cells. In agreement, *prdm14*-GR promoted proliferation and expansion of the progenitor pool in the neural plate, while neuronal differentiation was delayed. Prdm14 was shown to positively regulate the canonical Wnt pathway and the key neural plate border specifying genes, *pax3* and *zic1*. Correspondingly, Prdm14 was sufficient to promote derivatives of the neural plate border in pluripotent cells and embryos including neural crest cells and Rohon-Beard glutamatergic sensory neurons. *Prdm14* was also positively regulated by the proneural transcription factor Neurog2 and expressed in postmitotic neurons suggesting an additional function in the context of the development of the nervous system.

4.1 Prdm14 maintains the proliferation of precursor cells

Previous studies have described a role for Prdm14 in the establishment of primordial germ cells (PGC) in mice. In this context, Prdm14 together with Prdm1 (Blimp1) promotes stemness characteristics through activation of the pluripotency gene *sox2* (Yamaji et al., 2008). In hESCs, Prdm14 interacts with the core pluripotency genes by co-occupying target genes together with Sox2,

Nanog and Oct4. During the development of the nervous system, *sox2* serves a marker for multipotent proliferating neural progenitor cells and is expressed throughout the entire neural plate (Graham *et al.,* 2003; Ellis *et al.,* 2004). Similar to a role in ESCs, *prdm14* overexpression in *X. laevis* embryos resulted in an expansion of *sox2* expression and an increase in the number of pH3 positive cells, which marks mitotically active cells. This increase in proliferation occurred at the expense of differentiation, as shown by the transient inhibition of the post-mitotic neuronal marker *tubb2b*. The ability to promote proliferation and maintenance of a progenitor cell fate fits well with the strong and specific expression of *prdm14* in the prospective neuroectoderm at the onset of gastrulation. *Prdm14* is also present in the anterior neural plate at the end of gastrulation, which maintains its proliferative capacity and undergoes delayed neuronal differentiation (Hartenstein, 1989; Eagleson and Harris, 1990; Hartenstein, 1993; Papalopulu and Kintner, 1996).

In the RNA-sequencing analysis, *sox2* was only weakly (log2FC, 0.6) induced by *prdm14* compared to control caps at the equivalent of neural plate stage. This suggests that *prdm14* may not be sufficient to promote *sox2* expression and requires the cooperation with other factors. Another possible explanation might be that the levels of *sox2* are already decreasing in *prdm14*-GR overexpressing animal cap cells. Therefore, analysis of earlier time points might provide more insight in the transcript levels of *sox2* in *prdm14*-GR overexpressing animal caps.

Intriguingly, RNA-sequencing analysis revealed that *prdm14* overexpression in animal caps activated the expression of *prdm1* at neural plate stage. This is of particular interest, as Prdm14 in combination with Prdm1 is known to activate the expression of *sox2* during mouse PGC specification (Yamaji *et al.,* 2008). However, it must be mentioned, that *prdm14* expression in mice is specific for PGCs and has not been show in the central nervous system (Yabuta *et al.,* 2006; Yamaji *et al.,* 2008). Conversely, in *X. laevis prdm14* expression cannot be detected in PGCs and is restricted to the developing nervous system. As the genomic locus with respect to flanking genes of *prdm14* is the same in mice and *X. laevis*, the regulation of *prdm14* expression must have changed during evolution. The lack of expression of *prdm14* in *X. laevis* PGCs compared to mice may be attributed to the different mechanisms of PGC

specification in both species. While mice PGCs are specified by signals from the surrounding somatic tissue, the specification of PGCs in *X. laevis* and zebrafish requires the inheritance of maternal germ plasm (Johnson *et al.,* 2011). Therefore it is possible, that the interaction of Prdm14 and Prdm1 is conserved, although in a different developmental context. This is supported by the fact that in *X. laevis* and zebrafish *prdm1* is also not expressed in PGCs, but in the neural plate border where it is required for Rohon-Beard sensory neurons (de Souza *et al.,* 1999; Rossi *et al.,* 2009; Klymkowsky *et al.,* 2010). Furthermore, *X. laevis prdm1* plays a role in the anterior endomesoderm, where it is required for head induction (de Souza *et al.,* 1999).

As the overexpression of *prdm14* influences the expression of the neural plate marker *sox2* in *X. laevis*, Prdm14 might be involved in the establishment of the neuroectoderm. Furthermore, overexpression of *prdm14* in animal caps induced the expression of components of the FGF signaling pathway (*fgf3, fgfr1*), whose activity is required for neural induction (Kengaku and Okamoto, 1995; Lamb and Harland, 1995; Streit *et al.,* 2000; Pera *et al.,* 2003; Linker and Stern, 2004, Delaune *et al.,* 2005). In summary, the maintained proliferation upon *prdm14* overexpression is in agreement with the known function of *prdm14* to promote and maintain the stemness character in mESC and hESC (Tsuneyoshi *et al.,* 2008, Chia *et al.,* 2010; Ma *et al.,* 2011)

4.2 Prdm14 activates canonical Wnt-signaling in *X. laevis*

The balance between stemness and differentiation in adult stem cell niches requires the activity of canonical Wnt-signaling (Fodde and Brabletz, 2007; Holland *et al.,* 2013). Consequently, the deregulation of canonical Wnt-signaling is a common occurrence in the formation of cancer. A Wnt-pathway modulating activity has been described so far only for Prdm5 (Meani *et al.,* 2009; Shu *et al.,* 2011). It has been shown that Prdm5 functions as a tumor suppressor in part through down regulation of the canonical Wnt-signaling pathway (Meani *et al.,* 2009; Shu *et al.,* 2011). Interestingly, overexpression of *prdm14* activated several components of the Wnt-pathway in *X. laevis* animal caps. Additionally, as demonstrated by the TOPFlash luciferase reporter, *prdm14* led to an increase in canonical Wnt-signaling.

Prdm14 has also been described to play a role in carcinogenesis, where it was first described to promote the proliferation of breast cancer cells (Nishikawa *et al.,* 2007). Furthermore, an involvement of Prdm14 in other cancer types like lymphoblastic lymphoma, lung cancer, testicular cancer and HPV-positive cancers was shown (Dettman and Justice, 2008; Simko *et al.,* 2012; Zhang *et al.,* 2013; Ruark *et al.,* 2013; Snellenberg *et al.,* 2014; Hubers *et al.,* 2015). Interestingly, in *X. laevis* embryos and animal caps the overexpression of *prdm14* promotes the expression of the glutamatergic sensory marker *tlx3,* which has also been described to be upregulated in pediatric T-cell acute lymphoblastic leukemia (T-ALL) (Sayitoğlu *et al.*, 2012; Moussa and Sidhom, 2013). This type of cancer is also characterized by elevated levels of *prdm14* (Dettman *et al.,* 2011; Simko *et al.,* 2012; Carofino *et al.,* 2013). Therefore, it might be of interest to study if and how these genes interact in the formation of T-ALL in humans.

Although *prdm14* is deregulated in many types of cancer and its overexpression activates canonical Wnt-signaling in *X. laevis*, no connection between the deregulation of Wnt-signaling and Prdm14 in the context of carcinogenesis has been shown thus far. However, consistent with the observation that Prdm14 activates canonical Wnt-signaling, several downstream targets were activated such as the glutamatergic sensory marker *tlx3,* posterior neural plate markers *cdx1/2/5* and the neural plate border specifiers *pax3* and *zic1.*

4.3 Prdm14 activates the expression of neural plate border genes

The neural plate border (NPB) is the source for multiple derivatives such as the neurogenic placodes, Rohon-Beard sensory neurons and neural crest cells (Hong and Saint-Jeannet, 2007; Rossi *et al.,* 2009). The establishment of the NPB requires FGF-, Notch-, Wnt- signaling and intermediate levels of BMP signaling (Pegoraro and Monsoro-Burq, 2012; Simões-Costa and Bronner, 2015). The activity of these different signaling pathways induces the expression of neural plate border specifier genes such as *msx1, dlx3*, *pax3* and *zic1. Pax3* and *zic1* in combination are sufficient to induce the expression of neural crest specifying genes such as *sox8/9/10*, *snai2* and *foxd3* (Milet *et al.,* 2013;

Plouhinec *et al.,* 2014). Recently, large scale screening approaches could identify several *pax3* and *zic1* target genes, which might be involved in the formation of the developing neural crest (Plouhinec *et al.,* 2014; Bae *et al.,* 2014).

Interestingly, *prdm14* overexpression led to the expansion of the neural plate border and induced the expression of the neural plate border specifying genes *pax3* and *zic1*. In *X. laevis,* the regulation of *pax3* and *zic1* requires canonical Wnt-signaling (Bang *et al.,* 1999, Sato *et al.,* 2005). As previously mentioned, *prdm14* overexpression in neural plate stage animal caps activated canonical Wnt-signaling and downstream targets such as *cdx1/2/4* and *sp5,* which are known to be required for Wnt-mediated *pax3* expression (Sanchez-Ferras *et al.,* 2012; Park *et al.,* 2013). Hence, *prdm14* might activate canonical Wnt-signaling, which in turn, activates *pax3* through the action of *cdx1/2/4* and *sp5*. The observation that *pax3* was much stronger activated than *zic1* in *prdm14* overexpressing animal caps might be the result of a positive autoregulation of *pax3* (Plouhinec *et al.,* 2014). It is of interest that other neural plate border specifying genes such as *msx1* and *dlx3* were not found to be upregulated in *prdm14*-GR overexpressing animal caps. Recently described *pax3*/*zic1* target genes such as *lmx1b.1*, *xarp*, *elavl3, axin2* and *pnhd* (Plouhinec *et al.,* 2014) have also been identified as *prdm14* downstream targets in the animal cap assay, supporting the notion that *prdm14* activates *pax3* and *zic1* expression.

Consistent with the early activity of *prdm14* to promote proliferation and to maintain a progenitor cell fate, the neural crest specifying genes *sox10* and *foxd3* were inhibited at neural plate stage in *prdm14*-GR mRNA microinjected embryos. However, this inhibition was only transient as tailbud stage embryos showed ectopic expression of *sox10* and *foxd3* in the cranial neural crest. It remains to be addressed, if the ectopic expression at tailbud stage is due to an increased pool of progenitors or due to the increased expression of *pax3* and *zic1*.

It is known that *pax3* and *zic1* are sufficient to activate the gene regulatory network for neural crest formation (Hong and Saint-Jeannet, 2007; Plouhinec *et al.*, 2014). Therefore, the induced expression of neural crest specifying genes such as *snai2*, *foxd3*, *sox9/10* and *tfap2b/e* in *prdm14*-GR

overexpressing animal caps may be the consequence of *pax3* and *zic1* activation. These findings support a role for *prdm14* in the early establishment of the neural plate border. However, it will be of interest to test how other neural crest genes, which are not activated in *prdm14*-GR overexpressing animal caps, behave upon *prdm14*-GR overexpression.

4.4 *Prdm14* gain of function phenocopies *zic1/2/3* overexpression

Overexpression of the neural plate border genes *zic1, 2* and *3* in *X. laevis* promotes neural crest formation and causes an expansion of the neural plate (Nakata *et al.,* 1997, Nakata *et al.,* 1998). At tailbud stage an enlargement of the neural tube and mesenchymal tissue on the injected side is observed when *zic1, 2* and *3* are overexpressed. Interestingly, the expansion of the neural plate as well as the enlargement of the neural tube and mesenchymal tissue can also be detected upon ectopic *prdm14* expression in whole embryos. Consistently, in *prdm14* overexpressing animal caps and embryos the expression of *zic1, zic2* and *zic3* is increased. Therefore, it is possible that the *prdm14*-induced expansion of *sox2* expression, as well as the enlargement of the neural tube and mesenchymal tissue, are the result of *zic* activation. *Zic2* might be responsible for the inhibition of *tubb2b* at neural plate stage as it inhibits neuronal differentiation (Brewster *et al.,* 1998) and is also activated by *prdm14*-GR.

Zic genes are not only described as activators (Merzdorf and Sive, 2006), but also as inhibitors of canonical Wnt-signalling (Fujimi *et al.,* 2012; Pourebrahim *et al.,* 2011), which would conflict with the finding that Prdm14-GR activates canonical Wnt-signaling. Further analyses will clarify, whether the activation of *wnt8a* by Prdm14-GR is required for its downstream activity and if the activation of *wnt8a* is direct or indirect.

4.5 Prdm14 promotes sensory neuron formation

The expression of *prdm14* in the prospective neuroectoderm suggests an early function in the establishment of the neural plate. In addition to this early role, the expression of *prdm14* in the territories of primary neurogenesis and in

the postmitotic neurons in the neural tube is indicative for a later role in neuronal subtype differentiation and maturation. This notion is further supported by the positive regulation of *prdm14* by Neurog2.

Recently, it has been shown that Prdm12 is required for the specification of *X. laevis* sensory neurons (Nagy *et al.,* 2015). Overexpression of *prdm12* induces the expression of transcription factors required for sensory neuron specification such as *brn3d* (*pou4f1.2*), *sncg*, *drgx* and *tlx3.* Interestingly, overexpression of *prdm14* activates the same set of genes in animal caps, suggesting that Prdm14 might also be involved in the specification of sensory neurons. This idea is further supported by the finding that *prdm14* overexpression induces ectopic neuronal cells that express markers indicative for glutamatergic sensory neurons.

Glutamatergic Rohon-Beard sensory neurons are the first to be born and arise from the neural plate border (Hernandez-Lagunas *et al.,* 2005; Rossi *et al.,* 2009; Olesnicky *et al.,* 2010). Well-characterized transcription factors involved in the specification of this class of neurons are *prdm1*, *neurog1* and *neurog2,* which upon overexpression induce ectopic sensory neuron formation (Olson *et al.,* 1998; Perez *et al.,* 1999; Perron *et al.,* 1999; Cornell and Eisen, 2002; Hernandez-Lagunas *et al.,* 2005). Interestingly, the expression of these transcription factors was activated by Prdm14, indicating an upstream role of Prdm14 on sensory neuron formation. The observation that *prdm14* precedes the expression of *neurog1* suggests that Prdm14 may be a direct regulator of *neurog1.*

The specification of sensory neurons has also been linked to canonical Wnt-signaling. Kondo and colleagues showed, that neuralized mesenchymal stem cells are able to differentiate into neurons in the presence of canonical Wnt-signaling. Interestingly, these differentiating cells express *neurog1* and *tlx3* (Kondo *et al.,* 2011). As *prdm14* activates canonical Wnt-signaling as well as the expression of *neurog1* and *tlx3*, there is the intriguing possibility that canonical Wnt-signaling is involved in the process of sensory neuron specification in *X. laevis*.

Similar to *X. laevis*, *prdm14* is expressed in zebrafish throughout the anterior neural plate at bud stage (Liu *et al.,* 2012). At the 3-somite stage, *prdm14* is co-expressed with *neurog1* in dorsal and ventral neuron precursors

and at the 26-somite stage in Rohon-Beard sensory and motor neurons. Prdm14 knock down in zebrafish does not influence neuronal differentiation (Liu *et al.,* 2012). However, shortened axon outgrowth of CaP motor neurons can be observed at 26 hpf, which leads to impaired touch response and swimming behavior. This is only a transient effect as axon outgrowth is restored in embryos at 2.5 dpf, which was attributed to residual Prdm14 activity.

In this study, functionally verified splicing morpholinos for *prdm14a* and *prdm14b* were used to knock down both *prdm14* paralogs. Similar to zebrafish, the knock down of Prdm14 in *X. laevis* embryos had no effect on neuronal differentiation. In addition, the expression of the selected candidate genes, identified in the RNA-sequencing analysis of *prdm14*-GR overexpressing animal caps, was not affected. Furthermore, the motor neuron axon outgrowth was not affected in tailbud stage *X. laevis* embryos after Prdm14 knock down suggesting that *prdm14* is not necessary in these contexts. As Prdm14 is maternally supplied, it cannot be ruled out that the use of the splicing morpholinos is not effective enough and that the residual Prdm14 proteins might be sufficient to exert their function. A further explanation might be the existence of functional redundancies, as described in zebrafish for *prdm3*, *5* and *16* (Ding *et al.,* 2013). This is likely, considering that all members of the *prdm* family are expressed in the developing central nervous system of *X. laevis* (Eguchi *et al*., 2015). A potential candidate might be *prdm12,* which also promotes the specification of sensory neurons and therefore might compensate the Prdm14 knock down. To address the question, if redundancies might exist between different Prdms, it would be of interest to knock down more than one Prdm or use gene editing tools like TALENs or CRISPR/Cas to efficiently knock out *prdm14*.

5. Conclusion

In summary, this study suggests a role for the PR domain protein Prdm14 in the establishment of the neuroectoderm and maintenance of a proliferative state. As a consequence the pool of progenitor cells is expanded in the neural plate and neural plate border at the expense of differentiation. Since Prdm14 is able to induce the expression of *zic1, 2* and *3,* this expansion may also occur due to their activity. Through the *prdm14*-mediated activation of canonical Wnt-signaling the neural plate border specifying genes *pax3* and *zic1* are induced, which promote the formation of neural crest. The expansion of the neural plate border might also play a role in this context. The ectopic specification of Rohon-Beard sensory neurons could be caused by the expansion of the neural plate border or the activation of *neurog1* by Prdm14. However, if the promotion of neural plate border derivatives is the direct consequence of an expanded progenitor pool or requires the activity of other factors remains to be further addressed.

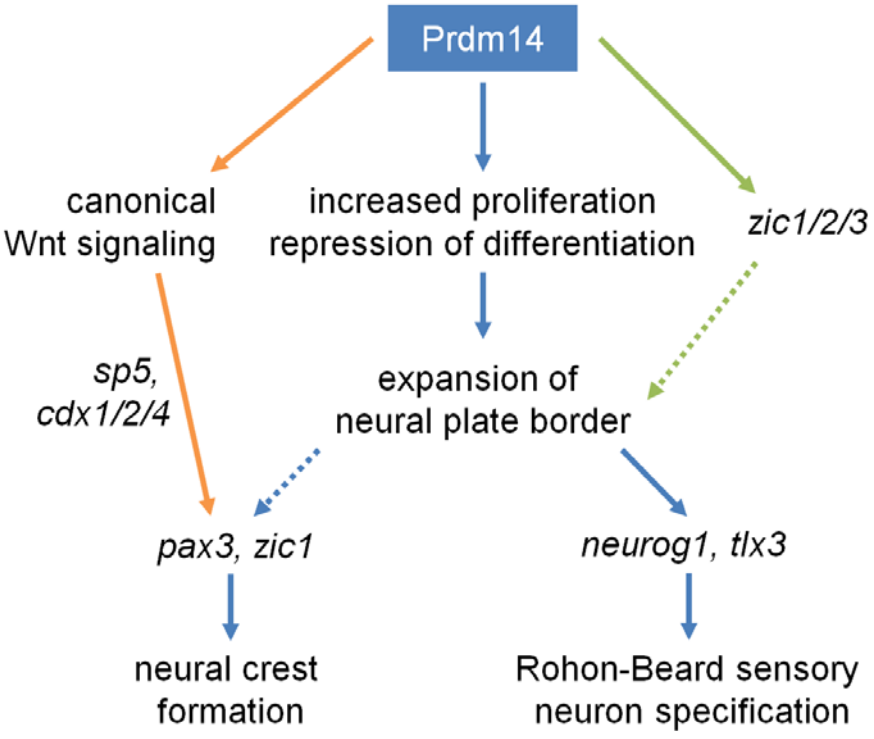

Fig. 5.1 Model for the function of Prdm14 in *X. laevis*. Prdm14 promotes a proliferative, undifferentiated state of progenitor cells. Furthermore, the expression of the *zic* genes is activated by Prdm14. Both processes might lead to the expansion of the neural plate border. Additionally, Prdm14 activates canonical Wnt-signaling which induces *pax3*/*zic1* and promotes neural crest formation. The ectopic differentiation of Rohon-Beard sensory neurons is likely due to the expansion of the neural plate border or the induction of *neurog1* by Prdm14.

Bibliography

Alaynick, W. A., T. M. Jessell, and S. L. Pfaff. 2011. SnapShot: spinal cord development. Cell 146: 178-178 e171.

Amaya, E. 2005. Xenomics. Genome research 15: 1683-1691.

Anders, S., and W. Huber. 2010. Differential expression analysis for sequence count data. Genome biology 11: R106.

Aoki, Y., N. Saint-Germain, M. Gyda, E. Magner-Fink, Y. H. Lee, C. Credidio, and J. P. Saint-Jeannet. 2003. Sox10 regulates the development of neural crest-derived melanocytes in Xenopus. Developmental biology 259: 19-33.

Ariizumi, T., S. Takahashi, T. C. Chan, Y. Ito, T. Michiue, and M. Asashima. 2009. Isolation and differentiation of Xenopus animal cap cells. Current protocols in stem cell biology Chapter 1: Unit 1D 5.

Aruga, J., and K. Mikoshiba. 2011. Role of BMP, FGF, calcium signaling, and Zic proteins in vertebrate neuroectodermal differentiation. Neurochemical research 36: 1286-1292.

Bae, C. J., B. Y. Park, Y. H. Lee, J. W. Tobias, C. S. Hong, and J. P. Saint-Jeannet. 2014. Identification of Pax3 and Zic1 targets in the developing neural crest. Developmental biology 386: 473-483.

Bang, A. G., N. Papalopulu, M. D. Goulding, and C. Kintner. 1999. Expression of Pax-3 in the lateral neural plate is dependent on a Wnt-mediated signal from posterior nonaxial mesoderm. Developmental biology 212: 366-380.

Bard-Chapeau, E. A., J. Jeyakani, C. H. Kok, J. Muller, B. Q. Chua, J. Gunaratne, A. Batagov, P. Jenjaroenpun, V. A. Kuznetsov, C. L. Wei, R. J. D'Andrea, G. Bourque, N. A. Jenkins, and N. G. Copeland. 2012. Ecotopic viral integration site 1 (EVI1) regulates multiple cellular processes important for cancer and is a synergistic partner for FOS protein in invasive tumors. Proceedings of the National Academy of Sciences of the United States of America 109: 2168-2173.

Baudat, F., J. Buard, C. Grey, A. Fledel-Alon, C. Ober, M. Przeworski, G. Coop, and B. de Massy. 2010. PRDM9 is a major determinant of meiotic recombination hotspots in humans and mice. Science 327: 836-840.

Beatus, P., and U. Lendahl. 1998. Notch and neurogenesis. Journal of neuroscience research 54: 125-136.

Bellefroid, E. J., C. Bourguignon, T. Hollemann, Q. Ma, D. J. Anderson, C. Kintner, and T. Pieler. 1996. X-MyT1, a Xenopus C2HC-type zinc finger protein with a regulatory function in neuronal differentiation. Cell 87: 1191-1202.

Bellmeyer, A., J. Krase, J. Lindgren, and C. LaBonne. 2003. The protooncogene c-myc is an essential regulator of neural crest formation in xenopus. Developmental cell 4: 827-839.

Bertrand, N., D. S. Castro, and F. Guillemot. 2002. Proneural genes and the specification of neural cell types. Nature reviews. Neuroscience 3: 517-530.

Bhat, N., H. J. Kwon, and B. B. Riley. 2013. A gene network that coordinates preplacodal competence and neural crest specification in zebrafish. Developmental biology 373: 107-117.

Bonev, B., P. Stanley, and N. Papalopulu. 2012. MicroRNA-9 Modulates Hes1 ultradian oscillations by forming a double-negative feedback loop. Cell reports 2: 10-18.

Borchers, A., and T. Pieler. 2010. Programming pluripotent precursor cells derived from Xenopus embryos to generate specific tissues and organs. Genes 1: 413-426.

Bouwmeester, T., S. Kim, Y. Sasai, B. Lu, and E. M. De Robertis. 1996. Cerberus is a head-inducing secreted factor expressed in the anterior endoderm of Spemann's organizer. Nature 382: 595-601.

Boy, S., J. Souopgui, M. A. Amato, M. Wegnez, T. Pieler, and M. Perron. 2004. XSEB4R, a novel RNA-binding protein involved in retinal cell differentiation downstream of bHLH proneural genes. Development 131: 851-862.

Boyer, L. A., T. I. Lee, M. F. Cole, S. E. Johnstone, S. S. Levine, J. P. Zucker, M. G. Guenther, R. M. Kumar, H. L. Murray, R. G. Jenner, D. K. Gifford, D. A. Melton, R. Jaenisch, and R. A. Young. 2005. Core transcriptional regulatory circuitry in human embryonic stem cells. Cell 122: 947-956.

Bray, S. J. 2006. Notch signalling: a simple pathway becomes complex. Nature reviews. Molecular cell biology 7: 678-689.

Brewster, R., J. Lee, and A. Ruiz i Altaba. 1998. Gli/Zic factors pattern the neural plate by defining domains of cell differentiation. Nature 393: 579-583.

Burton, A., J. Muller, S. Tu, P. Padilla-Longoria, E. Guccione, and M. E. Torres-Padilla. 2013. Single-cell profiling of epigenetic modifiers identifies PRDM14 as an inducer of cell fate in the mammalian embryo. Cell reports 5: 687-701.

Carofino, B. L., B. Ayanga, and M. J. Justice. 2013. A mouse model for inducible overexpression of Prdm14 results in rapid-onset and highly penetrant T-cell acute lymphoblastic leukemia (T-ALL). Disease models & mechanisms 6: 1494-1506.

Cau, E., S. Casarosa, and F. Guillemot. 2002. Mash1 and Ngn1 control distinct steps of determination and differentiation in the olfactory sensory neuron lineage. Development 129: 1871-1880.

Chalmers, A. D., D. Welchman, and N. Papalopulu. 2002. Intrinsic differences between the superficial and deep layers of the Xenopus ectoderm control primary neuronal differentiation. Developmental cell 2: 171-182.

Chan, Y. S., J. Goke, X. Lu, N. Venkatesan, B. Feng, I. H. Su, and H. H. Ng. 2013. A PRC2-dependent repressive role of PRDM14 in human embryonic stem cells and induced pluripotent stem cell reprogramming. Stem cells (Dayton, Ohio) 31: 682-692.

Chang, J. C., D. M. Meredith, P. R. Mayer, M. D. Borromeo, H. C. Lai, Y. H. Ou, and J. E. Johnson. 2013. Prdm13 mediates the balance of inhibitory and excitatory neurons in somatosensory circuits. Developmental cell 25: 182-195.

Cheung, M., M. C. Chaboissier, A. Mynett, E. Hirst, A. Schedl, and J. Briscoe. 2005. The transcriptional control of trunk neural crest induction, survival, and delamination. Developmental cell 8: 179-192.

Chia, N. Y., Y. S. Chan, B. Feng, X. Lu, Y. L. Orlov, D. Moreau, P. Kumar, L. Yang, J. Jiang, M. S. Lau, M. Huss, B. S. Soh, P. Kraus, P. Li, T.

Lufkin, B. Lim, N. D. Clarke, F. Bard, and H. H. Ng. 2010. A genome-wide RNAi screen reveals determinants of human embryonic stem cell identity. Nature 468: 316-320.

Chitnis, A., D. Henrique, J. Lewis, D. Ish-Horowicz, and C. Kintner. 1995. Primary neurogenesis in Xenopus embryos regulated by a homologue of the Drosophila neurogenic gene Delta. Nature 375: 761-766.

Chitnis, A. and C. Kintner. 1996. Sensitivity of proneural genes to lateral inhibition affects the pattern of primary neurons in Xenopus embryos. *Development* 122, 2295-301.

Christian, J. L., and R. T. Moon. 1993. Interactions between Xwnt-8 and Spemann organizer signaling pathways generate dorsoventral pattern in the embryonic mesoderm of Xenopus. Genes & development 7: 13-28.

Coffman, C. R., P. Skoglund, W. A. Harris, and C. R. Kintner. 1993. Expression of an extracellular deletion of Xotch diverts cell fate in Xenopus embryos. Cell 73: 659-671.

Coles, E. G., L. A. Taneyhill, and M. Bronner-Fraser. 2007. A critical role for Cadherin6B in regulating avian neural crest emigration. Developmental biology 312: 533-544.

Cornell, R. A., and J. S. Eisen. 2002. Delta/Notch signaling promotes formation of zebrafish neural crest by repressing Neurogenin 1 function. Development 129: 2639-2648.

Couly, G., A. Grapin-Botton, P. Coltey, B. Ruhin, and N. M. Le Douarin. 1998. Determination of the identity of the derivatives of the cephalic neural crest: incompatibility between Hox gene expression and lower jaw development. Development 125: 3445-3459.

Creazzo, T. L., R. E. Godt, L. Leatherbury, S. J. Conway, and M. L. Kirby. 1998. Role of cardiac neural crest cells in cardiovascular development. Annual review of physiology 60: 267-286.

Damianitsch, K., J. Melchert, and T. Pieler. 2009. XsFRP5 modulates endodermal organogenesis in Xenopus laevis. Developmental biology 329: 327-337.

Dawson, S. R., D. L. Turner, H. Weintraub, and S. M. Parkhurst. 1995. Specificity for the hairy/enhancer of split basic helix-loop-helix (bHLH) proteins maps outside the bHLH domain and suggests two separable modes of transcriptional repression. Molecular and cellular biology 15: 6923-6931.

de Croze, N., F. Maczkowiak, and A. H. Monsoro-Burq. 2011. Reiterative AP2a activity controls sequential steps in the neural crest gene regulatory network. Proceedings of the National Academy of Sciences of the United States of America 108: 155-160.

de la Calle-Mustienes, E., A. Glavic, J. Modolell, and J. L. Gomez-Skarmeta. 2002. Xiro homeoproteins coordinate cell cycle exit and primary neuron formation by upregulating neuronal-fate repressors and downregulating the cell-cycle inhibitor XGadd45-gamma. Mechanisms of development 119: 69-80.

de Souza, F. S., V. Gawantka, A. P. Gomez, H. Delius, S. L. Ang, and C. Niehrs. 1999. The zinc finger gene Xblimp1 controls anterior endomesodermal cell fate in Spemann's organizer. The EMBO journal 18: 6062-6072.

Delaune, E., P. Lemaire, and L. Kodjabachian. 2005. Neural induction in Xenopus requires early FGF signalling in addition to BMP inhibition. Development 132: 299-310.

Delwel, R., T. Funabiki, B. L. Kreider, K. Morishita, and J. N. Ihle. 1993. Four of the seven zinc fingers of the Evi-1 myeloid-transforming gene are required for sequence-specific binding to GA(C/T)AAGA(T/C)AAGATAA. Molecular and cellular biology 13: 4291-4300.

Dennis, G., Jr., B. T. Sherman, D. A. Hosack, J. Yang, W. Gao, H. C. Lane, and R. A. Lempicki. 2003. DAVID: Database for Annotation, Visualization, and Integrated Discovery. Genome biology 4: P3.

Dent, J. A., A. G. Polson, and M. W. Klymkowsky. 1989. A whole-mount immunocytochemical analysis of the expression of the intermediate filament protein vimentin in Xenopus. Development 105: 61-74.

Dettman, E. J., and M. J. Justice. 2008. The zinc finger SET domain gene Prdm14 is overexpressed in lymphoblastic lymphomas with retroviral insertions at Evi32. PloS one 3: e3823.

Dettman, E. J., S. J. Simko, B. Ayanga, B. L. Carofino, J. F. Margolin, H. C. Morse, 3rd, and M. J. Justice. 2011. Prdm14 initiates lymphoblastic leukemia after expanding a population of cells resembling common lymphoid progenitors. Oncogene 30: 2859-2873.

Ding, H. L., D. E. Clouthier, and K. B. Artinger. 2013. Redundant roles of PRDM family members in zebrafish craniofacial development. Developmental dynamics : an official publication of the American Association of Anatomists 242: 67-79.

Dobin, A., C. A. Davis, F. Schlesinger, J. Drenkow, C. Zaleski, S. Jha, P. Batut, M. Chaisson, and T. R. Gingeras. 2013. STAR: ultrafast universal RNA-seq aligner. Bioinformatics 29: 15-21.

Dottori, M., M. K. Gross, P. Labosky, and M. Goulding. 2001. The winged-helix transcription factor Foxd3 suppresses interneuron differentiation and promotes neural crest cell fate. Development 128: 4127-4138.

Duan, Z., R. E. Person, H. H. Lee, S. Huang, J. Donadieu, R. Badolato, H. L. Grimes, T. Papayannopoulou, and M. S. Horwitz. 2007. Epigenetic regulation of protein-coding and microRNA genes by the Gfi1-interacting tumor suppressor PRDM5. Molecular and cellular biology 27: 6889-6902.

Dubois, L., L. Bally-Cuif, M. Crozatier, J. Moreau, L. Paquereau, and A. Vincent. 1998. XCoe2, a transcription factor of the Col/Olf-1/EBF family involved in the specification of primary neurons in Xenopus. Current biology : CB 8: 199-209.

Eagleson, G. W., and W. A. Harris. 1990. Mapping of the presumptive brain regions in the neural plate of Xenopus laevis. Journal of neurobiology 21: 427-440.

Eguchi, R., E. Yoshigai, T. Koga, S. Kuhara, and K. Tashiro. 2015. Spatiotemporal expression of Prdm genes during Xenopus development. Cytotechnology.

Ellis, P., B. M. Fagan, S. T. Magness, S. Hutton, O. Taranova, S. Hayashi, A. McMahon, M. Rao, and L. Pevny. 2004. SOX2, a persistent marker for multipotential neural stem cells derived from embryonic stem cells, the embryo or the adult. Developmental neuroscience 26: 148-165.

Endo, Y., N. Osumi, and Y. Wakamatsu. 2002. Bimodal functions of Notch-mediated signaling are involved in neural crest formation during avian ectoderm development. Development 129: 863-873.

Eom, G. H., K. Kim, S. M. Kim, H. J. Kee, J. Y. Kim, H. M. Jin, J. R. Kim, J. H. Kim, N. Choe, K. B. Kim, J. Lee, H. Kook, N. Kim, and S. B. Seo. 2009. Histone methyltransferase PRDM8 regulates mouse testis steroidogenesis. Biochemical and biophysical research communications 388: 131-136.

Fodde, R., and T. Brabletz. 2007. Wnt/beta-catenin signaling in cancer stemness and malignant behavior. Current opinion in cell biology 19: 150-158.

Fog, C. K., G. G. Galli, and A. H. Lund. 2012. PRDM proteins: important players in differentiation and disease. BioEssays : news and reviews in molecular, cellular and developmental biology 34: 50-60.

Friedmann, D. R., A. Aguilar, J. Fan, M. V. Nachury, and R. Marmorstein. 2012. Structure of the alpha-tubulin acetyltransferase, alphaTAT1, and implications for tubulin-specific acetylation. Proceedings of the National Academy of Sciences of the United States of America 109: 19655-19660.

Fujimi, T. J., M. Hatayama, and J. Aruga. 2012. Xenopus Zic3 controls notochord and organizer development through suppression of the Wnt/beta-catenin signaling pathway. Developmental biology 361: 220-231.

Funabiki, T., B. L. Kreider, and J. N. Ihle. 1994. The carboxyl domain of zinc fingers of the Evi-1 myeloid transforming gene binds a consensus sequence of GAAGATGAG. Oncogene 9: 1575-1581.

Gammill, L. S., and M. Bronner-Fraser. 2002. Genomic analysis of neural crest induction. Development 129: 5731-5741.

Gammill, L. S., and M. Bronner-Fraser. 2003. Neural crest specification: migrating into genomics. Nature reviews. Neuroscience 4: 795-805.

Ge, W., F. He, K. J. Kim, B. Blanchi, V. Coskun, L. Nguyen, X. Wu, J. Zhao, J. I. Heng, K. Martinowich, J. Tao, H. Wu, D. Castro, M. M. Sobeih, G. Corfas, J. G. Gleeson, M. E. Greenberg, F. Guillemot, and Y. E. Sun. 2006. Coupling of cell migration with neurogenesis by proneural bHLH factors. Proceedings of the National Academy of Sciences of the United States of America 103: 1319-1324.

Geach, T. J., and L. B. Zimmerman. 2011. Developmental genetics in Xenopus tropicalis. Methods in molecular biology (Clifton, N.J.) 770: 77-117.

Gleason, K. K., V. R. Dondeti, H. L. Hsia, E. R. Cochran, J. Gumulak-Smith, and M. S. Saha. 2003. The vesicular glutamate transporter 1 (xVGlut1) is expressed in discrete regions of the developing Xenopus laevis nervous system. Gene expression patterns : GEP 3: 503-507.

Goodfellow, M., N. E. Phillips, C. Manning, T. Galla, and N. Papalopulu. 2014. microRNA input into a neural ultradian oscillator controls emergence and timing of alternative cell states. Nature communications 5: 3399.

Grabole, N., J. Tischler, J. A. Hackett, S. Kim, F. Tang, H. G. Leitch, E. Magnusdottir, and M. A. Surani. 2013. Prdm14 promotes germline fate and naive pluripotency by repressing FGF signalling and DNA methylation. EMBO reports 14: 629-637.

Graham, V., J. Khudyakov, P. Ellis, and L. Pevny. 2003. SOX2 functions to maintain neural progenitor identity. Neuron 39: 749-765.

Grainger, R. M. 2012. Xenopus tropicalis as a model organism for genetics and genomics: past, present, and future. Methods in molecular biology (Clifton, N.J.) 917: 3-15.

Groves, A. K., and C. LaBonne. 2014. Setting appropriate boundaries: fate, patterning and competence at the neural plate border. Developmental biology 389: 2-12.

Grunz, H., and L. Tacke. 1989. Neural differentiation of Xenopus laevis ectoderm takes place after disaggregation and delayed reaggregation without inducer. Cell differentiation and development : the official journal of the International Society of Developmental Biologists 28: 211-217.

Guo, X., T. Zhang, Z. Hu, Y. Zhang, Z. Shi, Q. Wang, Y. Cui, F. Wang, H. Zhao, and Y. Chen. 2014. Efficient RNA/Cas9-mediated genome editing in Xenopus tropicalis. Development 141: 707-714.

Hackett, J. A., S. Dietmann, K. Murakami, T. A. Down, H. G. Leitch, and M. A. Surani. 2013. Synergistic mechanisms of DNA demethylation during transition to ground-state pluripotency. Stem cell reports 1: 518-531.

Hanotel, J., N. Bessodes, A. Thelie, M. Hedderich, K. Parain, B. Van Driessche, O. Brandao Kde, S. Kricha, M. C. Jorgensen, A. Grapin-Botton, P. Serup, C. Van Lint, M. Perron, T. Pieler, K. A. Henningfeld, and E. J. Bellefroid. 2014. The Prdm13 histone methyltransferase encoding gene is a Ptf1a-Rbpj downstream target that suppresses glutamatergic and promotes GABAergic neuronal fate in the dorsal neural tube. Developmental biology 386: 340-357.

Hardcastle, Z., and N. Papalopulu. 2000. Distinct effects of XBF-1 in regulating the cell cycle inhibitor p27(XIC1) and imparting a neural fate. Development 127: 1303-1314.

Harland, R. M. 1991. In situ hybridization: an improved whole-mount method for Xenopus embryos. Methods in cell biology 36: 685-695.

Hartenstein, V. 1989. Early neurogenesis in Xenopus: the spatio-temporal pattern of proliferation and cell lineages in the embryonic spinal cord. Neuron 3: 399-411.

Hartenstein, V. 1993. Early pattern of neuronal differentiation in the Xenopus embryonic brainstem and spinal cord. The Journal of comparative neurology 328: 213-231.

Hatakeyama, J., and R. Kageyama. 2006. Notch1 expression is spatiotemporally correlated with neurogenesis and negatively regulated by Notch1-independent Hes genes in the developing nervous system. Cereb Cortex 16 Suppl 1: i132-137.

Hayashi, K., K. Yoshida, and Y. Matsui. 2005. A histone H3 methyltransferase controls epigenetic events required for meiotic prophase. Nature 438: 374-378.

Heasman, J. 2002. Morpholino oligos: making sense of antisense? Developmental biology 243: 209-214.

Heasman, J., M. Kofron, and C. Wylie. 2000. Beta-catenin signaling activity dissected in the early Xenopus embryo: a novel antisense approach. Developmental biology 222: 124-134.

Hemmati-Brivanlou, A., and D. A. Melton. 1992. A truncated activin receptor inhibits mesoderm induction and formation of axial structures in Xenopus embryos. Nature 359: 609-614.

Hemmati-Brivanlou, A., and D. A. Melton. 1994. Inhibition of activin receptor signaling promotes neuralization in Xenopus. Cell 77: 273-281.

Hemmati-Brivanlou, A., and D. Melton. 1997. Vertebrate neural induction. Annual review of neuroscience 20: 43-60.

Hemmati-Brivanlou, A., O. G. Kelly, and D. A. Melton. 1994. Follistatin, an antagonist of activin, is expressed in the Spemann organizer and displays direct neuralizing activity. Cell 77: 283-295.

Hernandez-Lagunas, L., D. R. Powell, J. Law, K. A. Grant, and K. B. Artinger. 2011. prdm1a and olig4 act downstream of Notch signaling to regulate cell fate at the neural plate border. Developmental biology 356: 496-505.

Hernandez-Lagunas, L., I. F. Choi, T. Kaji, P. Simpson, C. Hershey, Y. Zhou, L. Zon, M. Mercola, and K. B. Artinger. 2005. Zebrafish narrowminded disrupts the transcription factor prdm1 and is required for neural crest and sensory neuron specification. Developmental biology 278: 347-357.

Hirata, H., S. Yoshiura, T. Ohtsuka, Y. Bessho, T. Harada, K. Yoshikawa, and R. Kageyama. 2002. Oscillatory expression of the bHLH factor Hes1 regulated by a negative feedback loop. Science 298: 840-843.

Hohenauer, T., and A. W. Moore. 2012. The Prdm family: expanding roles in stem cells and development. Development 139: 2267-2282.

Holland, J. D., A. Klaus, A. N. Garratt, and W. Birchmeier. 2013. Wnt signaling in stem and cancer stem cells. Current opinion in cell biology 25: 254-264.

Hollemann, T., and T. Pieler. 1999. Xpitx-1: a homeobox gene expressed during pituitary and cement gland formation of Xenopus embryos. Mechanisms of development 88: 249-252.

Hong, C. S., and J. P. Saint-Jeannet. 2007. The activity of Pax3 and Zic1 regulates three distinct cell fates at the neural plate border. Molecular biology of the cell 18: 2192-2202.

Houtmeyers, R., J. Souopgui, S. Tejpar, and R. Arkell. 2013. The ZIC gene family encodes multi-functional proteins essential for patterning and morphogenesis. Cellular and molecular life sciences : CMLS 70: 3791-3811.

Huang, S. 2002. Histone methyltransferases, diet nutrients and tumour suppressors. Nature reviews. Cancer 2: 469-476.

Hubers, A. J., D. A. Heideman, S. A. Burgers, G. J. Herder, P. J. Sterk, R. J. Rhodius, H. J. Smit, F. Krouwels, A. Welling, B. I. Witte, S. Duin, R. Koning, E. F. Comans, R. D. Steenbergen, P. E. Postmus, G. A. Meijer, P. J. Snijders, E. F. Smit, and E. Thunnissen. 2015. DNA hypermethylation analysis in sputum for the diagnosis of lung cancer: training validation set approach. British journal of cancer 112: 1105-1113.

Imayoshi, I., and R. Kageyama. 2011. The role of Notch signaling in adult neurogenesis. Molecular neurobiology 44: 7-12.

Imayoshi, I., and R. Kageyama. 2014. bHLH factors in self-renewal, multipotency, and fate choice of neural progenitor cells. Neuron 82: 9-23.

Jessell, T. M. 2000. Neuronal specification in the spinal cord: inductive signals and transcriptional codes. Nature reviews. Genetics 1: 20-29.

Johnson, A. D., E. Richardson, R. F. Bachvarova, and B. I. Crother. 2011. Evolution of the germ line-soma relationship in vertebrate embryos. Reproduction (Cambridge, England) 141: 291-300.

Kageyama, R., T. Ohtsuka, H. Shimojo, and I. Imayoshi. 2008. Dynamic Notch signaling in neural progenitor cells and a revised view of lateral inhibition. Nature neuroscience 11: 1247-1251.

Kengaku, M., and H. Okamoto. 1995. bFGF as a possible morphogen for the anteroposterior axis of the central nervous system in Xenopus. Development 121: 3121-3130.

Khudyakov, J., and M. Bronner-Fraser. 2009. Comprehensive spatiotemporal analysis of early chick neural crest network genes. Developmental dynamics : an official publication of the American Association of Anatomists 238: 716-723.

Kim, K. C., L. Geng, and S. Huang. 2003. Inactivation of a histone methyltransferase by mutations in human cancers. Cancer research 63: 7619-7623.

Kinameri, E., T. Inoue, J. Aruga, I. Imayoshi, R. Kageyama, T. Shimogori, and A. W. Moore. 2008. Prdm proto-oncogene transcription factor family expression and interaction with the Notch-Hes pathway in mouse neurogenesis. PloS one 3: e3859.

Kiyota, T., and T. Kinoshita. 2002. Cysteine-rich region of X-Serrate-1 is required for activation of Notch signaling in Xenopus primary neurogenesis. The International journal of developmental biology 46: 1057-1060.

Kiyota, T., H. Jono, S. Kuriyama, K. Hasegawa, S. Miyatani, and T. Kinoshita. 2001. X-Serrate-1 is involved in primary neurogenesis in Xenopus laevis in a complementary manner with X-Delta-1. Development genes and evolution 211: 367-376.

Klisch, T. 2006. Transcriptional control in the context of primary neurogenesis. Göttingen Center for Molecular Biosciences

Klymkowsky, M. W., C. C. Rossi, and K. B. Artinger. 2010. Mechanisms driving neural crest induction and migration in the zebrafish and Xenopus laevis. Cell adhesion & migration 4: 595-608.

Kolm, P. J., and H. L. Sive. 1995. Efficient hormone-inducible protein function in Xenopus laevis. Developmental biology 171: 267-272.

Komai, T., H. Iwanari, Y. Mochizuki, T. Hamakubo, and Y. Shinkai. 2009. Expression of the mouse PR domain protein Prdm8 in the developing central nervous system. Gene expression patterns : GEP 9: 503-514.

Kondo, T., A. J. Matsuoka, A. Shimomura, K. R. Koehler, R. J. Chan, J. M. Miller, E. F. Srour, and E. Hashino. 2011. Wnt signaling promotes neuronal differentiation from mesenchymal stem cells through activation of Tlx3. Stem cells (Dayton, Ohio) 29: 836-846.

Korinek, V., N. Barker, P. J. Morin, D. van Wichen, R. de Weger, K. W. Kinzler, B. Vogelstein, and H. Clevers. 1997. Constitutive transcriptional activation by a beta-catenin-Tcf complex in APC-/- colon carcinoma. Science 275: 1784-1787.

Kouzarides, T. 2007. Chromatin modifications and their function. Cell 128: 693-705.

Koyano-Nakagawa, N., and C. Kintner. 2005. The expression and function of MTG/ETO family proteins during neurogenesis. Developmental biology 278: 22-34.

Koyano-Nakagawa, N., J. Kim, D. Anderson, and C. Kintner. 2000. Hes6 acts in a positive feedback loop with the neurogenins to promote neuronal differentiation. Development 127: 4203-4216.

Kroll, K. L., A. N. Salic, L. M. Evans, and M. W. Kirschner. 1998. Geminin, a neuralizing molecule that demarcates the future neural plate at the onset of gastrulation. Development 125: 3247-3258.

Kuo, T. C., and K. L. Calame. 2004. B lymphocyte-induced maturation protein (Blimp)-1, IFN regulatory factor (IRF)-1, and IRF-2 can bind to the same regulatory sites. J Immunol 173: 5556-5563.

Kuroda, H., O. Wessely, and E. M. De Robertis. 2004. Neural induction in Xenopus: requirement for ectodermal and endomesodermal signals via Chordin, Noggin, beta-Catenin, and Cerberus. PLoS biology 2: E92.

Kuroda, H., L. Fuentealba, A. Ikeda, B. Reversade, and E. M. De Robertis. 2005. Default neural induction: neuralization of dissociated Xenopus cells is mediated by Ras/MAPK activation. Genes & development 19: 1022-1027.

Laemmli, U. K. 1970. Cleavage of structural proteins during the assembly of the head of bacteriophage T4. Nature 227: 680-685.

Lamb, T. M., and R. M. Harland. 1995. Fibroblast growth factor is a direct neural inducer, which combined with noggin generates anterior-posterior neural pattern. Development 121: 3627-3636.

Lamb, T. M., A. K. Knecht, W. C. Smith, S. E. Stachel, A. N. Economides, N. Stahl, G. D. Yancopolous, and R. M. Harland. 1993. Neural induction by the secreted polypeptide noggin. Science 262: 713-718.

Lamborghini, J. E. 1980. Rohon-beard cells and other large neurons in Xenopus embryos originate during gastrulation. The Journal of comparative neurology 189: 323-333.

Le Douarin, N. M., and M. A. Teillet. 1973. The migration of neural crest cells to the wall of the digestive tract in avian embryo. Journal of embryology and experimental morphology 30: 31-48.

Le Douarin, N. M., and J. Smith. 1988. Development of the peripheral nervous system from the neural crest. Annual review of cell biology 4: 375-404.

Le Douarin, N. M., S. Creuzet, G. Couly, and E. Dupin. 2004. Neural crest cell plasticity and its limits. Development 131: 4637-4650.

Le Dreau, G., and E. Marti. 2012. Dorsal-ventral patterning of the neural tube: a tale of three signals. Developmental neurobiology 72: 1471-1481.

Leclerc, C., I. Neant, and M. Moreau. 2012. The calcium: an early signal that initiates the formation of the nervous system during embryogenesis. Frontiers in molecular neuroscience 5: 3.

Lefebvre, V., B. Dumitriu, A. Penzo-Mendez, Y. Han, and B. Pallavi. 2007. Control of cell fate and differentiation by Sry-related high-mobility-group box (Sox) transcription factors. The international journal of biochemistry & cell biology 39: 2195-2214.

Lei, Y., X. Guo, Y. Liu, Y. Cao, Y. Deng, X. Chen, C. H. Cheng, I. B. Dawid, Y. Chen, and H. Zhao. 2012. Efficient targeted gene disruption in Xenopus embryos using engineered transcription activator-like effector nucleases (TALENs). Proceedings of the National Academy of Sciences of the United States of America 109: 17484-17489.

Lewis, J. 1996. Neurogenic genes and vertebrate neurogenesis. Current opinion in neurobiology 6: 3-10.

Li, Y., and N. E. Baker. 2001. Proneural enhancement by Notch overcomes Suppressor-of-Hairless repressor function in the developing Drosophila eye. Current biology : CB 11: 330-338.

Lindsell, C. E., J. Boulter, G. diSibio, A. Gossler, and G. Weinmaster. 1996. Expression patterns of Jagged, Delta1, Notch1, Notch2, and Notch3 genes identify ligand-receptor pairs that may function in neural development. Molecular and cellular neurosciences 8: 14-27.

Linker, C., and C. D. Stern. 2004. Neural induction requires BMP inhibition only as a late step, and involves signals other than FGF and Wnt antagonists. Development 131: 5671-5681.

Liu, C., W. Ma, W. Su, and J. Zhang. 2012. Prdm14 acts upstream of islet2 transcription to regulate axon growth of primary motoneurons in zebrafish. Development 139: 4591-4600.

Liu, Y., D. Luo, Y. Lei, W. Hu, H. Zhao, and C. H. Cheng. 2014. A highly effective TALEN-mediated approach for targeted gene disruption in Xenopus tropicalis and zebrafish. Methods 69: 58-66.

Louvi, A., and S. Artavanis-Tsakonas. 2006. Notch signalling in vertebrate neural development. Nature reviews. Neuroscience 7: 93-102.

Luo, T., Y. H. Lee, J. P. Saint-Jeannet, and T. D. Sargent. 2003. Induction of neural crest in Xenopus by transcription factor AP2alpha. Proceedings of the National Academy of Sciences of the United States of America 100: 532-537.

Ma, Q., C. Kintner, and D. J. Anderson. 1996. Identification of neurogenin, a vertebrate neuronal determination gene. Cell 87: 43-52.

Ma, Z., T. Swigut, A. Valouev, A. Rada-Iglesias, and J. Wysocka. 2011. Sequence-specific regulator Prdm14 safeguards mouse ESCs from entering extraembryonic endoderm fates. Nature structural & molecular biology 18: 120-127.

McGrew, L. L., S. Hoppler, and R. T. Moon. 1997. Wnt and FGF pathways cooperatively pattern anteroposterior neural ectoderm in Xenopus. Mechanisms of development 69: 105-114.

Meani, N., F. Pezzimenti, G. Deflorian, M. Mione, and M. Alcalay. 2009. The tumor suppressor PRDM5 regulates Wnt signaling at early stages of zebrafish development. PloS one 4: e4273.

Merzdorf, C. S., and H. L. Sive. 2006. The zic1 gene is an activator of Wnt signaling. The International journal of developmental biology 50: 611-617.

Meulemans, D., and M. Bronner-Fraser. 2004. Gene-regulatory interactions in neural crest evolution and development. Developmental cell 7: 291-299.

Milet, C., F. Maczkowiak, D. D. Roche, and A. H. Monsoro-Burq. 2013. Pax3 and Zic1 drive induction and differentiation of multipotent, migratory, and functional neural crest in Xenopus embryos. Proceedings of the National Academy of Sciences of the United States of America 110: 5528-5533.

Miyata, T., M. Okamoto, T. Shinoda, and A. Kawaguchi. 2014. Interkinetic nuclear migration generates and opposes ventricular-zone crowding: insight into tissue mechanics. Frontiers in cellular neuroscience 8: 473.

Mizuseki, K., M. Kishi, M. Matsui, S. Nakanishi, and Y. Sasai. 1998a. Xenopus Zic-related-1 and Sox-2, two factors induced by chordin, have distinct activities in the initiation of neural induction. Development 125: 579-587.

Mizuseki, K., M. Kishi, K. Shiota, S. Nakanishi, and Y. Sasai. 1998b. SoxD: an essential mediator of induction of anterior neural tissues in Xenopus embryos. Neuron 21: 77-85.

Momiji, H., and N. A. Monk. 2009. Oscillatory Notch-pathway activity in a delay model of neuronal differentiation. Physical review. E, Statistical, nonlinear, and soft matter physics 80: 021930.

Monsoro-Burq, A. H., R. B. Fletcher, and R. M. Harland. 2003. Neural crest induction by paraxial mesoderm in Xenopus embryos requires FGF signals. Development 130: 3111-3124.

Monsoro-Burq, A. H., E. Wang, and R. Harland. 2005. Msx1 and Pax3 cooperate to mediate FGF8 and WNT signals during Xenopus neural crest induction. Developmental cell 8: 167-178.

Moody, S. A., and H. S. Je. 2002. Neural induction, neural fate stabilization, and neural stem cells. TheScientificWorldJournal 2: 1147-1166.

Moreau, M., I. Neant, S. E. Webb, A. L. Miller, and C. Leclerc. 2008. Calcium signalling during neural induction in Xenopus laevis embryos. Philosophical transactions of the Royal Society of London. Series B, Biological sciences 363: 1371-1375.

Moussa, H., and I. Sidhom. 2013. NKX2-5, SIL/TAL and TLX3/HOX11L2 expression in Egyptian pediatric T-cell acute lymphoblastic leukemia. Asia-Pacific journal of clinical oncology.

Munoz-Sanjuan, I., and A. H. Brivanlou. 2002. Neural induction, the default model and embryonic stem cells. Nature reviews. Neuroscience 3: 271-280.

Nagy, V., T. Cole, C. Van Campenhout, T. M. Khoung, C. Leung, S. Vermeiren, M. Novatchkova, D. Wenzel, D. Cikes, A. A. Polyansky, I. Kozieradzki, A. Meixner, E. J. Bellefroid, G. G. Neely, and J. M. Penninger. 2015. The evolutionarily conserved transcription factor PRDM12 controls sensory neuron development and pain perception. Cell Cycle: 0.

Nakaki, F., and M. Saitou. 2014. PRDM14: a unique regulator for pluripotency and epigenetic reprogramming. Trends in biochemical sciences 39: 289-298.

Nakata, K., T. Nagai, J. Aruga, and K. Mikoshiba. 1997. Xenopus Zic3, a primary regulator both in neural and neural crest development. Proceedings of the National Academy of Sciences of the United States of America 94: 11980-11985.

Nakata, K., T. Nagai, J. Aruga, and K. Mikoshiba. 1998. Xenopus Zic family and its role in neural and neural crest development. Mechanisms of development 75: 43-51.

Nakayama, T., M. B. Fish, M. Fisher, J. Oomen-Hajagos, G. H. Thomsen, and R. M. Grainger. 2013. Simple and efficient CRISPR/Cas9-mediated targeted mutagenesis in Xenopus tropicalis. Genesis 51: 835-843.

Nelson, B. R., and T. A. Reh. 2008. Relationship between Delta-like and proneural bHLH genes during chick retinal development. Developmental dynamics : an official publication of the American Association of Anatomists 237: 1565-1580.

Nguyen, L., A. Besson, J. I. Heng, C. Schuurmans, L. Teboul, C. Parras, A. Philpott, J. M. Roberts, and F. Guillemot. 2006. p27kip1 independently promotes neuronal differentiation and migration in the cerebral cortex. Genes & development 20: 1511-1524.

Nichane, M., N. de Croze, X. Ren, J. Souopgui, A. H. Monsoro-Burq, and E. J. Bellefroid. 2008. Hairy2-Id3 interactions play an essential role in

Xenopus neural crest progenitor specification. Developmental biology 322: 355-367.

Nieber, F., T. Pieler, and K. A. Henningfeld. 2009. Comparative expression analysis of the neurogenins in Xenopus tropicalis and Xenopus laevis. Developmental dynamics : an official publication of the American Association of Anatomists 238: 451-458.

Nieuwkoop, P.D., Faber, J. (Eds.) (1967). Normal table of *Xenopus laevis* (Daudin). Second Edition. North Holland Publ. Co. Amsterdam.

Nikitina, N., T. Sauka-Spengler, and M. Bronner-Fraser. 2008. Dissecting early regulatory relationships in the lamprey neural crest gene network. Proceedings of the National Academy of Sciences of the United States of America 105: 20083-20088.

Nishikawa, N., M. Toyota, H. Suzuki, T. Honma, T. Fujikane, T. Ohmura, T. Nishidate, M. Ohe-Toyota, R. Maruyama, T. Sonoda, Y. Sasaki, T. Urano, K. Imai, K. Hirata, and T. Tokino. 2007. Gene amplification and overexpression of PRDM14 in breast cancers. Cancer research 67: 9649-9657.

Nutt, S. L., O. J. Bronchain, K. O. Hartley, and E. Amaya. 2001. Comparison of morpholino based translational inhibition during the development of Xenopus laevis and Xenopus tropicalis. Genesis 30: 110-113.

Ohinata, Y., H. Ohta, M. Shigeta, K. Yamanaka, T. Wakayama, and M. Saitou. 2009. A signaling principle for the specification of the germ cell lineage in mice. Cell 137: 571-584.

Ohinata, Y., B. Payer, D. O'Carroll, K. Ancelin, Y. Ono, M. Sano, S. C. Barton, T. Obukhanych, M. Nussenzweig, A. Tarakhovsky, M. Saitou, and M. A. Surani. 2005. Blimp1 is a critical determinant of the germ cell lineage in mice. Nature 436: 207-213.

Ohkawara, B., and C. Niehrs. 2011. An ATF2-based luciferase reporter to monitor non-canonical Wnt signaling in Xenopus embryos. Developmental dynamics : an official publication of the American Association of Anatomists 240: 188-194.

Okashita, N., Y. Kumaki, K. Ebi, M. Nishi, Y. Okamoto, M. Nakayama, S. Hashimoto, T. Nakamura, K. Sugasawa, N. Kojima, T. Takada, M. Okano, and Y. Seki. 2014. PRDM14 promotes active DNA demethylation through the ten-eleven translocation (TET)-mediated base excision repair pathway in embryonic stem cells. Development 141: 269-280.

Olesnicky, E., L. Hernandez-Lagunas, and K. B. Artinger. 2010. prdm1a Regulates sox10 and islet1 in the development of neural crest and Rohon-Beard sensory neurons. Genesis 48: 656-666.

Olson, E. C., A. F. Schinder, J. L. Dantzker, E. A. Marcus, N. C. Spitzer, and W. A. Harris. 1998. Properties of ectopic neurons induced by Xenopus neurogenin1 misexpression. Molecular and cellular neurosciences 12: 281-299.

Ozair, M. Z., C. Kintner, and A. H. Brivanlou. 2013. Neural induction and early patterning in vertebrates. Wiley interdisciplinary reviews. Developmental biology 2: 479-498.

Papalopulu, N., and C. Kintner. 1996. A posteriorising factor, retinoic acid, reveals that anteroposterior patterning controls the timing of neuronal differentiation in Xenopus neuroectoderm. Development 122: 3409-3418.

Papanayotou, C., A. Mey, A. M. Birot, Y. Saka, S. Boast, J. C. Smith, J. Samarut, and C. D. Stern. 2008. A mechanism regulating the onset of Sox2 expression in the embryonic neural plate. PLoS biology 6: e2.

Park, D. S., J. H. Seo, M. Hong, W. Bang, J. K. Han, and S. C. Choi. 2013. Role of Sp5 as an essential early regulator of neural crest specification in xenopus. Developmental dynamics : an official publication of the American Association of Anatomists 242: 1382-1394.

Patterson, K. D., and P. A. Krieg. 1999. Hox11-family genes XHox11 and XHox11L2 in xenopus: XHox11L2 expression is restricted to a subset of the primary sensory neurons. Developmental dynamics : an official publication of the American Association of Anatomists 214: 34-43.

Pegoraro, C., and A. H. Monsoro-Burq. 2013. Signaling and transcriptional regulation in neural crest specification and migration: lessons from xenopus embryos. Wiley interdisciplinary reviews. Developmental biology 2: 247-259.

Penzel, R., R. Oschwald, Y. Chen, L. Tacke, and H. Grunz. 1997. Characterization and early embryonic expression of a neural specific transcription factor xSOX3 in Xenopus laevis. The International journal of developmental biology 41: 667-677.

Pera, E. M., A. Ikeda, E. Eivers, and E. M. De Robertis. 2003. Integration of IGF, FGF, and anti-BMP signals via Smad1 phosphorylation in neural induction. Genes & development 17: 3023-3028.

Pera, E. M., H. Acosta, N. Gouignard, M. Climent, and I. Arregi. 2014. Active signals, gradient formation and regional specificity in neural induction. Experimental cell research 321: 25-31.

Perez, S. E., S. Rebelo, and D. J. Anderson. 1999. Early specification of sensory neuron fate revealed by expression and function of neurogenins in the chick embryo. Development 126: 1715-1728.

Perron, M., K. Opdecamp, K. Butler, W. A. Harris, and E. J. Bellefroid. 1999. X-ngnr-1 and Xath3 promote ectopic expression of sensory neuron markers in the neurula ectoderm and have distinct inducing properties in the retina. Proceedings of the National Academy of Sciences of the United States of America 96: 14996-15001.

Pevny, L., and M. Placzek. 2005. SOX genes and neural progenitor identity. Current opinion in neurobiology 15: 7-13.

Piccolo, S., Y. Sasai, B. Lu, and E. M. De Robertis. 1996. Dorsoventral patterning in Xenopus: inhibition of ventral signals by direct binding of chordin to BMP-4. Cell 86: 589-598.

Piccolo, S., E. Agius, L. Leyns, S. Bhattacharyya, H. Grunz, T. Bouwmeester, and E. M. De Robertis. 1999. The head inducer Cerberus is a multifunctional antagonist of Nodal, BMP and Wnt signals. Nature 397: 707-710.

Pinheiro, I., R. Margueron, N. Shukeir, M. Eisold, C. Fritzsch, F. M. Richter, G. Mittler, C. Genoud, S. Goyama, M. Kurokawa, J. Son, D. Reinberg, M. Lachner, and T. Jenuwein. 2012. Prdm3 and Prdm16 are H3K9me1 methyltransferases required for mammalian heterochromatin integrity. Cell 150: 948-960.

Plouhinec, J. L., D. D. Roche, C. Pegoraro, A. L. Figueiredo, F. Maczkowiak, L. J. Brunet, C. Milet, J. P. Vert, N. Pollet, R. M. Harland, and A. H. Monsoro-Burq. 2014. Pax3 and Zic1 trigger the

early neural crest gene regulatory network by the direct activation of multiple key neural crest specifiers. Developmental biology 386: 461-472.

Pohl, B. S., and W. Knochel. 2001. Overexpression of the transcriptional repressor FoxD3 prevents neural crest formation in Xenopus embryos. Mechanisms of development 103: 93-106.

Pourebrahim, R., R. Houtmeyers, S. Ghogomu, S. Janssens, A. Thelie, H. T. Tran, T. Langenberg, K. Vleminckx, E. Bellefroid, J. J. Cassiman, and S. Tejpar. 2011. Transcription factor Zic2 inhibits Wnt/beta-catenin protein signaling. The Journal of biological chemistry 286: 37732-37740.

Powell, D. R., L. Hernandez-Lagunas, K. LaMonica, and K. B. Artinger. 2013. Prdm1a directly activates foxd3 and tfap2a during zebrafish neural crest specification. Development 140: 3445-3455.

Powell, L. M., and A. P. Jarman. 2008. Context dependence of proneural bHLH proteins. Current opinion in genetics & development 18: 411-417.

Pozzoli, O., A. Bosetti, L. Croci, G. G. Consalez, and M. L. Vetter. 2001. Xebf3 is a regulator of neuronal differentiation during primary neurogenesis in Xenopus. Developmental biology 233: 495-512.

Rea, S., F. Eisenhaber, D. O'Carroll, B. D. Strahl, Z. W. Sun, M. Schmid, S. Opravil, K. Mechtler, C. P. Ponting, C. D. Allis, and T. Jenuwein. 2000. Regulation of chromatin structure by site-specific histone H3 methyltransferases. Nature 406: 593-599.

Roberts, A. 2000. Early functional organization of spinal neurons in developing lower vertebrates. Brain research bulletin 53: 585-593.

Roberts, A., W. C. Li, and S. R. Soffe. 2012. A functional scaffold of CNS neurons for the vertebrates: the developing Xenopus laevis spinal cord. Developmental neurobiology 72: 575-584.

Rogers, C. D., S. A. Moody, and E. S. Casey. 2009. Neural induction and factors that stabilize a neural fate. Birth defects research. Part C, Embryo today : reviews 87: 249-262.

Ross, S. E., A. E. McCord, C. Jung, D. Atan, S. I. Mok, M. Hemberg, T. K. Kim, J. Salogiannis, L. Hu, S. Cohen, Y. Lin, D. Harrar, R. R. McInnes, and M. E. Greenberg. 2012. Bhlhb5 and Prdm8 form a repressor complex involved in neuronal circuit assembly. Neuron 73: 292-303.

Rossi, C. C., T. Kaji, and K. B. Artinger. 2009. Transcriptional control of Rohon-Beard sensory neuron development at the neural plate border. Developmental dynamics : an official publication of the American Association of Anatomists 238: 931-943.

Rossi, C. C., L. Hernandez-Lagunas, C. Zhang, I. F. Choi, L. Kwok, M. Klymkowsky, and K. B. Artinger. 2008. Rohon-Beard sensory neurons are induced by BMP4 expressing non-neural ectoderm in Xenopus laevis. Developmental biology 314: 351-361.

Ruark, E., S. Seal, H. McDonald, F. Zhang, A. Elliot, K. Lau, E. Perdeaux, E. Rapley, R. Eeles, J. Peto, Z. Kote-Jarai, K. Muir, J. Nsengimana, J. Shipley, D. T. Bishop, M. R. Stratton, D. F. Easton, R. A. Huddart, N. Rahman, and C. Turnbull. 2013. Identification of nine new susceptibility loci for testicular cancer, including variants near DAZL and PRDM14. Nature genetics 45: 686-689.

Rubenstein, A., J. Merriam, and M. W. Klymkowsky. 1997. Localizing the adhesive and signaling functions of plakoglobin. Developmental genetics 20: 91-102.

Saha, M. S., R. R. Miles, and R. M. Grainger. 1997. Dorsal-ventral patterning during neural induction in Xenopus: assessment of spinal cord regionalization with xHB9, a marker for the motor neuron region. Developmental biology 187: 209-223.

Sambrook, J. and Russel, D.W. (Eds.) (2001). Molecular Cloning: a laboratory manual. Third Edition. *Cold Spring Harbour Laboratory Press*, Cold Spring Harbour, New York.

Sanchez-Ferras, O., B. Coutaud, T. Djavanbakht Samani, I. Tremblay, O. Souchkova, and N. Pilon. 2012. Caudal-related homeobox (Cdx) protein-dependent integration of canonical Wnt signaling on paired-box 3 (Pax3) neural crest enhancer. The Journal of biological chemistry 287: 16623-16635.

Sanger, F., S. Nicklen, and A. R. Coulson. 1977. DNA sequencing with chain-terminating inhibitors. Proceedings of the National Academy of Sciences of the United States of America 74: 5463-5467.

Sasai, Y. 1998. Identifying the missing links: genes that connect neural induction and primary neurogenesis in vertebrate embryos. Neuron 21: 455-458.

Sasai, Y., B. Lu, H. Steinbeisser, D. Geissert, L. K. Gont, and E. M. De Robertis. 1994. Xenopus chordin: a novel dorsalizing factor activated by organizer-specific homeobox genes. Cell 79: 779-790.

Sato, S. M., and T. D. Sargent. 1989. Development of neural inducing capacity in dissociated Xenopus embryos. Developmental biology 134: 263-266.

Sato, T., N. Sasai, and Y. Sasai. 2005. Neural crest determination by co-activation of Pax3 and Zic1 genes in Xenopus ectoderm. Development 132: 2355-2363.

Sayitoglu, M., Y. Erbilgin, O. Hatirnaz Ng, I. Yildiz, T. Celkan, S. Anak, O. Devecioglu, G. Aydogan, S. Karaman, N. Sarper, C. Timur, U. Ure, and U. Ozbek. 2012. Upregulation of T-Cell-Specific Transcription Factor Expression in Pediatric T-Cell Acute Lymphoblastic Leukemia (T-ALL). Turkish journal of haematology : official journal of Turkish Society of Haematology 29: 325-333.

Schneider, M. L., D. L. Turner, and M. L. Vetter. 2001. Notch signaling can inhibit Xath5 function in the neural plate and developing retina. Molecular and cellular neurosciences 18: 458-472.

Schroeter, E. H., J. A. Kisslinger, and R. Kopan. 1998. Notch-1 signalling requires ligand-induced proteolytic release of intracellular domain. Nature 393: 382-386.

Seale, P., S. Kajimura, W. Yang, S. Chin, L. M. Rohas, M. Uldry, G. Tavernier, D. Langin, and B. M. Spiegelman. 2007. Transcriptional control of brown fat determination by PRDM16. Cell metabolism 6: 38-54.

Selkoe, D., and R. Kopan. 2003. Notch and Presenilin: regulated intramembrane proteolysis links development and degeneration. Annual review of neuroscience 26: 565-597.

Seo, S., and K. L. Kroll. 2006. Geminin's double life: chromatin connections that regulate transcription at the transition from proliferation to differentiation. Cell Cycle 5: 374-379.

Sharp, P. A., B. Sugden, and J. Sambrook. 1973. Detection of two restriction endonuclease activities in Haemophilus parainfluenzae using analytical agarose--ethidium bromide electrophoresis. Biochemistry 12: 3055-3063.

Shimojo, H., T. Ohtsuka, and R. Kageyama. 2008. Oscillations in notch signaling regulate maintenance of neural progenitors. Neuron 58: 52-64.

Shu, X. S., H. Geng, L. Li, J. Ying, C. Ma, Y. Wang, F. F. Poon, X. Wang, Y. Ying, W. Yeo, G. Srivastava, S. W. Tsao, J. Yu, J. J. Sung, S. Huang, A. T. Chan, and Q. Tao. 2011. The epigenetic modifier PRDM5 functions as a tumor suppressor through modulating WNT/beta-catenin signaling and is frequently silenced in multiple tumors. PloS one 6: e27346.

Simko, S. J., H. Voicu, B. L. Carofino, and M. J. Justice. 2012. Mouse Lymphoblastic Leukemias Induced by Aberrant Expression Demonstrate Widespread Copy Number Alterations Also Found in Human ALL. Cancers 4: 1050-1066.

Simoes-Costa, M., and M. E. Bronner. 2015. Establishing neural crest identity: a gene regulatory recipe. Development 142: 242-257.

Sive, H. L., R. M. Grainger, and R. M. Harland. 2010. Microinjection of Xenopus embryos. Cold Spring Harbor protocols 2010: pdb ip81.

Smith, W. C., and R. M. Harland. 1992. Expression cloning of noggin, a new dorsalizing factor localized to the Spemann organizer in Xenopus embryos. Cell 70: 829-840.

Snellenberg, S., S. A. Cillessen, W. Van Criekinge, L. Bosch, C. J. Meijer, P. J. Snijders, and R. D. Steenbergen. 2014. Methylation-mediated repression of PRDM14 contributes to apoptosis evasion in HPV-positive cancers. Carcinogenesis 35: 2611-2618.

Solter, M., M. Koster, T. Hollemann, A. Brey, T. Pieler, and W. Knochel. 1999. Characterization of a subfamily of related winged helix genes, XFD-12/12'/12" (XFLIP), during Xenopus embryogenesis. Mechanisms of development 89: 161-165.

Souopgui, J., M. Solter, and T. Pieler. 2002. XPak3 promotes cell cycle withdrawal during primary neurogenesis in Xenopus laevis. The EMBO journal 21: 6429-6439.

Spear, P. C., and C. A. Erickson. 2012. Interkinetic nuclear migration: a mysterious process in search of a function. Development, growth & differentiation 54: 306-316.

Stern, C. D. 2005. Neural induction: old problem, new findings, yet more questions. Development 132: 2007-2021.

Streit, A., A. J. Berliner, C. Papanayotou, A. Sirulnik, and C. D. Stern. 2000. Initiation of neural induction by FGF signalling before gastrulation. Nature 406: 74-78.

Sullivan, S. A., L. Akers, and S. A. Moody. 2001. foxD5a, a Xenopus winged helix gene, maintains an immature neural ectoderm via transcriptional repression that is dependent on the C-terminal domain. Developmental biology 232: 439-457.

Sun, X. J., P. F. Xu, T. Zhou, M. Hu, C. T. Fu, Y. Zhang, Y. Jin, Y. Chen, S. J. Chen, Q. H. Huang, T. X. Liu, and Z. Chen. 2008. Genome-wide survey and developmental expression mapping of zebrafish SET domain-containing genes. PloS one 3: e1499.

Taverna, E., and W. B. Huttner. 2010. Neural progenitor nuclei IN motion. Neuron 67: 906-914.

Towbin, H., T. Staehelin, and J. Gordon. 1992. Electrophoretic transfer of proteins from polyacrylamide gels to nitrocellulose sheets: procedure and some applications. 1979. Biotechnology (Reading, Mass.) 24: 145-149.

Tsuneyoshi, N., T. Sumi, H. Onda, H. Nojima, N. Nakatsuji, and H. Suemori. 2008. PRDM14 suppresses expression of differentiation marker genes in human embryonic stem cells. Biochemical and biophysical research communications 367: 899-905.

Uchikawa, M., Y. Kamachi, and H. Kondoh. 1999. Two distinct subgroups of Group B Sox genes for transcriptional activators and repressors: their expression during embryonic organogenesis of the chicken. Mechanisms of development 84: 103-120.

van der Sanden, M. H., H. Meems, M. Houweling, J. B. Helms, and A. B. Vaandrager. 2004. Induction of CCAAT/enhancer-binding protein (C/EBP)-homologous protein/growth arrest and DNA damage-inducible protein 153 expression during inhibition of phosphatidylcholine synthesis is mediated via activation of a C/EBP-activating transcription factor-responsive element. The Journal of biological chemistry 279: 52007-52015.

Vasconcelos, F. F., and D. S. Castro. 2014. Transcriptional control of vertebrate neurogenesis by the proneural factor Ascl1. Frontiers in cellular neuroscience 8: 412.

Vernon, A. E., and A. Philpott. 2003. A single cdk inhibitor, p27Xic1, functions beyond cell cycle regulation to promote muscle differentiation in Xenopus. Development 130: 71-83.

Wang, S., and B. A. Barres. 2000. Up a notch: instructing gliogenesis. Neuron 27: 197-200.

Wettstein, D. A., D. L. Turner, and C. Kintner. 1997. The Xenopus homolog of Drosophila Suppressor of Hairless mediates Notch signaling during primary neurogenesis. Development 124: 693-702.

Wilson, P. A., and A. Hemmati-Brivanlou. 1995. Induction of epidermis and inhibition of neural fate by Bmp-4. Nature 376: 331-333.

Wu, Y., J. E. Ferguson, 3rd, H. Wang, R. Kelley, R. Ren, H. McDonough, J. Meeker, P. C. Charles, and C. Patterson. 2008. PRDM6 is enriched in vascular precursors during development and inhibits endothelial cell proliferation, survival, and differentiation. Journal of molecular and cellular cardiology 44: 47-58.

Wullimann, M. F., E. Rink, P. Vernier, and G. Schlosser. 2005. Secondary neurogenesis in the brain of the African clawed frog, Xenopus laevis, as revealed by PCNA, Delta-1, Neurogenin-related-1, and NeuroD expression. The Journal of comparative neurology 489: 387-402.

Yabuta, Y., K. Kurimoto, Y. Ohinata, Y. Seki, and M. Saitou. 2006. Gene expression dynamics during germline specification in mice identified by quantitative single-cell gene expression profiling. Biology of reproduction 75: 705-716.

Yamaji, M., Y. Seki, K. Kurimoto, Y. Yabuta, M. Yuasa, M. Shigeta, K. Yamanaka, Y. Ohinata, and M. Saitou. 2008. Critical function of Prdm14 for the establishment of the germ cell lineage in mice. Nature genetics 40: 1016-1022.

Yamaji, M., J. Ueda, K. Hayashi, H. Ohta, Y. Yabuta, K. Kurimoto, R. Nakato, Y. Yamada, K. Shirahige, and M. Saitou. 2013. PRDM14 ensures naive pluripotency through dual regulation of signaling and epigenetic pathways in mouse embryonic stem cells. Cell stem cell 12: 368-382.

Yardley, N., and M. I. Garcia-Castro. 2012. FGF signaling transforms non-neural ectoderm into neural crest. Developmental biology 372: 166-177.

Zannino, D. A., G. B. Downes, and C. G. Sagerstrom. 2014. prdm12b specifies the p1 progenitor domain and reveals a role for V1 interneurons in swim movements. Developmental biology 390: 247-260.

Zhang, T., L. Meng, W. Dong, H. Shen, S. Zhang, Q. Liu, and J. Du. 2013. High expression of PRDM14 correlates with cell differentiation and is a novel prognostic marker in resected non-small cell lung cancer. Medical oncology (Northwood, London, England) 30: 605.

Zwane, T. B., and N. V. Nikitina. 2015. Spatiotemporal expression analysis of Prdm1 and Prdm1 binding partners in early chick embryo. Gene expression patterns : GEP 17: 56-68.

6. Appendix

6.1 Candidate gene list for the RNA-sequencing analysis of *prdm14*-GR overexpressing animal caps

Given are the genes which were differentially expressed between *prdm14*-GR overexpressing animal caps and uninjected control caps, equivalent to stage 14 and 27, in three independent experiments.

6.1.1 Differentially expressed genes at stage 14

Given are the ensembl id, official gene name, log2 fold change and the adjusted P-value with respect to multiple testing using the FDR method. Genes were sorted according to the highest and lowest log2 fold change, respectively.

Table 6.1 Summary of differentially expressed genes at stage 14

upregulated			
ensembl id	Gene	log2 fold change	adjust. P-value
ENSXETG00000015915	*prdm14*	9.33	1.55E-68
ENSXETG00000010282	*cdx1*	8.98	3.26E-29
ENSXETG00000024458	*zic3*	8.23	3.45E-23
ENSXETG00000004589	*cdx4*	8.14	1.08E-46
ENSXETG00000025525	*pnhd*	7.71	2.67E-18
ENSXETG00000025407	*sp5*	7.21	3.15E-39
ENSXETG00000003826	*wnt8a*	7.13	1.02E-18
ENSXETG00000001801	*hoxd1*	6.60	4.96E-17
ENSXETG00000007898	*neurog1*	6.52	1.17E-10
ENSXETG00000019220	*bmpr1b*	5.80	1.02E-09
ENSXETG00000022950	*zbtb16*	5.79	4.80E-18
ENSXETG00000022080	*emx2*	5.66	1.72E-29
ENSXETG00000011788	*cdx2*	5.57	1.96E-22
ENSXETG00000007640	*pax3*	5.51	8.74E-08
ENSXETG00000031623	*wnt10a*	5.39	2.05E-12
ENSXETG00000023986	*barhl2*	5.29	4.73E-07
ENSXETG00000000742	*lmx1b.1*	5.18	2.26E-13
ENSXETG00000002761	*fgf3*	5.17	1.30E-06
ENSXETG00000020167	*tox*	4.94	7.99E-29

downregulated			
ensembl id	Gene	log2 fold change	adjust. P-value
ENSXETG00000014812	*htr1a*	-3.44	5.72E-06
ENSXETG00000001728	*slc6a3*	-3.08	5.28E-04
ENSXETG00000027551	*ces5a*	-3.02	4.91E-03
ENSXETG00000009166	*hmp19*	-2.77	1.97E-05
ENSXETG00000017117	*vstm5*	-2.75	3.44E-03
ENSXETG00000012215	*hhex*	-2.67	2.49E-03
ENSXETG00000022118	*gpr37*	-2.63	1.30E-14
ENSXETG00000011262	*c20orf85*	-2.55	2.42E-03
ENSXETG00000032792	*gnrh2*	-2.50	4.63E-05
ENSXETG00000023176	*prox1*	-2.50	1.11E-03
ENSXETG00000014758	*dner*	-2.47	4.76E-06
ENSXETG00000017493	*tmtops*	-2.46	1.79E-03
ENSXETG00000004406		-2.44	2.87E-02
ENSXETG00000005224		-2.36	5.23E-04
ENSXETG00000033983	*dmrt2*	-2.31	3.83E-11
ENSXETG00000013115	*kiaa0895*	-2.31	5.83E-04
ENSXETG00000033308	*efhb*	-2.31	5.97E-09
ENSXETG00000013407	*aatk*	-2.30	2.02E-04
ENSXETG00000001353	*hmcn2*	-2.30	1.80E-02

ENSXETG00000025183	*hoxc5*	4.77	1.25E-27	ENSXETG00000032462	*smpx*	-2.27	6.19E-13
ENSXETG00000023476	*hoxc8*	4.74	1.69E-29	ENSXETG00000017916	*galntl1*	-2.27	2.27E-04
ENSXETG00000000722	*hoxa7*	4.70	9.15E-11	ENSXETG00000012021	*sema5b*	-2.25	1.99E-06
ENSXETG00000009083	*hes7.2*	4.69	5.01E-06	ENSXETG00000031621	*c2orf70*	-2.23	5.25E-08
ENSXETG00000000802	*ror2*	4.55	3.83E-31	ENSXETG00000009727	*prkag1*	-2.22	1.83E-22
ENSXETG00000000724	*hoxa9*	4.54	4.99E-07	ENSXETG00000013371	*plcb2*	-2.21	1.79E-02
ENSXETG00000019927	*crabp2*	4.52	3.42E-05	ENSXETG00000000901		-2.19	4.18E-13
ENSXETG00000000237	*zeb2*	4.48	4.04E-06	ENSXETG00000005160	*march3*	-2.14	6.21E-04
ENSXETG00000023479	*hoxc6*	4.41	3.07E-19	ENSXETG00000000594	*foxc1*	-2.12	3.35E-02
ENSXETG00000023475	*hoxc9*	4.38	1.83E-16	ENSXETG00000024302	*atp10a*	-2.12	6.81E-03
ENSXETG00000018660	*tpbg*	4.31	2.80E-24	ENSXETG00000001696	*syt6*	-2.11	2.31E-02
ENSXETG00000021703	*fmnl2*	4.30	1.41E-06	ENSXETG00000015108	*rdh7*	-2.11	1.07E-03
ENSXETG00000001068	*gcm2*	4.29	3.43E-05	ENSXETG00000022840	*lphn1*	-2.11	5.03E-03
ENSXETG00000000728	*hoxa10*	4.28	3.14E-05	ENSXETG00000018291	*cebpa*	-2.10	7.44E-05
ENSXETG00000010153	*ebf2*	4.27	1.38E-05	ENSXETG00000016618	*ngf*	-2.07	4.71E-04
ENSXETG00000008000	*hnf1b*	4.17	3.22E-05	ENSXETG00000019537	*tbc1d24.2*	-2.07	4.56E-28
ENSXETG00000013607	*axin2*	4.05	3.35E-06	ENSXETG00000014344	*celf5*	-2.07	3.82E-03
ENSXETG00000012490	*gast*	3.95	5.28E-05	ENSXETG00000008779	*fbn1*	-2.06	3.11E-03
ENSXETG00000033673	*fam155b*	3.81	1.29E-10	ENSXETG00000030605	*loxhd1*	-2.05	7.17E-04
ENSXETG00000026355	*akap12*	3.75	6.41E-06	ENSXETG00000018430	*nkx2-3*	-2.05	6.22E-07
ENSXETG00000022636	*prss35*	3.65	2.78E-11	ENSXETG00000033418		-2.05	2.11E-03
ENSXETG00000006226	*gli1.2*	3.65	2.64E-07	ENSXETG00000015427	*adra2c*	-2.04	6.14E-04
ENSXETG00000018365	*kremen2*	3.63	8.94E-21	ENSXETG00000031925		-2.04	3.00E-02
ENSXETG00000001879	*nr3c1*	3.62	7.96E-25	ENSXETG00000009502		-2.03	4.01E-04
ENSXETG00000021987	*hoxb6*	3.61	7.21E-04	ENSXETG00000001273	*psd4*	-2.02	2.70E-02
ENSXETG00000018386	*pou4f1.2*	3.59	1.26E-05	ENSXETG00000001035	*fam132a*	-2.02	4.56E-03
ENSXETG00000027510	*itgb6*	3.58	4.61E-04	ENSXETG00000011726	*ntrk2*	-2.01	3.78E-02
ENSXETG00000007794	*cldn3*	3.54	1.09E-15	ENSXETG00000007316	*slc38a3*	-2.01	3.70E-13
ENSXETG00000000720	*hoxa5*	3.53	3.35E-06	ENSXETG00000021301	*akd1*	-2.00	5.28E-03
ENSXETG00000024347	*znf703*	3.52	1.96E-22	ENSXETG00000015542	*ccdc78*	-1.98	1.24E-07
ENSXETG00000010120	*mpzl2*	3.51	6.06E-12	ENSXETG00000030611	*lrrd1*	-1.98	5.30E-10
ENSXETG00000020467	*cdh11*	3.47	5.49E-04	ENSXETG00000033531	*tsc22d4*	-1.97	3.94E-02
ENSXETG00000021035	*pdgfra*	3.44	3.73E-04	ENSXETG00000010505	*phox2a*	-1.96	3.61E-03
ENSXETG00000012821	*sult1a1*	3.31	5.55E-05	ENSXETG00000021999	*ak1*	-1.96	1.20E-10
ENSXETG00000001223	*emilin1*	3.30	1.91E-06	ENSXETG00000017952	*efcab5*	-1.96	3.56E-09
ENSXETG00000010128	*nefm*	3.29	7.76E-10	ENSXETG00000005731	*sstr5*	-1.96	1.53E-09
ENSXETG00000018864	*zic2*	3.23	2.39E-08	ENSXETG00000017078	*s100z*	-1.96	3.11E-02

ENSXETG00000008971	*ywhag*	3.23	2.53E-10
ENSXETG00000001974	*st3gal5*	3.19	3.14E-07
ENSXETG00000025936	*cnrip1*	3.18	3.59E-03
ENSXETG00000031488	*pcdh19*	3.18	2.69E-04
ENSXETG00000010435	*prss23*	3.17	4.14E-07
ENSXETG00000019101	*nova2*	3.11	3.60E-06
ENSXETG00000003251	*limd2*	3.11	1.26E-11
ENSXETG00000033139	*zbtb16*	3.09	5.77E-05
ENSXETG00000006965	*pxdn*	3.06	4.16E-41
ENSXETG00000023975		3.06	2.18E-05
ENSXETG00000023080	*kif26a*	3.04	2.71E-04
ENSXETG00000034301		3.00	1.08E-07
ENSXETG00000016174		2.99	1.63E-06
ENSXETG00000001613	*emilin2*	2.97	4.94E-03
ENSXETG00000022798	*sostdc1*	2.95	7.83E-05
ENSXETG00000003565	*foxf1*	2.93	5.36E-04
ENSXETG00000026058	*cnfn.1*	2.91	3.30E-06
ENSXETG00000002879	*tspan4*	2.89	2.01E-04
ENSXETG00000019550	*pdgfc*	2.87	3.38E-03
ENSXETG00000012556	*itgb4*	2.84	9.95E-05
ENSXETG00000009114	*ucma*	2.82	2.17E-08
ENSXETG00000021674	*tfap2b*	2.81	2.45E-05
ENSXETG00000007633	*slco3a1*	2.81	1.87E-03
ENSXETG00000018715	*olfm4*	2.79	1.19E-08
ENSXETG00000034215	*sipa1*	2.77	3.31E-02
ENSXETG00000014867	*pltp*	2.75	2.41E-06
ENSXETG00000021993	*hoxb8*	2.72	1.36E-02
ENSXETG00000010058	*xarp*	2.68	5.91E-32
ENSXETG00000015096	*snap25*	2.64	2.05E-04
ENSXETG00000008088		2.63	4.42E-06
ENSXETG00000013886	*ngef*	2.62	1.23E-11
ENSXETG00000016741	*elavl3*	2.57	5.94E-03
ENSXETG00000027601	*mex3b*	2.54	1.06E-07
ENSXETG00000015467	*zic1*	2.54	7.17E-07
ENSXETG00000003871	*thrb*	2.53	3.27E-03
ENSXETG00000006797	*prickle1*	2.52	6.10E-15
ENSXETG00000007330	*hyal2*	2.50	2.99E-12

ENSXETG00000015694	*kcnrg*	-1.95	2.45E-05
ENSXETG00000014625	*nell2*	-1.95	3.86E-02
ENSXETG00000014639	*palm*	-1.95	1.59E-02
ENSXETG00000021296	*ppil6*	-1.95	2.95E-06
ENSXETG00000008426	*ehbp1l1*	-1.94	7.66E-06
ENSXETG00000031406	*lnx2*	-1.94	1.53E-02
ENSXETG00000017940	*c11orf41*	-1.94	3.93E-04
ENSXETG00000031483	*dnah6*	-1.94	2.94E-08
ENSXETG00000005172	*ccdc33*	-1.93	2.59E-10
ENSXETG00000010345	*stx1a*	-1.93	7.13E-03
ENSXETG00000010434	*fzd4*	-1.92	1.89E-03
ENSXETG00000004621	*tnni2*	-1.92	8.08E-10
ENSXETG00000007237	*zfyve28*	-1.91	2.55E-10
ENSXETG00000003267	*ttll1*	-1.89	1.08E-07
ENSXETG00000009789	*adcy6*	-1.89	1.67E-05
ENSXETG00000013478	*gas2l2*	-1.88	4.00E-04
ENSXETG00000017418		-1.87	3.08E-13
ENSXETG00000032935		-1.87	1.36E-02
ENSXETG00000032659	*ces3*	-1.86	3.33E-02
ENSXETG00000032002		-1.86	1.53E-04
ENSXETG00000025398	*gata3*	-1.85	1.01E-07
ENSXETG00000006186	*ahrr*	-1.85	2.83E-02
ENSXETG00000017275	*dvl3*	-1.85	1.09E-06
ENSXETG00000016042	*tm4sf1*	-1.85	1.30E-02
ENSXETG00000021393	*dnhd1*	-1.84	4.29E-02
ENSXETG00000021314	*c6orf186*	-1.82	4.26E-02
ENSXETG00000000586	*jak2*	-1.81	6.06E-12
ENSXETG00000005916	*msrb2*	-1.80	2.73E-06
ENSXETG00000008821	*sorbs1*	-1.80	2.18E-06
ENSXETG00000031224	*cdhr4*	-1.80	1.22E-02
ENSXETG00000001935	*foxi4.1*	-1.79	1.74E-04
ENSXETG00000030156	*casc1*	-1.79	1.18E-03
ENSXETG00000032214	*lrrtm3*	-1.79	3.70E-02
ENSXETG00000008299	*dnah2*	-1.78	5.73E-04
ENSXETG00000033707		-1.78	5.48E-03
ENSXETG00000033377		-1.77	1.04E-04
ENSXETG00000020893	*spag17*	-1.77	9.64E-06

ENSXETG00000002878	*polr2l.2*	2.49	9.62E-03
ENSXETG00000006798	*btc*	2.48	3.04E-11
ENSXETG00000031898		2.47	3.53E-04
ENSXETG00000012934	*bgn*	2.47	2.35E-03
ENSXETG00000007804	*smad3*	2.47	1.46E-04
ENSXETG00000018417	*sall1*	2.44	1.74E-06
ENSXETG00000013266	*s1pr1*	2.36	3.04E-04
ENSXETG00000019108	*ckm*	2.34	2.96E-06
ENSXETG00000003071	*fbln1*	2.32	6.94E-04
ENSXETG00000010230	*grk5*	2.31	4.36E-04
ENSXETG00000012029	*cass4*	2.31	3.58E-05
ENSXETG00000022662	*epn1*	2.30	4.54E-14
ENSXETG00000005738	*rasd1*	2.29	1.62E-04
ENSXETG00000027666	*tmeff1*	2.27	2.61E-04
ENSXETG00000011508	*manea*	2.26	3.45E-03
ENSXETG00000005370	*t*	2.26	1.83E-03
ENSXETG00000014363	*vash2*	2.25	7.98E-07
ENSXETG00000016758	*xb-gene-1002559*	2.24	3.07E-04
ENSXETG00000021973	*hoxb4*	2.23	2.38E-02
ENSXETG00000018322	*mcf2*	2.23	8.30E-03
ENSXETG00000018908	*c13orf15*	2.22	4.05E-06
ENSXETG00000004773	*col9a2*	2.22	4.12E-06
ENSXETG00000017823	*plxnb1*	2.21	3.77E-05
ENSXETG00000020971	*robo1*	2.19	6.08E-10
ENSXETG00000027351	*hoxb7*	2.17	3.17E-02
ENSXETG00000027392	*sncaip*	2.17	7.27E-03
ENSXETG00000018304	*tlx3*	2.17	1.30E-02
ENSXETG00000009704	*tnfrsf19*	2.14	9.39E-05
ENSXETG00000030035	*abcb9*	2.14	7.94E-03
ENSXETG00000019934	*srrm4*	2.13	1.32E-02
ENSXETG00000021450	*ampd1*	2.13	3.28E-03
ENSXETG00000022554	*dhx32*	2.11	1.14E-09
ENSXETG00000017807	*spry2*	2.11	3.93E-07
ENSXETG00000014718	*shb*	2.10	4.72E-17
ENSXETG00000022348	*sox9*	2.09	2.27E-04
ENSXETG00000010142	*nefl*	2.09	4.21E-06
ENSXETG00000006598	*dkk1*	2.08	4.04E-02

ENSXETG00000024528	*cfap70*	-1.76	1.16E-07
ENSXETG00000025109	*ankar*	-1.76	2.14E-07
ENSXETG00000011506	*xb-gene-5857146*	-1.76	9.44E-12
ENSXETG00000004373	*tekt2*	-1.75	1.40E-09
ENSXETG00000015719	*odf3*	-1.74	2.06E-08
ENSXETG00000030092		-1.74	2.28E-03
ENSXETG00000021988	*dcdc2*	-1.74	4.76E-06
ENSXETG00000024508		-1.74	1.42E-08
ENSXETG00000032283	*dnah3*	-1.73	8.46E-07
ENSXETG00000021518	*kcnn2*	-1.73	1.91E-03
ENSXETG00000018025	*slc22a23*	-1.73	2.39E-04
ENSXETG00000030029	*dnah1*	-1.73	4.20E-08
ENSXETG00000000659	*efhc1*	-1.72	1.11E-09
ENSXETG00000031311		-1.72	8.25E-05
ENSXETG00000013506	*rnf32*	-1.72	2.64E-02
ENSXETG00000004208	*rtdr1*	-1.71	1.52E-08
ENSXETG00000031053	*ttc6*	-1.71	3.26E-05
ENSXETG00000001388	*dhrs3*	-1.71	5.67E-07
ENSXETG00000024630	*ccdc153*	-1.70	8.28E-03
ENSXETG00000016412	*rasal1*	-1.70	9.02E-09
ENSXETG00000023103	*spata18*	-1.70	2.05E-06
ENSXETG00000003039		-1.70	4.29E-03
ENSXETG00000021297	*ak9*	-1.69	1.55E-06
ENSXETG00000004297	*ppp1r1a*	-1.69	3.11E-02
ENSXETG00000002217	*kiaa1841*	-1.69	4.85E-04
ENSXETG00000009722	*ca12*	-1.68	5.65E-04
ENSXETG00000015133	*phldb3*	-1.68	2.17E-03
ENSXETG00000022889	*zbbx*	-1.68	2.32E-02
ENSXETG00000006838	*rab37*	-1.68	2.58E-04
ENSXETG00000019163	*itgb3*	-1.68	1.29E-03
ENSXETG00000007116	*ttc29*	-1.68	5.83E-05
ENSXETG00000014624	*gmpr2*	-1.68	9.38E-13
ENSXETG00000032601	*akna*	-1.68	4.08E-02
ENSXETG00000003663	*pcdh10*	-1.67	6.34E-03
ENSXETG00000016964	*btbd11*	-1.67	1.39E-02
ENSXETG00000001718		-1.67	1.99E-02
ENSXETG00000006261	*c9orf9*	-1.67	1.60E-05

ENSXETG00000 011173	*wnt10b*	2.07	4.97E-02
ENSXETG00000 025522	*esr10*	2.06	2.47E-02
ENSXETG00000 003296	*cxcr7*	2.06	1.26E-05
ENSXETG00000 003938	*robo3*	2.06	5.52E-23
ENSXETG00000 031424		2.05	3.76E-03
ENSXETG00000 013228	*egflam*	2.04	2.21E-04
ENSXETG00000 016415	*gas2l1*	2.04	1.59E-04
ENSXETG00000 022245	*hes9.1*	2.04	4.43E-02
ENSXETG00000 005880	*hip1*	2.02	2.18E-03
ENSXETG00000 001058	*klf17*	2.02	3.99E-08
ENSXETG00000 023193	*p2ry4*	1.99	2.23E-10
ENSXETG00000 017641	*xb-gene-5781886*	1.98	8.76E-05
ENSXETG00000 000377	*fras1*	1.95	2.49E-03
ENSXETG00000 004222	*adora2a*	1.94	1.06E-03
ENSXETG00000 007241	*dbn1*	1.94	1.62E-03
ENSXETG00000 010865	*aldh1a2*	1.94	2.14E-03
ENSXETG00000 008399	*flt4*	1.94	2.75E-02
ENSXETG00000 015816	*blvra*	1.94	2.83E-06
ENSXETG00000 021140	*cyp1a1*	1.92	4.73E-02
ENSXETG00000 012279	*lamb1*	1.90	2.28E-05
ENSXETG00000 029924	*stxbp5*	1.90	8.96E-11
ENSXETG00000 030428		1.90	3.35E-02
ENSXETG00000 012216	*msi1*	1.88	2.56E-07
ENSXETG00000 010662	*ap3b2*	1.88	1.06E-02
ENSXETG00000 019579	*pmp22*	1.88	1.57E-02
ENSXETG00000 001066	*gpr63*	1.88	4.97E-02
ENSXETG00000 032528	*sspo*	1.87	4.28E-02
ENSXETG00000 000758	*pcsk5*	1.87	1.18E-06
ENSXETG00000 005259	*stk40*	1.86	1.36E-04
ENSXETG00000 019568	*spry4*	1.86	3.22E-03
ENSXETG00000 009686	*insm1*	1.85	1.22E-02
ENSXETG00000 015431	*mylip*	1.85	1.00E-04
ENSXETG00000 029928	*gas1*	1.85	3.30E-06
ENSXETG00000 018847	*plk2*	1.83	7.47E-16
ENSXETG00000 008674	*prdm1*	1.83	1.55E-05
ENSXETG00000 030115	*sp8*	1.81	2.17E-08
ENSXETG00000 016853	*slc23a2*	1.80	8.61E-05

ENSXETG00000 023392	*rassf6*	-1.67	7.65E-05
ENSXETG00000 026100	*c5orf42*	-1.67	5.28E-07
ENSXETG00000 030387	*c3orf84*	-1.67	1.88E-02
ENSXETG00000 018416	*clcnkb*	-1.67	1.16E-02
ENSXETG00000 013869	*ccdc108*	-1.66	1.06E-09
ENSXETG00000 013373	*fam81b*	-1.65	1.33E-04
ENSXETG00000 018707	*capsl*	-1.65	2.04E-03
ENSXETG00000 016146	*sec14l3*	-1.65	1.81E-07
ENSXETG00000 016844	*wdr38*	-1.65	2.47E-06
ENSXETG00000 019005		-1.65	2.70E-05
ENSXETG00000 006227	*arhgef25*	-1.64	3.33E-02
ENSXETG00000 010988	*ndrg1*	-1.64	3.87E-02
ENSXETG00000 008688		-1.64	3.89E-08
ENSXETG00000 009174	*c9orf21*	-1.64	1.13E-03
ENSXETG00000 012367	*syne1*	-1.63	4.50E-07
ENSXETG00000 000658	*paqr8*	-1.63	3.61E-02
ENSXETG00000 024641	*elovl2*	-1.63	2.69E-07
ENSXETG00000 027678	*gnaz*	-1.63	1.16E-07
ENSXETG00000 011269	*cdh15*	-1.63	6.04E-04
ENSXETG00000 004835	*efhc2*	-1.63	7.34E-05
ENSXETG00000 017994	*pkhd1l1*	-1.63	3.27E-02
ENSXETG00000 019512	*pik3r6*	-1.62	1.43E-02
ENSXETG00000 005336	*prr29*	-1.62	9.81E-05
ENSXETG00000 022781	*ets1*	-1.62	4.57E-04
ENSXETG00000 015189	*c2orf73*	-1.62	5.92E-06
ENSXETG00000 003686	*als2cl*	-1.62	1.60E-09
ENSXETG00000 018553	*dnah14*	-1.62	1.61E-04
ENSXETG00000 013834	*c17orf105*	-1.61	7.94E-04
ENSXETG00000 014590	*ccdc170*	-1.61	3.51E-09
ENSXETG00000 010527	*rsph1*	-1.61	1.43E-09
ENSXETG00000 033037		-1.61	2.12E-07
ENSXETG00000 032089	*spef1*	-1.61	3.57E-05
ENSXETG00000 007897	*h2afy*	-1.61	2.08E-03
ENSXETG00000 008812	*fzd8*	-1.61	4.77E-04
ENSXETG00000 006725	*c11orf66*	-1.60	2.42E-06
ENSXETG00000 005595	*tns1*	-1.60	1.30E-02
ENSXETG00000 007384	*spag6*	-1.60	2.40E-11

ENSXETG00000021344	*fyn*	1.79	4.12E-02
ENSXETG00000017665	*lhx5*	1.78	3.52E-02
ENSXETG00000016286	*trps1*	1.77	1.89E-03
ENSXETG00000002103	*ndnf*	1.76	2.45E-02
ENSXETG00000015557	*vsnl1*	1.76	1.43E-09
ENSXETG00000007560	*elf5*	1.76	4.11E-02
ENSXETG00000022354	*nos1*	1.76	3.36E-02
ENSXETG00000011941	*tmem132a*	1.75	7.19E-04
ENSXETG00000014993	*kcp*	1.75	4.64E-02
ENSXETG00000003934	*slc37a2*	1.74	2.81E-09
ENSXETG00000010956	*mycl1*	1.73	1.62E-04
ENSXETG00000002931	*fzd10*	1.73	2.78E-10
ENSXETG00000023872	*ngfr*	1.72	2.74E-07
ENSXETG00000023832	*tmcc3*	1.71	8.11E-04
ENSXETG00000000251	*hmox1*	1.71	1.23E-07
ENSXETG00000005911	*hes6.1*	1.69	5.58E-05
ENSXETG00000001837	*trim2*	1.69	2.04E-03
ENSXETG00000016100	*tcf7*	1.67	2.16E-06
ENSXETG00000010491	*pcbp2*	1.67	4.05E-02
ENSXETG00000001802	*mtx2*	1.66	1.27E-03
ENSXETG00000010410	*phf15*	1.65	3.72E-02
ENSXETG00000021972	*col27a1*	1.65	2.04E-04
ENSXETG00000007198	*nudt22*	1.65	9.82E-03
ENSXETG00000006532	*fbxo10*	1.63	2.26E-02
ENSXETG00000025626	*tmem69*	1.63	1.52E-08
ENSXETG00000019257	*rab34*	1.62	1.15E-02
ENSXETG00000016157	*znf219*	1.62	4.30E-02
ENSXETG00000023439	*sox11*	1.61	2.18E-05
ENSXETG00000011665	*ncam1*	1.61	2.58E-02
ENSXETG00000002340	*jag1*	1.60	2.30E-03
ENSXETG00000021454	*dennd2c*	1.60	2.25E-02
ENSXETG00000013354	*slitrk1*	1.60	1.93E-02
ENSXETG00000005062	*etv1*	1.60	1.67E-04
ENSXETG00000022669	*mmp14*	1.58	1.86E-05
ENSXETG00000012404	*fzd7*	1.57	1.90E-04
ENSXETG00000017378	*ptgs2*	1.57	2.37E-05
ENSXETG00000018892	*ptch2*	1.55	4.19E-03

ENSXETG00000026587	*ccdc180*	-1.60	7.03E-05
ENSXETG00000030126		-1.60	1.53E-06
ENSXETG00000023295	*lmo4.1*	-1.60	2.98E-08
ENSXETG00000005917	*armc3*	-1.60	1.04E-06
ENSXETG00000010437	*ccdc81*	-1.59	1.59E-04
ENSXETG00000008630	*wdr63*	-1.59	1.38E-08
ENSXETG00000022691	*dzip1l*	-1.59	2.18E-06
ENSXETG00000016326	*morn5*	-1.59	8.25E-05
ENSXETG00000030661		-1.59	1.16E-03
ENSXETG00000000514	*mgat5*	-1.58	6.29E-03
ENSXETG00000014934	*c2orf62*	-1.58	2.27E-05
ENSXETG00000034198		-1.58	4.56E-02
ENSXETG00000016481	*gjb3*	-1.58	8.65E-03
ENSXETG00000008519	*add2*	-1.58	5.20E-03
ENSXETG00000022961	*kcnj16*	-1.58	4.91E-03
ENSXETG00000032300	*stmnd1*	-1.58	1.79E-09
ENSXETG00000022016	*ribc1*	-1.57	2.39E-08
ENSXETG00000024952	*tnnt3*	-1.57	4.02E-02
ENSXETG00000019324	*bcam*	-1.57	1.85E-02
ENSXETG00000024951	*stard9*	-1.57	4.38E-04
ENSXETG00000018735	*tcf7l2*	-1.57	2.47E-02
ENSXETG00000008892	*irx4*	-1.57	1.66E-04
ENSXETG00000015159	*eml6*	-1.57	4.61E-04
ENSXETG00000020037		-1.56	1.14E-02
ENSXETG00000015289	*anxa2*	-1.56	7.39E-06
ENSXETG00000021497	*epb41l4a*	-1.56	3.55E-04
ENSXETG00000015923	*xb-gene-5949053*	-1.56	1.33E-02
ENSXETG00000005341	*cxorf22*	-1.56	9.91E-03
ENSXETG00000004292	*rapgef3*	-1.55	1.31E-03
ENSXETG00000016804	*inpp5a.2*	-1.55	5.98E-03
ENSXETG00000032500	*fam179a*	-1.55	7.63E-04
ENSXETG00000007146	*lrrc18*	-1.55	5.24E-06
ENSXETG00000001021	*acap3*	-1.55	4.86E-04
ENSXETG00000030526	*tsga10*	-1.55	5.57E-05
ENSXETG00000022934	*xb-gene-5992704*	-1.55	5.46E-07
ENSXETG00000015878	*hydin*	-1.54	6.21E-07
ENSXETG00000011560	*foxp2*	-1.54	7.09E-03

ENSXETG00000034300		1.54	6.43E-06
ENSXETG00000013631	*adamts1*	1.53	6.68E-03
ENSXETG00000016416	*rasl10a*	1.53	1.65E-03
ENSXETG00000011490	*col6a2*	1.52	1.72E-02
ENSXETG00000005928	*dag1*	1.52	4.70E-06
ENSXETG00000032223	*cltcl1*	1.52	1.62E-03
ENSXETG00000012718	*dpysl3*	1.52	2.90E-02
ENSXETG00000021813	*cttnbp2*	1.51	4.42E-05
ENSXETG00000014353	*tle2*	1.51	2.04E-06
ENSXETG00000010707	*sparc*	1.51	9.66E-03
ENSXETG00000004642	*cdc42ep4*	1.50	9.92E-05
ENSXETG00000027807	*cited2*	1.50	3.36E-02
ENSXETG00000000904	*il17rd*	1.48	6.79E-03
ENSXETG00000026881	*nr2c2ap*	1.48	3.37E-02
ENSXETG00000025478	*lum*	1.48	2.02E-02
ENSXETG00000009405	*wnt5b*	1.48	3.23E-03
ENSXETG00000011877	*cd74*	1.47	2.22E-03
ENSXETG00000000581	*fmnl3*	1.46	7.96E-04
ENSXETG00000000696	*rai14*	1.46	2.06E-04
ENSXETG00000016573	*dlx6*	1.46	7.31E-04
ENSXETG00000023744	*ptp4a3*	1.45	7.14E-04
ENSXETG00000031265	*raph1*	1.45	9.02E-05
ENSXETG00000006108	*col9a3*	1.45	9.54E-04
ENSXETG00000018919	*cnn3*	1.44	5.10E-06
ENSXETG00000026104	*st3gal6*	1.44	1.62E-02
ENSXETG00000014751	*atp1b3*	1.43	1.25E-03
ENSXETG00000012324	*lin28a*	1.42	4.50E-02
ENSXETG00000025992	*cdh3*	1.41	5.13E-12
ENSXETG00000000076	*mapkapk3*	1.41	1.18E-02
ENSXETG00000011231	*cmtm3*	1.39	1.31E-02
ENSXETG00000010393		1.39	1.36E-02
ENSXETG00000003952	*nrarp*	1.39	5.89E-04
ENSXETG00000017085	*pkp1*	1.39	3.86E-02
ENSXETG00000031404	*draxin*	1.38	1.57E-02
ENSXETG00000015391	*cadm1*	1.37	6.52E-04
ENSXETG00000025060	*shprh*	1.37	3.85E-03
ENSXETG00000030338		1.36	5.28E-03

ENSXETG00000024614	*tbcel*	-1.54	1.43E-13
ENSXETG00000019733	*ccdc146*	-1.54	7.95E-08
ENSXETG00000021596	*gpr146*	-1.54	4.01E-04
ENSXETG00000024914	*rab36*	-1.54	1.10E-05
ENSXETG00000023542	*xb-gene-5950142*	-1.53	2.12E-04
ENSXETG00000016135	*hhla2*	-1.53	1.18E-02
ENSXETG00000008117	*fam63a*	-1.53	4.31E-07
ENSXETG00000019168	*c13orf26*	-1.53	2.42E-11
ENSXETG00000014319	*eno4*	-1.53	4.50E-10
ENSXETG00000012713	*stk33*	-1.53	8.82E-04
ENSXETG00000002847	*c14orf45*	-1.52	4.61E-04
ENSXETG00000012703	*klhdc9*	-1.52	6.90E-03
ENSXETG00000027390	*znf474*	-1.52	4.49E-13
ENSXETG00000033778	*tbata*	-1.51	3.06E-07
ENSXETG00000030130		-1.51	9.46E-04
ENSXETG00000025251	*dnah9*	-1.51	2.32E-02
ENSXETG00000033908	*ube2u*	-1.51	3.92E-02
ENSXETG00000005487	*arhgap42*	-1.51	6.21E-07
ENSXETG00000015093	*ankrd5*	-1.50	1.54E-11
ENSXETG00000022383	*mapk4*	-1.50	3.43E-02
ENSXETG00000030188	*dnah10*	-1.50	2.63E-06
ENSXETG00000019423	*plcg1*	-1.49	7.63E-04
ENSXETG00000000693	*sox7*	-1.49	7.80E-17
ENSXETG00000010195	*c9orf96*	-1.49	1.85E-03
ENSXETG00000001452	*mdm1*	-1.49	7.51E-04
ENSXETG00000032973	*iqca1*	-1.49	4.11E-06
ENSXETG00000019904	*lrrc3b*	-1.48	1.06E-02
ENSXETG00000033755	*speg*	-1.48	2.90E-02
ENSXETG00000016710		-1.48	7.58E-09
ENSXETG00000010185	*dixdc1*	-1.48	1.33E-03
ENSXETG00000032155		-1.47	8.54E-04
ENSXETG00000000335	*cdkl2*	-1.47	9.22E-06
ENSXETG00000013463	*zmynd12*	-1.47	3.37E-07
ENSXETG00000010186	*coro2a*	-1.47	4.42E-02
ENSXETG00000003349	*poc5*	-1.47	3.57E-06
ENSXETG00000001383	*c1orf158*	-1.47	2.84E-08
ENSXETG00000021173	*ncoa1*	-1.46	8.28E-04

ENSXETG00000021749		1.36	4.26E-03
ENSXETG00000020160	*pros1*	1.35	3.74E-02
ENSXETG00000027751	*marcks*	1.35	1.54E-02
ENSXETG00000004371	*tspan1*	1.34	1.06E-03
ENSXETG00000008603	*akt1*	1.33	8.43E-04
ENSXETG00000020280	*fam171a1*	1.33	7.09E-03
ENSXETG00000002238	*akap2*	1.32	1.99E-04
ENSXETG00000025083	*c6orf35*	1.32	3.59E-02
ENSXETG00000005091	*lrp4*	1.31	2.47E-05
ENSXETG00000016127	*cblb*	1.31	1.82E-05
ENSXETG00000033405	*cbr1*	1.30	1.43E-13
ENSXETG00000025368	*best2*	1.30	7.43E-03
ENSXETG00000018074	*rasgrp1*	1.29	1.14E-02
ENSXETG00000016775	*fgfr1*	1.29	2.64E-07
ENSXETG00000016111	*slc27a2*	1.29	3.30E-06
ENSXETG00000022029	*pfkfb1*	1.29	1.10E-12
ENSXETG00000018375	*anxa11*	1.29	4.86E-04
ENSXETG00000005683		1.28	6.74E-05
ENSXETG00000011781	*rab11fip5*	1.28	3.22E-02
ENSXETG00000018359	*zmiz1*	1.27	4.54E-04
ENSXETG00000010302	*chga*	1.27	1.25E-02
ENSXETG00000027667	*c9orf6*	1.27	6.90E-08
ENSXETG00000009866	*znf503*	1.27	2.61E-05
ENSXETG00000033367	*tmem2*	1.27	5.59E-07
ENSXETG00000015500	*mllt3*	1.26	3.26E-02
ENSXETG00000010460	*nos1ap*	1.26	1.23E-05
ENSXETG00000019965	*kcnq1*	1.25	1.52E-07
ENSXETG00000019763	*mospd1*	1.25	1.30E-04
ENSXETG00000011217	*thbs1*	1.24	2.50E-02
ENSXETG00000011962	*dact1*	1.24	1.10E-03
ENSXETG00000004387	*cept1*	1.24	6.80E-04
ENSXETG00000019267	*c6orf203*	1.23	2.55E-02
ENSXETG00000020924	*ippk*	1.23	3.24E-02
ENSXETG00000025190	*lrrc8b*	1.23	5.40E-03
ENSXETG00000016563	*tcf12*	1.23	6.41E-06
ENSXETG00000010357	*nme3*	1.22	2.58E-02
ENSXETG00000017315	*adcy9*	1.21	4.81E-07

ENSXETG00000004761	*xb-gene-5817486*	-1.46	3.65E-03
ENSXETG00000017409	*kiaa0513*	-1.46	9.09E-04
ENSXETG00000006299	*xepsin*	-1.46	1.50E-02
ENSXETG00000021376	*mpped2*	-1.46	3.99E-02
ENSXETG00000019539	*wdr16*	-1.46	3.67E-14
ENSXETG00000006312	*casz1*	-1.46	1.69E-11
ENSXETG00000000118	*slc2a12*	-1.46	4.79E-02
ENSXETG00000013421	*crocc*	-1.46	5.04E-04
ENSXETG00000030034	*lrrc73*	-1.45	1.81E-02
ENSXETG00000025205	*xb-gene-5922677*	-1.45	3.09E-08
ENSXETG00000012154		-1.45	7.82E-04
ENSXETG00000013950	*ak7*	-1.45	5.91E-09
ENSXETG00000016747	*rgl3*	-1.45	3.15E-03
ENSXETG00000018928	*c2orf77*	-1.45	9.09E-04
ENSXETG00000023781	*c2orf50*	-1.45	1.33E-04
ENSXETG00000005240	*dcdc2b*	-1.45	6.88E-05
ENSXETG00000008873	*kndc1*	-1.44	2.63E-03
ENSXETG00000021705		-1.44	7.51E-04
ENSXETG00000013234	*cdc14a*	-1.44	8.29E-07
ENSXETG00000022874	*wdr49*	-1.44	1.53E-04
ENSXETG00000017416	*fam92b*	-1.44	2.54E-05
ENSXETG00000001591	*cetn4*	-1.43	1.89E-05
ENSXETG00000032161	*morn3*	-1.43	9.27E-07
ENSXETG00000025413	*mest*	-1.43	2.34E-02
ENSXETG00000011276	*slc22a31*	-1.43	5.65E-04
ENSXETG00000014603	*slc7a8*	-1.43	3.49E-05
ENSXETG00000005961		-1.43	4.49E-04
ENSXETG00000000061	*dnal1*	-1.43	1.42E-08
ENSXETG00000010363	*tekt1*	-1.43	1.15E-09
ENSXETG00000020932	*esrrg*	-1.42	7.37E-03
ENSXETG00000032986		-1.42	7.63E-08
ENSXETG00000026362	*xb-gene-5902318*	-1.42	2.88E-03
ENSXETG00000013823	*elmo3*	-1.41	2.18E-03
ENSXETG00000012922	*pde4c*	-1.41	2.28E-02
ENSXETG00000004839	*maob*	-1.41	1.58E-02
ENSXETG00000018269	*cep89*	-1.41	1.06E-05
ENSXETG00000012560	*c2cd3*	-1.41	4.28E-06

ENSXETG00000007197	*dnajc4*	1.21	4.27E-03
ENSXETG00000017793	*zc4h2*	1.21	4.92E-03
ENSXETG00000030893		1.21	4.43E-02
ENSXETG00000026157	*cdk5rap2*	1.21	3.04E-02
ENSXETG00000033372		1.20	2.81E-02
ENSXETG00000027014	*traf4*	1.20	4.72E-02
ENSXETG00000034081	*cul5*	1.19	1.18E-02
ENSXETG00000017566	*smarca5*	1.19	4.24E-08
ENSXETG00000011565	*mdfic*	1.18	3.45E-02
ENSXETG00000018620	*prrg1*	1.18	1.50E-10
ENSXETG00000009218	*mynn*	1.18	6.04E-04
ENSXETG00000025335	*rnd3*	1.17	1.47E-02
ENSXETG00000014857	*ostm1*	1.17	1.99E-06
ENSXETG00000011833	*ptprd*	1.17	1.36E-03
ENSXETG00000012186	*ccnj*	1.16	1.41E-03
ENSXETG00000011897	*eno1*	1.15	6.82E-03
ENSXETG00000012289	*rps6ka1*	1.15	1.65E-04
ENSXETG00000023793	*greb1*	1.15	4.28E-03
ENSXETG00000013793	*setd6*	1.15	5.09E-06
ENSXETG00000010313	*otub2*	1.14	2.75E-02
ENSXETG00000030447	*dusp8*	1.14	3.97E-03
ENSXETG00000012743	*rcor1*	1.13	5.45E-03
ENSXETG00000021414	*egln1*	1.12	1.22E-02
ENSXETG00000010841	*dock7*	1.12	6.22E-06
ENSXETG00000005431	*sema3d*	1.12	4.72E-02
ENSXETG00000024679	*spats2*	1.12	6.57E-06
ENSXETG00000004155	*abi2*	1.11	7.67E-07
ENSXETG00000024397	*nr1d1*	1.10	1.28E-02
ENSXETG00000003253	*pik3r3*	1.10	8.28E-03
ENSXETG00000005342	*arhgap6*	1.10	1.28E-03
ENSXETG00000011818	*ryk*	1.08	7.21E-04
ENSXETG00000017437	*cdk2ap2*	1.08	2.16E-02
ENSXETG00000012160	*srebf1*	1.08	2.11E-04
ENSXETG00000030743	*mb*	1.08	2.10E-04
ENSXETG00000000543	*gldc*	1.08	4.85E-02
ENSXETG00000011111	*hes3.1*	1.08	5.91E-03
ENSXETG00000001573	*spry1*	1.07	3.26E-02

ENSXETG00000002998	*c1orf173*	-1.41	7.13E-03
ENSXETG00000024765	*dynlrb2*	-1.41	1.97E-05
ENSXETG00000034073	*mdh1b*	-1.41	4.57E-06
ENSXETG00000016262	*enpp4*	-1.41	3.35E-02
ENSXETG00000011397	*neurl*	-1.40	9.95E-05
ENSXETG00000003974	*clic3*	-1.40	9.96E-05
ENSXETG00000022138	*iqub*	-1.40	1.40E-08
ENSXETG00000006354	*kiaa1370*	-1.39	8.74E-08
ENSXETG00000013608	*cep112*	-1.39	1.33E-02
ENSXETG00000008631	*lpar3*	-1.39	4.69E-03
ENSXETG00000017777	*wdr52*	-1.39	7.33E-03
ENSXETG00000018653		-1.39	4.47E-02
ENSXETG00000019906	*nek10*	-1.39	3.52E-03
ENSXETG00000030298	*pifo*	-1.39	4.22E-02
ENSXETG00000014097	*rarres1*	-1.38	1.00E-03
ENSXETG00000022093	*dnah7*	-1.38	7.46E-05
ENSXETG00000023071	*fam102a*	-1.38	3.07E-02
ENSXETG00000005871	*fam149a*	-1.37	1.57E-02
ENSXETG00000032269	*lrrfip1*	-1.37	6.92E-04
ENSXETG00000026283	*gjb1*	-1.37	1.16E-02
ENSXETG00000022580	*nhsl2*	-1.37	2.94E-03
ENSXETG00000007409	*rapgef5*	-1.36	8.92E-07
ENSXETG00000009576	*oat.2*	-1.36	5.05E-09
ENSXETG00000004679	*lox*	-1.36	3.17E-02
ENSXETG00000032814	*clhc1*	-1.36	3.35E-06
ENSXETG00000023923	*lrrc23*	-1.36	8.85E-09
ENSXETG00000025131	*sgpp1*	-1.35	1.25E-04
ENSXETG00000033099	*jag2*	-1.35	2.94E-03
ENSXETG00000031301	*cdc20b*	-1.35	9.59E-05
ENSXETG00000013238	*fos*	-1.35	4.00E-03
ENSXETG00000015673	*arl11*	-1.35	1.33E-02
ENSXETG00000026793	*tmem30b*	-1.35	1.44E-03
ENSXETG00000002371	*kif27*	-1.35	2.63E-03
ENSXETG00000021433	*snta1*	-1.35	1.15E-04
ENSXETG00000032805		-1.34	4.75E-02
ENSXETG00000002233	*fam161a*	-1.34	2.10E-04
ENSXETG00000010212	*hopx*	-1.34	3.49E-03

ENSXETG00000014939	*smo*	1.06	4.08E-02
ENSXETG00000012949	*ctps*	1.06	3.88E-06
ENSXETG00000015984	*nol12*	1.06	2.84E-02
ENSXETG00000011847	*med20*	1.05	4.16E-04
ENSXETG00000007756	*shf*	1.05	2.88E-02
ENSXETG00000012714	*arhgef37*	1.05	3.32E-05
ENSXETG00000007514	*ipo8*	1.05	1.27E-02
ENSXETG00000009119	*lrr1*	1.04	3.06E-02
ENSXETG00000013749	*polr1b*	1.04	1.37E-06
ENSXETG00000021731	*epha2*	1.03	3.73E-04
ENSXETG00000014976	*slc39a6*	1.03	2.94E-02
ENSXETG00000017414	*ubiad1*	1.03	2.65E-03
ENSXETG00000003247	*znf451*	1.03	2.14E-03
ENSXETG00000022626	*prmt5*	1.02	9.08E-04
ENSXETG00000021932	*c18orf21*	1.02	3.88E-04
ENSXETG00000015231	*sulf1*	1.01	3.12E-02
ENSXETG00000021691	*mapk8*	1.01	2.22E-03
ENSXETG00000012163	*ppp1r7*	1.01	1.87E-03
ENSXETG00000021431	*cbfa2t2*	1.01	1.85E-05
ENSXETG00000020027	*cbfb*	1.01	1.74E-02
ENSXETG00000012969	*rcc1*	1.01	2.38E-03
ENSXETG00000018603	*mvk*	1.00	8.54E-05
ENSXETG00000015037	*taf1a*	1.00	1.76E-02

ENSXETG00000021129	*bmper*	-1.34	8.22E-03
ENSXETG00000018451	*dlec1*	-1.34	4.35E-03
ENSXETG00000031212	*lrrc61*	-1.34	1.09E-03
ENSXETG00000007364	*slc4a1*	-1.33	4.86E-04
ENSXETG00000000511	*tubal3*	-1.33	1.37E-06
ENSXETG00000025129	*fam154b*	-1.32	4.36E-07
ENSXETG00000019254		-1.32	2.59E-09
ENSXETG00000011664	*ttc12*	-1.32	1.31E-03
ENSXETG00000013794	*c20orf12*	-1.32	3.25E-07
ENSXETG00000006039	*lrrc56*	-1.32	1.06E-02
ENSXETG00000005411	*meig1*	-1.32	9.85E-05
ENSXETG00000032730		-1.31	7.02E-04
ENSXETG00000021807	*cdkl5*	-1.31	3.26E-02
ENSXETG00000020259	*fam195a*	-1.31	1.98E-04
ENSXETG00000024054	*rsph10b*	-1.31	8.25E-05
ENSXETG00000004553	*armc4*	-1.30	3.19E-06
ENSXETG00000008083	*sptlc3*	-1.29	3.39E-06
ENSXETG00000019807	*cntrl*	-1.29	1.05E-06
ENSXETG00000000221	*sertad4*	-1.29	2.78E-02
ENSXETG00000001621	*fam83b*	-1.29	3.56E-03
ENSXETG00000019246		-1.29	4.71E-04
ENSXETG00000021922	*pfkp*	-1.29	4.43E-02
ENSXETG00000010513	*rhobtb2*	-1.29	2.63E-02
ENSXETG00000030628	*cep41*	-1.29	9.00E-10
ENSXETG00000003474	*eya2*	-1.29	3.26E-02
ENSXETG00000008832	*syt7*	-1.29	1.15E-02
ENSXETG00000000853	*nfatc1*	-1.28	1.68E-04
ENSXETG00000020342	*lrrc49*	-1.28	6.07E-05
ENSXETG00000018749	*b9d2*	-1.28	2.85E-05
ENSXETG00000025359	*spef2*	-1.28	5.05E-09
ENSXETG00000007441	*c7orf63*	-1.28	5.83E-06
ENSXETG00000023547	*cidec*	-1.28	1.50E-06
ENSXETG00000018054	*c3orf15*	-1.28	1.46E-06
ENSXETG00000021532	*atp6v1b1*	-1.28	2.40E-02
ENSXETG00000010337	*ern2*	-1.28	8.25E-05
ENSXETG00000025736	*id4*	-1.27	4.86E-04
ENSXETG00000017121	*ccdc67*	-1.27	2.00E-07

ENSXETG00000030250		-1.27	1.39E-08
ENSXETG00000005339	*ankrd9*	-1.27	2.69E-05
ENSXETG00000017407	*fbxo31*	-1.27	3.35E-06
ENSXETG00000021693	*c12orf63*	-1.27	1.12E-02
ENSXETG00000017719	*pde7b*	-1.27	1.47E-03
ENSXETG00000017468		-1.27	3.35E-02
ENSXETG00000015230	*c8orf34*	-1.26	4.70E-02
ENSXETG00000008245	*ctgf*	-1.26	1.35E-02
ENSXETG00000025254	*ccdc60*	-1.26	3.53E-02
ENSXETG00000000681	*mtus1*	-1.26	5.58E-08
ENSXETG00000016064	*tekt4*	-1.26	2.37E-07
ENSXETG00000019283	*ptprn*	-1.26	3.54E-02
ENSXETG00000017281	*ttc16*	-1.26	7.21E-03
ENSXETG00000030994	*kiaa0226*	-1.26	7.60E-03
ENSXETG00000033370		-1.25	1.04E-02
ENSXETG00000003003	*lrrc45*	-1.25	2.07E-02
ENSXETG00000014869	*efna5*	-1.25	1.06E-02
ENSXETG00000004470	*c9orf117*	-1.25	5.77E-05
ENSXETG00000024488	*c1orf177*	-1.25	1.97E-05
ENSXETG00000027042	*eif2c3*	-1.25	3.15E-03
ENSXETG00000015826	*egfr*	-1.25	5.39E-03
ENSXETG00000016661		-1.25	2.20E-02
ENSXETG00000007211	*esrra*	-1.25	2.98E-05
ENSXETG00000014773		-1.25	9.49E-03
ENSXETG00000005016	*wrap73*	-1.25	3.28E-03
ENSXETG00000031073	*katnal1*	-1.24	7.19E-03
ENSXETG00000030978	*cfap57*	-1.24	3.23E-06
ENSXETG00000023111	*slc26a5*	-1.24	4.75E-02
ENSXETG00000001379	*pdgfa*	-1.24	2.53E-02
ENSXETG00000026042	*rgs12*	-1.24	3.14E-02
ENSXETG00000029983		-1.24	1.50E-02
ENSXETG00000021994	*pip5kl1*	-1.24	3.01E-04
ENSXETG00000009776	*ezr*	-1.24	2.16E-02
ENSXETG00000000346	*rbl2*	-1.23	3.82E-03
ENSXETG00000000961	*ubr1*	-1.23	9.39E-03
ENSXETG00000033951	*ccdc96*	-1.23	1.64E-03
ENSXETG00000007177	*iqsec2*	-1.23	1.13E-02

ENSXETG00000010016	*pde9a*	-1.23	5.57E-03
ENSXETG00000006790	*tctex1d1*	-1.23	2.60E-09
ENSXETG00000009243	*pvrl1*	-1.23	2.09E-13
ENSXETG00000001752	*tuba8*	-1.23	1.48E-03
ENSXETG00000033873		-1.23	4.29E-05
ENSXETG00000004522	*lypd6*	-1.23	1.71E-02
ENSXETG00000018935	*bbs5*	-1.22	4.73E-07
ENSXETG00000007584	*baz2b*	-1.22	5.37E-03
ENSXETG00000013287	*atp2c2*	-1.22	2.24E-03
ENSXETG00000010879	*rsph9*	-1.22	2.28E-03
ENSXETG00000021049	*kit*	-1.22	4.85E-04
ENSXETG00000004424	*scube2*	-1.22	1.93E-02
ENSXETG00000016981	*lrrc9*	-1.22	1.60E-03
ENSXETG00000004770	*fbxw9*	-1.22	2.01E-04
ENSXETG00000030456	*mgst2*	-1.21	3.00E-03
ENSXETG00000030879	*efcab11*	-1.21	1.13E-02
ENSXETG00000019577	*tekt3*	-1.21	1.27E-05
ENSXETG00000025737	*c4orf47*	-1.21	2.18E-06
ENSXETG00000012662	*ccdc14*	-1.21	2.97E-02
ENSXETG00000006697	*egr1*	-1.20	3.32E-02
ENSXETG00000034354	*nek11*	-1.20	1.39E-03
ENSXETG00000006172	*c6orf165*	-1.20	4.60E-07
ENSXETG00000007394	*c10orf140*	-1.20	1.63E-02
ENSXETG00000030283	*fgd1*	-1.20	6.07E-05
ENSXETG00000017882	*fbxo43*	-1.20	2.39E-06
ENSXETG00000009988		-1.20	4.46E-02
ENSXETG00000013759	*ccdc135*	-1.20	1.41E-05
ENSXETG00000030281	*sntb2*	-1.20	2.07E-08
ENSXETG00000023804	*gfra1*	-1.19	3.01E-02
ENSXETG00000016145	*ccdc157*	-1.19	4.21E-05
ENSXETG00000033712	*fry*	-1.19	3.31E-03
ENSXETG00000009697	*c20orf26*	-1.19	9.83E-03
ENSXETG00000008640	*ctbs*	-1.19	1.58E-02
ENSXETG00000023191	*fam83a*	-1.19	2.91E-02
ENSXETG00000006027	*xb-gene-5818700*	-1.19	1.66E-02
ENSXETG00000003627	*wdr90*	-1.19	4.85E-10
ENSXETG00000031278		-1.18	1.14E-03

ENSXETG00000009994	*mycbpap*	-1.18	1.86E-04
ENSXETG00000016761	*cep19*	-1.18	1.16E-02
ENSXETG00000033547		-1.18	3.25E-02
ENSXETG00000019549	*foxj1*	-1.18	2.77E-06
ENSXETG00000030692	*sh3tc2*	-1.18	3.87E-02
ENSXETG00000023988	*zfpm1*	-1.18	4.71E-04
ENSXETG00000020484	*zfyve28*	-1.18	4.37E-02
ENSXETG00000001893	*c12orf55*	-1.18	3.86E-02
ENSXETG00000008804	*atf5.2*	-1.18	2.02E-02
ENSXETG00000002166	*dnali1*	-1.18	2.26E-04
ENSXETG00000016124	*alcam*	-1.18	5.01E-03
ENSXETG00000009215	*lrrc31*	-1.18	1.13E-02
ENSXETG00000006170	*ccdc13*	-1.17	1.84E-02
ENSXETG00000013405	*mapk15*	-1.17	5.67E-07
ENSXETG00000004564	*fut1*	-1.17	9.55E-03
ENSXETG00000017730	*wdr93*	-1.17	2.46E-02
ENSXETG00000013740	*ca2*	-1.17	1.42E-02
ENSXETG00000023881	*kif9*	-1.17	1.09E-06
ENSXETG00000022522	*plk4*	-1.16	1.43E-09
ENSXETG00000001302	*noxred1*	-1.16	1.09E-02
ENSXETG00000019671	*cep76*	-1.16	7.08E-05
ENSXETG00000000715	*hoxa1*	-1.16	1.27E-02
ENSXETG00000001588	*bbs12*	-1.16	5.58E-04
ENSXETG00000005936	*fam126a*	-1.16	3.35E-03
ENSXETG00000006579	*tbx3*	-1.16	3.00E-02
ENSXETG00000009392	*fam160a1*	-1.15	2.64E-02
ENSXETG00000018333	*kiaa0556*	-1.15	2.84E-04
ENSXETG00000029925		-1.15	1.57E-02
ENSXETG00000013734	*atp6v0d2*	-1.15	6.65E-04
ENSXETG00000005517	*fermt1*	-1.15	4.18E-02
ENSXETG00000022616	*fam184a*	-1.15	6.17E-03
ENSXETG00000004200		-1.15	1.41E-02
ENSXETG00000021413	*tpp1*	-1.15	3.34E-02
ENSXETG00000018202	*fam228b*	-1.15	3.83E-02
ENSXETG00000022999	*ccdc18*	-1.14	2.89E-02
ENSXETG00000012882	*meis2*	-1.14	1.19E-02
ENSXETG00000031289		-1.14	1.06E-02

ENSXETG00000031455	*ift88*	-1.14	3.60E-06
ENSXETG00000003366	*rab27b*	-1.14	1.74E-02
ENSXETG00000032327	*ccdc92*	-1.14	1.57E-04
ENSXETG00000031527	*ccdc87*	-1.13	3.85E-03
ENSXETG00000001384	*aadacl4*	-1.13	8.16E-03
ENSXETG00000010779	*spata4*	-1.13	7.30E-07
ENSXETG00000030332	*kiaa1407*	-1.13	6.22E-03
ENSXETG00000012541	*dnajb13*	-1.13	7.30E-07
ENSXETG00000008955	*acaca*	-1.13	3.07E-02
ENSXETG00000015924	*lrrk1*	-1.13	2.03E-02
ENSXETG00000013007	*ugp2*	-1.13	1.30E-05
ENSXETG00000009728	*usp3*	-1.13	3.28E-05
ENSXETG00000004420	*ccdc89*	-1.13	1.50E-02
ENSXETG00000006535	*prickle2*	-1.12	6.21E-04
ENSXETG00000025336	*cxorf58*	-1.12	1.33E-02
ENSXETG00000003329	*ccdc164*	-1.12	3.28E-03
ENSXETG00000031946	*dennd1b*	-1.12	2.90E-02
ENSXETG00000024543	*tex9*	-1.12	2.65E-05
ENSXETG00000001355	*ncs1*	-1.12	9.94E-04
ENSXETG00000004106	*fzd6*	-1.12	1.06E-03
ENSXETG00000023039	*lrrc6*	-1.11	1.67E-02
ENSXETG00000016749	*eppk1*	-1.11	5.30E-03
ENSXETG00000024456	*fbxo46*	-1.11	8.98E-04
ENSXETG00000009961	*kcnk5*	-1.11	8.64E-03
ENSXETG00000004670	*mvp*	-1.11	2.28E-05
ENSXETG00000031364	*nsf*	-1.11	1.40E-02
ENSXETG00000019251	*tuba1a*	-1.11	5.42E-07
ENSXETG00000010700	*ccdc83*	-1.11	4.29E-02
ENSXETG00000009216	*lrriq4*	-1.11	2.62E-03
ENSXETG00000024111	*casp6*	-1.11	1.41E-03
ENSXETG00000012423	*scnn1g*	-1.11	4.68E-02
ENSXETG00000020096	*siah2*	-1.11	1.83E-02
ENSXETG00000019437	*ccdc39*	-1.11	4.28E-06
ENSXETG00000009902	*c21orf59*	-1.10	1.91E-07
ENSXETG00000016769	*hs6st1*	-1.10	2.91E-04
ENSXETG00000018842	*enkur*	-1.10	4.25E-05
ENSXETG00000010315	*ppp4r4*	-1.10	1.56E-04

ENSXETG00000021254	*ift172*	-1.10	1.59E-04
ENSXETG00000032001	*bicd1*	-1.10	3.80E-02
ENSXETG00000016745	*ccdc151*	-1.10	1.76E-03
ENSXETG00000020238	*agbl3*	-1.10	1.20E-02
ENSXETG00000033274	*mcidas*	-1.10	1.91E-03
ENSXETG00000009178	*c9orf93*	-1.10	2.63E-06
ENSXETG00000020322	*ccdc11*	-1.10	1.72E-05
ENSXETG00000002073	*c19orf44*	-1.09	6.09E-05
ENSXETG00000004663		-1.09	1.40E-02
ENSXETG00000002225	*rod1*	-1.09	6.26E-03
ENSXETG00000005963	*tmprss2*	-1.09	3.04E-03
ENSXETG00000020468	*ppargc1a*	-1.09	8.43E-04
ENSXETG00000021069	*cep135*	-1.09	2.69E-04
ENSXETG00000028091	*ccno*	-1.08	6.74E-03
ENSXETG00000031645	*efnb3*	-1.08	5.98E-03
ENSXETG00000010891	*tcte1*	-1.08	2.69E-03
ENSXETG00000030937	*fsip1*	-1.08	1.86E-05
ENSXETG00000033876		-1.08	6.42E-03
ENSXETG00000008997	*plekha8*	-1.08	2.03E-02
ENSXETG00000012970	*rap1gap2*	-1.08	1.89E-02
ENSXETG00000011732	*agtpbp1*	-1.08	6.01E-03
ENSXETG00000009217	*lrrc34*	-1.07	7.79E-05
ENSXETG00000025773	*c1orf222*	-1.07	1.15E-03
ENSXETG00000033996	*pcnt*	-1.07	5.57E-03
ENSXETG00000012328	*ubxn11*	-1.07	5.45E-03
ENSXETG00000017447	*c1orf21*	-1.07	2.59E-04
ENSXETG00000016556	*mns1*	-1.07	1.91E-03
ENSXETG00000019096	*rsph6a*	-1.07	9.66E-05
ENSXETG00000001463	*ift122*	-1.06	3.26E-02
ENSXETG00000025625	*agr2*	-1.06	1.55E-06
ENSXETG00000018105	*micall2*	-1.06	9.61E-06
ENSXETG00000008978	*styxl1*	-1.06	8.97E-09
ENSXETG00000013739	*ccdc113*	-1.06	4.01E-04
ENSXETG00000014260	*fam129b*	-1.05	2.20E-06
ENSXETG00000006071	*ccdc104*	-1.05	1.58E-08
ENSXETG00000009815	*ccdc65*	-1.05	3.14E-05
ENSXETG00000012155	*lrrc48*	-1.05	7.42E-03

ENSXETG00000001229	*mgc79783*	-1.05	1.85E-02
ENSXETG00000018573	*foxn4*	-1.05	7.60E-03
ENSXETG00000018017	*gpr156*	-1.04	2.45E-02
ENSXETG00000023264	*cspp1*	-1.03	3.00E-02
ENSXETG00000013130	*magi1*	-1.03	5.27E-03
ENSXETG00000001660	*xb-gene-5815363*	-1.03	1.68E-02
ENSXETG00000000979	*ttbk2*	-1.03	2.61E-02
ENSXETG00000007807	*iqch*	-1.03	1.02E-03
ENSXETG00000020472	*pacrgl*	-1.03	2.07E-02
ENSXETG00000000702	*ttc23l*	-1.02	7.11E-05
ENSXETG00000017228	*rnasek*	-1.02	8.47E-05
ENSXETG00000004733	*kifap3*	-1.02	3.20E-02
ENSXETG00000003223	*esyt3*	-1.02	4.47E-03
ENSXETG00000034059		-1.02	2.22E-04
ENSXETG00000033349	*mgc147546*	-1.02	2.66E-04
ENSXETG00000019937	*agbl2*	-1.02	2.16E-02
ENSXETG00000016014	*stoml3*	-1.02	8.64E-03
ENSXETG00000002292	*acly*	-1.02	1.92E-04
ENSXETG00000012554	*capn7*	-1.02	2.15E-04
ENSXETG00000007726	*plp2*	-1.01	1.50E-02
ENSXETG00000030278	*adam7*	-1.01	1.15E-03
ENSXETG00000008635	*ssx2ip*	-1.01	6.12E-03
ENSXETG00000016097	*pgp*	-1.01	1.95E-03
ENSXETG00000014740	*arhgap23*	-1.01	1.01E-02
ENSXETG00000015225	*arl3.1*	-1.01	7.82E-08
ENSXETG00000021305	*nbeal2*	-1.01	2.38E-02
ENSXETG00000014645	*slc4a11*	-1.00	5.41E-03
ENSXETG00000031231	*fbf1*	-1.00	3.12E-03
ENSXETG00000018458	*plcd1*	-1.00	1.45E-02
ENSXETG00000000967	*nadsyn1*	-1.00	2.05E-03
ENSXETG00000002421	*c1orf114*	-1.00	1.68E-04
ENSXETG00000020945	*ift81*	-1.00	6.89E-04
ENSXETG00000031398	*ccp110*	-1.00	3.74E-04
ENSXETG00000010380	*acvr1*	-1.00	7.74E-03

6.1.2 Differentially expressed genes at stage 27

Given are the ensembl id, official gene name, log2 fold change and the adjusted P-value with respect to multiple testing using the FDR method. Genes were sorted according to the highest and lowest log2 fold change, respectively.

Table 6.2 Summary of differentially expressed genes at stage 27

upregulated			
ensembl id	**Gene**	**log2 Fold Change**	**adjust. P-value**
ENSXETG00000006348	*sox10*	7.92	7.84E-21
ENSXETG00000023476	*hoxc8*	7.56	1.34E-37
ENSXETG00000015915	*prdm14*	7.44	1.19E-33
ENSXETG00000007863	*stmn2*	7.25	5.73E-11
ENSXETG00000005657	*penk*	6.80	3.34E-10
ENSXETG00000023475	*hoxc9*	6.65	7.84E-21
ENSXETG00000003618	*atp2b4*	6.61	4.11E-10
ENSXETG00000016479	*trpm1*	6.58	1.29E-10
ENSXETG00000023479	*hoxc6*	6.40	2.40E-15
ENSXETG00000010836	*foxd3*	6.34	3.01E-10
ENSXETG00000032598	*map1b*	6.34	1.85E-10
ENSXETG00000027815	*vcan*	6.28	1.89E-09
ENSXETG00000004874		6.24	1.60E-08
ENSXETG00000018387	*ednrb2*	6.20	1.29E-08
ENSXETG00000022336	*olfm1*	6.15	1.51E-09
ENSXETG00000015096	*snap25*	6.14	1.07E-17
ENSXETG00000008965	*scn3a*	6.12	2.24E-10
ENSXETG00000003388	*adam11*	5.97	3.77E-09
ENSXETG00000011738	*tyr*	5.91	2.04E-08
ENSXETG00000018304	*tlx3*	5.91	5.73E-11
ENSXETG00000030140	*stx1b*	5.84	2.36E-07
ENSXETG00000003399	*slc17a7*	5.78	4.18E-09
ENSXETG00000030402		5.77	4.41E-07
ENSXETG00000000237	*zeb2*	5.73	5.32E-09
ENSXETG00000019179	*adcyap1*	5.68	4.49E-08
ENSXETG00000013347	*gpm6b*	5.62	1.03E-09

downregulated			
ensembl id	**Gene**	**log2 Fold Change**	**adjust. P-value**
ENSXETG00000032850	*lrrn3*	-2.69	8.13E-03
ENSXETG00000001728	*slc6a3*	-2.50	2.79E-02
ENSXETG00000032366	*lgr5*	-2.49	7.86E-04
ENSXETG00000008859	*hkdc1*	-2.16	1.27E-03
ENSXETG00000012512	*xb-gene-990053*	-1.99	2.94E-04
ENSXETG00000001035	*fam132a*	-1.93	1.45E-02
ENSXETG00000017075	*pde8b*	-1.89	4.70E-02
ENSXETG00000027798	*pnmt*	-1.88	2.89E-02
ENSXETG00000022857		-1.83	9.72E-03
ENSXETG00000007353	*tgm5*	-1.78	6.28E-03
ENSXETG00000031045	*sepp1*	-1.64	1.91E-02
ENSXETG00000021580	*slc2a7*	-1.61	2.48E-03
ENSXETG00000014607	*calb1*	-1.60	1.15E-02
ENSXETG00000004839	*maob*	-1.56	4.89E-02
ENSXETG00000020701	*tpte2*	-1.56	2.91E-04
ENSXETG00000032779		-1.55	1.80E-04
ENSXETG00000032204	*plcl1*	-1.52	1.98E-02
ENSXETG00000020033	*serpinc1*	-1.51	8.88E-06
ENSXETG00000018739	*cdo1*	-1.49	4.41E-03
ENSXETG00000031991		-1.47	4.52E-05
ENSXETG00000033983	*dmrt2*	-1.47	3.72E-04
ENSXETG00000015904	*lctl*	-1.46	1.20E-02
ENSXETG00000018800		-1.42	3.28E-02
ENSXETG00000017719	*pde7b*	-1.42	5.79E-04
ENSXETG00000007364	*slc4a1*	-1.38	6.87E-04
ENSXETG00000002371	*kif27*	-1.36	2.12E-02

ENSXETG00000000724	*hoxa9*	5.56	1.29E-08
ENSXETG00000020467	*cdh11*	5.56	1.79E-08
ENSXETG00000003657	*sncg*	5.56	1.20E-14
ENSXETG00000019353	*cadm3*	5.45	6.81E-06
ENSXETG00000018040	*ntrk1*	5.35	2.73E-06
ENSXETG00000002556	*slc45a2*	5.35	1.29E-08
ENSXETG00000020978	*robo2*	5.34	3.74E-08
ENSXETG00000000719	*l1cam*	5.32	2.27E-10
ENSXETG00000011751	*rab38*	5.31	4.37E-06
ENSXETG00000006932	*cdh2*	5.29	2.71E-09
ENSXETG00000006230	*kif5a*	5.14	7.99E-07
ENSXETG00000009943	*ntng1*	5.14	1.82E-05
ENSXETG00000013534	*rtn4rl1*	5.11	9.82E-08
ENSXETG00000023938	*tnc*	5.10	1.24E-09
ENSXETG00000021492	*lrfn5*	5.08	2.01E-05
ENSXETG00000010942	*dct*	5.07	6.40E-06
ENSXETG00000015442	*syt4*	5.05	1.71E-05
ENSXETG00000026846	*sncb*	5.04	1.75E-07
ENSXETG00000032855	*tmem196*	5.02	4.07E-05
ENSXETG00000031363	*rab6b*	5.00	7.86E-08
ENSXETG00000006562	*shc2*	4.99	1.10E-05
ENSXETG00000005838	*mllt11*	4.99	8.53E-06
ENSXETG00000010153	*ebf2*	4.96	4.12E-06
ENSXETG00000009667	*c1orf216*	4.91	1.24E-05
ENSXETG00000032232	*mlph*	4.86	1.49E-05
ENSXETG00000023585	*dpysl4*	4.85	2.94E-08
ENSXETG00000034215	*sipa1*	4.84	6.25E-05
ENSXETG00000001025	*mapk8ip1*	4.82	3.30E-06
ENSXETG00000007640	*pax3*	4.82	1.65E-05
ENSXETG00000003477	*fgf13*	4.81	1.13E-05
ENSXETG00000016741	*elavl3*	4.81	6.64E-07
ENSXETG00000009037	*fam176b*	4.77	6.01E-05
ENSXETG00000019618	*nptx1*	4.74	6.05E-10
ENSXETG00000004068	*syt1*	4.73	2.36E-04
ENSXETG00000022924	*brsk1*	4.73	2.57E-04
ENSXETG00000014261	*stxbp1*	4.69	2.36E-09
ENSXETG00000030030	*kctd16*	4.68	2.25E-04

ENSXETG00000008892	*irx4*	-1.34	4.41E-03
ENSXETG00000010125	*tmprss13*	-1.29	4.31E-02
ENSXETG00000020335	*fgfbp2*	-1.28	2.71E-02
ENSXETG00000032404	*axdnd1*	-1.28	2.43E-02
ENSXETG00000013722	*ephb1*	-1.27	1.16E-05
ENSXETG00000000158	*xb-gene-5822257*	-1.25	1.59E-02
ENSXETG00000030875		-1.21	1.66E-03
ENSXETG00000000901		-1.13	2.45E-03
ENSXETG00000000157	*ppp1r14a*	-1.10	3.27E-03
ENSXETG00000032488		-1.09	8.57E-03
ENSXETG00000001660	*xb-gene-5815363*	-1.06	4.15E-02
ENSXETG00000009697	*c20orf26*	-1.06	4.10E-02
ENSXETG00000014867	*pltp*	-1.05	5.90E-03
ENSXETG00000020710	*nek5*	-1.01	3.59E-03
ENSXETG00000024858	*cyp2c18*	-1.00	1.07E-02

ENSXETG00000 022315	*cplx2*	4.66	1.29E-08
ENSXETG00000 000728	*hoxa10*	4.65	3.94E-05
ENSXETG00000 030920	*atp2b3*	4.63	1.27E-11
ENSXETG00000 015058	*klhl35*	4.63	1.56E-04
ENSXETG00000 021181	*pcdh9*	4.61	4.83E-05
ENSXETG00000 000722	*hoxa7*	4.58	1.65E-09
ENSXETG00000 025525	*pnhd*	4.51	1.13E-05
ENSXETG00000 015810	*cntn1*	4.50	6.57E-05
ENSXETG00000 015061	*map6*	4.48	3.33E-04
ENSXETG00000 018386	*pou4f1.2*	4.47	4.39E-08
ENSXETG00000 011339	*sez6l2*	4.47	9.87E-06
ENSXETG00000 000225	*kcnh1*	4.44	6.92E-04
ENSXETG00000 007718	*syp*	4.42	1.33E-06
ENSXETG00000 020282	*itga8*	4.39	5.23E-04
ENSXETG00000 005746	*sox8*	4.37	2.10E-05
ENSXETG00000 000910	*arl8a*	4.37	8.02E-09
ENSXETG00000 002939	*scg2*	4.35	1.95E-05
ENSXETG00000 022304	*svop*	4.34	2.91E-04
ENSXETG00000 007649	*c11orf87*	4.34	3.00E-04
ENSXETG00000 025183	*hoxc5*	4.29	5.89E-15
ENSXETG00000 007626	*sv2b*	4.28	1.66E-03
ENSXETG00000 006906	*nptxr*	4.25	7.19E-07
ENSXETG00000 016503	*apba2*	4.24	2.79E-07
ENSXETG00000 022780	*fli1*	4.24	8.94E-04
ENSXETG00000 010118	*adam23*	4.23	6.01E-05
ENSXETG00000 033967	*slc18a3*	4.18	4.68E-04
ENSXETG00000 015711	*grm7*	4.18	1.12E-03
ENSXETG00000 020846	*scn1a*	4.16	4.76E-04
ENSXETG00000 008680	*elavl4*	4.15	5.01E-07
ENSXETG00000 002245	*frmpd1*	4.14	2.06E-04
ENSXETG00000 023482	*bhlhe41*	4.13	6.73E-04
ENSXETG00000 001353	*hmcn2*	4.13	4.38E-07
ENSXETG00000 012179	*rtn4r*	4.10	2.27E-03
ENSXETG00000 006793	*pdzrn4*	4.09	1.56E-03
ENSXETG00000 022950	*zbtb16*	4.09	6.37E-16
ENSXETG00000 025936	*cnrip1*	4.05	4.52E-04
ENSXETG00000 027666	*tmeff1*	4.05	3.34E-10

ENSXETG00000 010674	*atp8a2*	4.04	1.52E-03
ENSXETG00000 034346	*dpysl2*	4.04	6.29E-07
ENSXETG00000 000742	*lmx1b.1*	4.00	4.22E-07
ENSXETG00000 004296	*xb-gene-987190*	4.00	1.18E-03
ENSXETG00000 001812	*postn*	3.99	4.62E-03
ENSXETG00000 032363	*pou4f3*	3.98	4.03E-03
ENSXETG00000 000108	*c6orf192*	3.96	3.59E-03
ENSXETG00000 004406		3.96	3.47E-05
ENSXETG00000 006083	*slc1a3*	3.92	1.12E-06
ENSXETG00000 007492	*kcnj12*	3.92	4.64E-03
ENSXETG00000 009344	*kank2*	3.90	4.39E-03
ENSXETG00000 025170	*gpr173*	3.89	5.75E-03
ENSXETG00000 026334	*cacnb1*	3.88	1.23E-04
ENSXETG00000 021973	*hoxb4*	3.87	6.89E-04
ENSXETG00000 005205	*parp6*	3.87	1.50E-03
ENSXETG00000 020236	*rbfox3*	3.86	3.11E-04
ENSXETG00000 030565	*drgx*	3.86	1.56E-04
ENSXETG00000 021993	*hoxb8*	3.85	1.81E-03
ENSXETG00000 021195		3.81	2.51E-04
ENSXETG00000 006675	*smpd3*	3.80	3.27E-05
ENSXETG00000 012718	*dpysl3*	3.80	8.12E-11
ENSXETG00000 022629	*snap91*	3.78	4.07E-05
ENSXETG00000 012629	*nrp1*	3.76	1.52E-04
ENSXETG00000 017979	*avp*	3.75	9.78E-03
ENSXETG00000 017099	*kif21b*	3.75	7.73E-03
ENSXETG00000 003405	*slit1*	3.74	4.74E-05
ENSXETG00000 020230	*hs3st5*	3.73	6.22E-03
ENSXETG00000 015595	*npr3*	3.73	8.99E-03
ENSXETG00000 032535	*fbn2*	3.71	1.12E-03
ENSXETG00000 011744	*mgat4c*	3.71	1.11E-02
ENSXETG00000 014639	*palm*	3.69	8.48E-08
ENSXETG00000 019847	*dbndd1*	3.69	1.09E-02
ENSXETG00000 003565	*foxf1*	3.67	3.68E-04
ENSXETG00000 014625	*nell2*	3.66	7.69E-05
ENSXETG00000 010136	*homer3*	3.66	3.26E-03
ENSXETG00000 013321	*phlda1*	3.65	1.20E-03
ENSXETG00000 025361	*xb-gene-5911701*	3.65	3.59E-03

ENSXETG00000 022236	*tspan18*	3.62	1.43E-02
ENSXETG00000 032009	*kcnq2*	3.61	3.91E-03
ENSXETG00000 009439	*pmel*	3.60	1.19E-04
ENSXETG00000 003071	*fbln1*	3.59	1.10E-05
ENSXETG00000 031277	*spry3*	3.58	9.78E-03
ENSXETG00000 009191	*trim63*	3.57	1.04E-02
ENSXETG00000 022008	*sh2d3c*	3.56	2.32E-03
ENSXETG00000 033300	*gareml*	3.55	1.74E-02
ENSXETG00000 011309	*ebf3*	3.55	2.57E-05
ENSXETG00000 009683	*tpbgl*	3.54	1.79E-02
ENSXETG00000 026804	*ptprr*	3.52	5.27E-03
ENSXETG00000 007501	*fscn1*	3.51	2.46E-09
ENSXETG00000 021591	*mcam*	3.51	3.00E-03
ENSXETG00000 011743	*htr1b*	3.50	2.03E-02
ENSXETG00000 007838	*adamts7*	3.49	1.50E-02
ENSXETG00000 005730		3.49	1.79E-02
ENSXETG00000 025181	*hoxc3*	3.48	2.46E-03
ENSXETG00000 011600	*crmp1*	3.47	1.26E-03
ENSXETG00000 019220	*bmpr1b*	3.47	1.81E-03
ENSXETG00000 010128	*nefm*	3.46	3.30E-09
ENSXETG00000 023484	*hoxc4*	3.44	9.95E-07
ENSXETG00000 018406	*slc24a5*	3.44	7.17E-05
ENSXETG00000 019915	*nes*	3.41	2.22E-02
ENSXETG00000 015623	*cdh19*	3.41	2.66E-02
ENSXETG00000 013268	*olfm3*	3.41	2.45E-03
ENSXETG00000 004054	*piezo2*	3.40	4.02E-05
ENSXETG00000 008490	*kcna1*	3.39	1.90E-02
ENSXETG00000 012905	*tyrp1*	3.39	1.26E-03
ENSXETG00000 030791	*mmrn2*	3.38	1.44E-02
ENSXETG00000 004192	*kcnk18*	3.36	6.66E-03
ENSXETG00000 023916	*clstn3*	3.36	8.71E-05
ENSXETG00000 019927	*crabp2*	3.35	1.18E-02
ENSXETG00000 013830	*plcd4*	3.33	4.88E-03
ENSXETG00000 008612	*slc6a8*	3.33	6.09E-03
ENSXETG00000 003449	*kcnt1*	3.31	1.25E-02
ENSXETG00000 018094	*scg5*	3.30	3.28E-04
ENSXETG00000 001801	*hoxd1*	3.30	5.01E-03

ENSXETG00000003372	*ppp1r9b*	3.30	3.84E-03
ENSXETG00000017530	*stmn4*	3.29	1.98E-02
ENSXETG00000017708	*foxb1*	3.29	3.35E-02
ENSXETG00000021987	*hoxb6*	3.28	1.70E-02
ENSXETG00000011726	*ntrk2*	3.27	7.97E-04
ENSXETG00000007556	*cd44*	3.25	2.30E-02
ENSXETG00000006011	*slc45a1*	3.21	6.83E-03
ENSXETG00000022371	*xb-gene-5730963*	3.20	5.42E-03
ENSXETG00000034183	*mapk8ip3*	3.20	8.96E-04
ENSXETG00000021035	*pdgfra*	3.19	1.17E-02
ENSXETG00000014391	*kcnc1*	3.19	4.71E-02
ENSXETG00000009066	*kcnab3*	3.18	1.67E-02
ENSXETG00000027289	*slmo1*	3.18	4.39E-02
ENSXETG00000018862	*dclk1*	3.16	2.42E-02
ENSXETG00000027719	*tfap2e*	3.16	7.86E-08
ENSXETG00000010491	*pcbp2*	3.16	6.55E-05
ENSXETG00000016492	*gng2*	3.16	5.44E-03
ENSXETG00000005309	*lrfn1*	3.14	2.92E-02
ENSXETG00000033812	*tmem116*	3.13	2.43E-02
ENSXETG00000022020	*fam198a*	3.12	1.26E-02
ENSXETG00000023385	*fst*	3.12	4.15E-02
ENSXETG00000005841	*nhlh1*	3.12	4.20E-02
ENSXETG00000031503	*grik5*	3.12	4.71E-02
ENSXETG00000000442	*optc*	3.11	3.68E-04
ENSXETG00000012138	*kif1a*	3.10	4.41E-03
ENSXETG00000006647	*igdcc4*	3.09	4.66E-02
ENSXETG00000005585	*cacna1a*	3.08	5.32E-03
ENSXETG00000000314	*nr5a2*	3.07	4.41E-03
ENSXETG00000023470	*hoxc12*	3.06	4.71E-02
ENSXETG00000013424	*mfap2*	3.06	7.38E-03
ENSXETG00000023751	*kiaa1274*	3.05	5.83E-04
ENSXETG00000022299	*kal1*	3.03	9.26E-03
ENSXETG00000004290	*ccdc165*	3.02	3.68E-04
ENSXETG00000010095	*nrp2*	3.01	4.41E-03
ENSXETG00000009083	*hes7.2*	2.99	4.29E-02
ENSXETG00000015532	*fbxl16*	2.97	3.47E-03
ENSXETG00000023880	*rgmb*	2.95	9.80E-04

ENSXETG00000 020755	*scg3*	2.95	4.91E-02
ENSXETG00000 030958	*kcnh5*	2.95	1.26E-02
ENSXETG00000 003986	*lmo2*	2.95	3.12E-02
ENSXETG00000 021660	*scarf2*	2.93	2.77E-02
ENSXETG00000 021341	*krt16*	2.93	1.75E-07
ENSXETG00000 006199	*mapk10*	2.93	9.02E-04
ENSXETG00000 012355	*dach1*	2.92	4.71E-02
ENSXETG00000 001772	*gdap1l1*	2.92	3.42E-04
ENSXETG00000 015485	*mycn*	2.92	3.31E-04
ENSXETG00000 020864	*ppp2r2b*	2.91	3.87E-04
ENSXETG00000 022243	*cadps*	2.89	2.12E-03
ENSXETG00000 033848		2.88	1.34E-04
ENSXETG00000 001405		2.87	4.71E-02
ENSXETG00000 031488	*pcdh19*	2.87	1.79E-02
ENSXETG00000 003707	*apc2*	2.85	2.77E-03
ENSXETG00000 030305	*amph*	2.85	3.50E-02
ENSXETG00000 014034	*lix1l*	2.81	5.84E-03
ENSXETG00000 003954	*ptgds*	2.79	1.25E-02
ENSXETG00000 007462	*vim*	2.77	1.92E-06
ENSXETG00000 008109	*xkr4*	2.77	5.57E-03
ENSXETG00000 018024	*c6orf145*	2.74	7.93E-03
ENSXETG00000 032893	*plekhg4b*	2.74	2.56E-02
ENSXETG00000 027686	*serpinf1*	2.72	3.81E-04
ENSXETG00000 020206	*timp2*	2.72	3.28E-02
ENSXETG00000 010662	*ap3b2*	2.71	4.76E-04
ENSXETG00000 002780	*clip3*	2.70	2.06E-03
ENSXETG00000 007241	*dbn1*	2.69	1.20E-05
ENSXETG00000 000735	*srpk2*	2.69	1.04E-02
ENSXETG00000 022354	*nos1*	2.69	1.12E-03
ENSXETG00000 013597	*unc13a*	2.63	2.92E-02
ENSXETG00000 003735	*pcdh8l*	2.63	3.64E-02
ENSXETG00000 020455	*krt18*	2.63	5.35E-10
ENSXETG00000 002894	*kcnab2*	2.62	2.43E-02
ENSXETG00000 011446	*plxna4*	2.60	3.41E-02
ENSXETG00000 032158	*wasf3*	2.60	2.92E-02
ENSXETG00000 009658	*mrz 09*	2.60	6.66E-03
ENSXETG00000 021674	*tfap2b*	2.57	1.17E-04

ENSXETG00000 022636	*prss35*	2.57	7.37E-05
ENSXETG00000 003570	*cxcl12*	2.55	7.71E-03
ENSXETG00000 015769	*nrcam*	2.53	1.70E-02
ENSXETG00000 002702	*mmp24*	2.52	1.78E-02
ENSXETG00000 023036	*kcnq3*	2.51	4.33E-02
ENSXETG00000 018853	*rab3c*	2.49	2.56E-02
ENSXETG00000 012785	*bsn*	2.46	2.90E-03
ENSXETG00000 001650	*ppp2r5b*	2.44	1.80E-02
ENSXETG00000 017780	*fez1*	2.43	1.79E-02
ENSXETG00000 003374	*col1a1*	2.42	1.29E-08
ENSXETG00000 011604	*ppp2r2c*	2.42	4.59E-02
ENSXETG00000 012934	*bgn*	2.41	8.09E-05
ENSXETG00000 031380	*gng3*	2.40	4.49E-03
ENSXETG00000 002263	*ttc28*	2.39	2.03E-02
ENSXETG00000 016983	*rtn1*	2.38	4.83E-03
ENSXETG00000 020369	*sgip1*	2.37	2.42E-02
ENSXETG00000 011375	*mmp25*	2.36	8.46E-04
ENSXETG00000 030341	*rab3il1*	2.35	2.86E-02
ENSXETG00000 029995	*sptbn1*	2.35	4.04E-06
ENSXETG00000 011332	*vwde*	2.32	4.71E-02
ENSXETG00000 000720	*hoxa5*	2.32	4.22E-03
ENSXETG00000 015555	*ank2*	2.31	6.66E-03
ENSXETG00000 009096	*vamp2*	2.31	4.71E-02
ENSXETG00000 006707	*b4galnt4*	2.31	1.27E-02
ENSXETG00000 011788	*cdx2*	2.30	2.20E-03
ENSXETG00000 017443	*glt25d2*	2.26	2.13E-02
ENSXETG00000 011665	*ncam1*	2.24	6.66E-03
ENSXETG00000 031133	*sema3e*	2.24	1.79E-02
ENSXETG00000 010393		2.23	2.08E-03
ENSXETG00000 034301		2.21	2.25E-04
ENSXETG00000 004486	*kif5c*	2.21	3.76E-02
ENSXETG00000 017239		2.20	2.76E-03
ENSXETG00000 011188	*prph*	2.19	4.41E-03
ENSXETG00000 007431	*adam22*	2.19	2.49E-03
ENSXETG00000 004589	*cdx4*	2.18	4.38E-03
ENSXETG00000 022798	*sostdc1*	2.16	3.47E-02
ENSXETG00000 026058	*cnfn.1*	2.13	1.07E-02

ENSXETG00000020346	*gabbr1*	2.09	3.51E-03
ENSXETG00000032203	*map1a*	2.08	3.10E-02
ENSXETG00000002308	*rims1*	2.08	4.63E-02
ENSXETG00000007363	*rundc3a*	2.06	9.90E-04
ENSXETG00000018184	*cyp26a1*	2.06	9.26E-03
ENSXETG00000025407	*sp5*	2.06	2.08E-02
ENSXETG00000030115	*sp8*	2.05	1.46E-08
ENSXETG00000012198	*nid2*	2.03	1.72E-06
ENSXETG00000015806	*hecw1*	2.03	3.37E-02
ENSXETG00000027090	*xb-gene-5768884*	2.01	6.07E-04
ENSXETG00000013742	*ndrg3*	2.00	6.66E-03
ENSXETG00000005949	*mst1*	1.99	3.48E-02
ENSXETG00000018032	*tubb2b*	1.98	4.85E-04
ENSXETG00000008971	*ywhag*	1.96	8.73E-04
ENSXETG00000021967	*hoxb3*	1.95	4.18E-02
ENSXETG00000016758	*xb-gene-1002559*	1.95	2.24E-06
ENSXETG00000020280	*fam171a1*	1.94	1.97E-04
ENSXETG00000024006	*snai2*	1.92	2.69E-03
ENSXETG00000031472	*tenm2*	1.91	1.85E-05
ENSXETG00000031338	*cntn4*	1.91	2.89E-02
ENSXETG00000014880	*xb-gene-5936529*	1.89	2.38E-02
ENSXETG00000017270	*c3*	1.88	1.04E-02
ENSXETG00000010655	*col2a1*	1.88	4.18E-06
ENSXETG00000017823	*plxnb1*	1.88	4.83E-03
ENSXETG00000016109	*gatm*	1.86	6.29E-07
ENSXETG00000007614	*epha4*	1.86	5.55E-03
ENSXETG00000013228	*egflam*	1.86	2.99E-03
ENSXETG00000019579	*pmp22*	1.80	1.04E-02
ENSXETG00000009499	*slc39a5*	1.80	8.81E-04
ENSXETG00000027751	*marcks*	1.79	1.71E-03
ENSXETG00000005960	*c3orf54*	1.79	9.28E-04
ENSXETG00000023647	*rufy3*	1.78	1.53E-03
ENSXETG00000008706	*flrt3*	1.71	1.18E-02
ENSXETG00000010898	*fn1*	1.66	8.57E-03
ENSXETG00000010192	*pde4dip*	1.66	2.43E-02
ENSXETG00000002710	*rcor2*	1.65	4.71E-02
ENSXETG00000005775	*gng13*	1.65	4.73E-03

ENSXETG00000004959	*epb41l3*	1.63	2.13E-02
ENSXETG00000000172	*maf*	1.61	3.27E-02
ENSXETG00000021398	*dgki*	1.61	4.26E-03
ENSXETG00000008088		1.58	4.81E-02
ENSXETG00000002597	*lpar1*	1.57	4.71E-02
ENSXETG00000007569	*hapln3*	1.57	9.12E-03
ENSXETG00000011877	*cd74*	1.53	1.60E-02
ENSXETG00000020022	*gnao1*	1.53	1.06E-02
ENSXETG00000031404	*draxin*	1.49	1.77E-03
ENSXETG00000018597	*aldh3b1*	1.47	6.85E-04
ENSXETG00000007165	*myo10.2*	1.47	4.55E-02
ENSXETG00000024138	*rgma*	1.46	2.76E-03
ENSXETG00000011757	*col5a3*	1.46	1.70E-02
ENSXETG00000011615	*fam171a2*	1.44	2.39E-02
ENSXETG00000013891	*kcnj13*	1.39	3.95E-02
ENSXETG00000012216	*msi1*	1.39	1.36E-02
ENSXETG00000025032	*mmp15*	1.36	2.21E-02
ENSXETG00000013633	*rab30*	1.36	1.92E-02
ENSXETG00000020090	*pfn2*	1.34	1.74E-02
ENSXETG00000003486	*st3gal3*	1.31	4.10E-02
ENSXETG00000010561	*dmd*	1.30	1.40E-02
ENSXETG00000018626	*xk*	1.30	4.71E-02
ENSXETG00000011231	*cmtm3*	1.30	2.96E-02
ENSXETG00000004468	*kiaa0182*	1.28	2.33E-03
ENSXETG00000034199	*prkg1*	1.26	8.08E-04
ENSXETG00000001502	*cyfip2*	1.21	1.65E-02
ENSXETG00000018465	*rell1*	1.21	3.90E-02
ENSXETG00000017308	*dlgap4*	1.18	5.73E-03
ENSXETG00000027945	*slc30a8*	1.09	2.24E-02
ENSXETG00000011833	*ptprd*	1.05	2.03E-02
ENSXETG00000023814	*angpt4*	1.05	3.06E-03
ENSXETG00000024861	*loxl1*	1.05	3.48E-02
ENSXETG00000018462	*nkd1*	1.03	7.00E-03
ENSXETG00000014931	*pnkd*	1.00	2.92E-02

6.2 GO analysis of candidate genes

Gene Ontology (GO) analysis was performed using DAVID (http://david.abcc.ncifcrf.gov) as previously described (Dennis *et al.,* 2003). Analyzed were genes which were up and downregulated at stage 14 and 27, respectively.

6.2.1 GO analysis of candidate genes upregulated at stage 14

Given is the biological process, the number of genes and the P-value. Biological processes were sorted according to the P-value from lowest to highest.

Table 6.3 Summary of GO analysis of genes upregulated at stage 14

Biological Processes	Count	P-value
GO:0007389~pattern specification process	33	5.20E-17
GO:0003002~regionalization	28	6.70E-16
GO:0001501~skeletal system development	34	1.55E-15
GO:0009952~anterior/posterior pattern formation	24	1.71E-15
GO:0009792~embryonic development ending in birth or egg hatching	30	7.64E-12
GO:0043009~chordate embryonic development	29	3.36E-11
GO:0048568~embryonic organ development	20	6.65E-10
GO:0048598~embryonic morphogenesis	26	8.97E-10
GO:0048706~embryonic skeletal system development	13	2.10E-08
GO:0048705~skeletal system morphogenesis	14	1.98E-07
GO:0016055~Wnt receptor signaling pathway	15	2.29E-07
GO:0030182~neuron differentiation	27	2.72E-07
GO:0006355~regulation of transcription, DNA-dependent	61	4.31E-06
GO:0048562~embryonic organ morphogenesis	13	8.57E-06
GO:0051252~regulation of RNA metabolic process	61	8.75E-06
GO:0045165~cell fate commitment	13	1.35E-05
GO:0035107~appendage morphogenesis	11	1.82E-05
GO:0035108~limb morphogenesis	11	1.82E-05
GO:0035295~tube development	16	2.02E-05
GO:0002009~morphogenesis of an epithelium	11	2.17E-05
GO:0048736~appendage development	11	2.57E-05
GO:0060173~limb development	11	2.57E-05
GO:0042127~regulation of cell proliferation	33	3.83E-05
GO:0006357~regulation of transcription from RNA polymerase II promoter	31	5.19E-05
GO:0045449~regulation of transcription	76	6.73E-05
GO:0001568~blood vessel development	16	6.99E-05

GO:0001944~vasculature development	16	9.18E-05
GO:0048704~embryonic skeletal system morphogenesis	8	9.68E-05
GO:0006350~transcription	64	1.05E-04
GO:0060429~epithelium development	15	1.13E-04
GO:0031175~neuron projection development	16	1.15E-04
GO:0060348~bone development	11	1.17E-04
GO:0048729~tissue morphogenesis	13	1.69E-04
GO:0030326~embryonic limb morphogenesis	9	2.44E-04
GO:0035113~embryonic appendage morphogenesis	9	2.44E-04
GO:0051960~regulation of nervous system development	13	3.07E-04
GO:0051893~regulation of focal adhesion formation	4	3.54E-04
GO:0070482~response to oxygen levels	11	3.59E-04
GO:0022610~biological adhesion	28	3.78E-04
GO:0007155~cell adhesion	28	3.78E-04
GO:0007223~Wnt receptor signaling pathway, calcium modulating pathway	5	5.90E-04
GO:0031328~positive regulation of cellular biosynthetic process	27	6.12E-04
GO:0030030~cell projection organization	18	6.79E-04
GO:0010557~positive regulation of macromolecule biosynthetic process	26	7.03E-04
GO:0030323~respiratory tube development	9	7.16E-04
GO:0048514~blood vessel morphogenesis	13	7.19E-04
GO:0009891~positive regulation of biosynthetic process	27	7.53E-04
GO:0051094~positive regulation of developmental process	15	8.82E-04
GO:0022604~regulation of cell morphogenesis	10	8.83E-04
GO:0001890~placenta development	7	9.41E-04
GO:0008284~positive regulation of cell proliferation	19	9.51E-04
GO:0045664~regulation of neuron differentiation	10	9.84E-04
GO:0001666~response to hypoxia	10	0.001037845
GO:0050767~regulation of neurogenesis	11	0.001277265
GO:0048146~positive regulation of fibroblast proliferation	5	0.001368572
GO:0045597~positive regulation of cell differentiation	13	0.001454326
GO:0031344~regulation of cell projection organization	8	0.001507788
GO:0001503~ossification	9	0.001564536
GO:0010810~regulation of cell-substrate adhesion	6	0.001727396
GO:0021915~neural tube development	7	0.001813197
GO:0006928~cell motion	20	0.001833765
GO:0060284~regulation of cell development	12	0.00188405
GO:0035270~endocrine system development	7	0.00195489
GO:0035282~segmentation	6	0.002092464
GO:0010975~regulation of neuron projection development	7	0.002104804
GO:0048666~neuron development	16	0.002122653
GO:0001822~kidney development	8	0.002332143
GO:0048812~neuron projection morphogenesis	12	0.002542962
GO:0001708~cell fate specification	6	0.002741333
GO:0051173~positive regulation of nitrogen compound metabolic process	24	0.002765258
GO:0045596~negative regulation of cell differentiation	12	0.002834022
GO:0035239~tube morphogenesis	9	0.002920086

GO:0060485~mesenchyme development	6	0.002986784
GO:0014033~neural crest cell differentiation	5	0.00337608
GO:0014032~neural crest cell development	5	0.00337608
GO:0010769~regulation of cell morphogenesis involved in differentiation	7	0.003409922
GO:0051895~negative regulation of focal adhesion formation	3	0.003461661
GO:0010604~positive regulation of macromolecule metabolic process	29	0.003550878
GO:0045935~positive regulation of nucleobase, nucleoside, nucleotide and nucleic acid metabolic process	23	0.003923674
GO:0048145~regulation of fibroblast proliferation	5	0.004193864
GO:0050770~regulation of axonogenesis	6	0.00445706
GO:0045893~positive regulation of transcription, DNA-dependent	19	0.004459939
GO:0030155~regulation of cell adhesion	9	0.004634042
GO:0045944~positive regulation of transcription from RNA polymerase II promoter	16	0.00488243
GO:0051254~positive regulation of RNA metabolic process	19	0.00490873
GO:0001655~urogenital system development	8	0.00498123
GO:0006469~negative regulation of protein kinase activity	7	0.006210497
GO:0016477~cell migration	13	0.006593595
GO:0000904~cell morphogenesis involved in differentiation	12	0.007032767
GO:0002011~morphogenesis of an epithelial sheet	3	0.007088879
GO:0060216~definitive hemopoiesis	3	0.007088879
GO:0048858~cell projection morphogenesis	12	0.007244738
GO:0033673~negative regulation of kinase activity	7	0.007306829
GO:0001570~vasculogenesis	5	0.007423532
GO:0010628~positive regulation of gene expression	21	0.007600185
GO:0010629~negative regulation of gene expression	19	0.007718019
GO:0051130~positive regulation of cellular component organization	10	0.007749873
GO:0035136~forelimb morphogenesis	4	0.007990003
GO:0007507~heart development	11	0.008095522
GO:0000902~cell morphogenesis	15	0.00825573
GO:0045892~negative regulation of transcription, DNA-dependent	15	0.00825573
GO:0043549~regulation of kinase activity	15	0.008437681
GO:0009855~determination of bilateral symmetry	5	0.008783876
GO:0009799~determination of symmetry	5	0.008783876
GO:0060562~epithelial tube morphogenesis	6	0.008824926
GO:0032989~cellular component morphogenesis	16	0.009012378
GO:0009954~proximal/distal pattern formation	4	0.009061354
GO:0051253~negative regulation of RNA metabolic process	15	0.009381825
GO:0043583~ear development	7	0.009434829
GO:0051348~negative regulation of transferase activity	7	0.009908341
GO:0032990~cell part morphogenesis	12	0.009912217
GO:0010720~positive regulation of cell development	6	0.00996161
GO:0042981~regulation of apoptosis	26	0.010494514
GO:0040012~regulation of locomotion	10	0.011167629
GO:0030324~lung development	7	0.01143017
GO:0050772~positive regulation of axonogenesis	4	0.011445024
GO:0045941~positive regulation of transcription	20	0.011537427

GO:0007409~axonogenesis	10	0.011545858
GO:0043067~regulation of programmed cell death	26	0.0118267
GO:0051338~regulation of transferase activity	15	0.011865452
GO:0031346~positive regulation of cell projection organization	5	0.011970439
GO:0010941~regulation of cell death	26	0.01219235
GO:0007423~sensory organ development	11	0.012269742
GO:0001952~regulation of cell-matrix adhesion	4	0.014156404
GO:0016481~negative regulation of transcription	17	0.014505195
GO:0048870~cell motility	13	0.014567628
GO:0051674~localization of cell	13	0.014567628
GO:0001953~negative regulation of cell-matrix adhesion	3	0.01463005
GO:0045859~regulation of protein kinase activity	14	0.01481493
GO:0030334~regulation of cell migration	9	0.015480762
GO:0010811~positive regulation of cell-substrate adhesion	4	0.015636844
GO:0014031~mesenchymal cell development	5	0.015816193
GO:0048762~mesenchymal cell differentiation	5	0.015816193
GO:0030278~regulation of ossification	6	0.016323553
GO:0016337~cell-cell adhesion	12	0.016588266
GO:0060541~respiratory system development	7	0.01697508
GO:0048839~inner ear development	6	0.017164717
GO:0043065~positive regulation of apoptosis	16	0.017541166
GO:0010812~negative regulation of cell-substrate adhesion	3	0.017659224
GO:0043405~regulation of MAP kinase activity	8	0.018111471
GO:0048667~cell morphogenesis involved in neuron differentiation	10	0.01852925
GO:0043068~positive regulation of programmed cell death	16	0.018540644
GO:0044087~regulation of cellular component biogenesis	8	0.018753038
GO:0060606~tube closure	4	0.01884975
GO:0001843~neural tube closure	4	0.01884975
GO:0010942~positive regulation of cell death	16	0.019262565
GO:0010033~response to organic substance	23	0.019360157
GO:0008285~negative regulation of cell proliferation	14	0.020732215
GO:0048566~embryonic gut development	3	0.020928455
GO:0042573~retinoic acid metabolic process	3	0.020928455
GO:0009719~response to endogenous stimulus	15	0.022644706
GO:0051174~regulation of phosphorus metabolic process	17	0.02297031
GO:0019220~regulation of phosphate metabolic process	17	0.02297031
GO:0009725~response to hormone stimulus	14	0.02326085
GO:0006351~transcription, DNA-dependent	12	0.023974942
GO:0016331~morphogenesis of embryonic epithelium	5	0.024243091
GO:0014020~primary neural tube formation	4	0.024303066
GO:0006775~fat-soluble vitamin metabolic process	4	0.024303066
GO:0070633~transepithelial transport	3	0.024427602
GO:0051726~regulation of cell cycle	13	0.024755656
GO:0048589~developmental growth	6	0.024939263
GO:0050769~positive regulation of neurogenesis	5	0.025630326
GO:0032774~RNA biosynthetic process	12	0.02613828

GO:0001756~somitogenesis	4	0.02629014
GO:0045785~positive regulation of cell adhesion	5	0.027064424
GO:0030902~hindbrain development	5	0.027064424
GO:0007169~transmembrane receptor protein tyrosine kinase signaling pathway	10	0.027491236
GO:0045668~negative regulation of osteoblast differentiation	3	0.028146821
GO:0003006~reproductive developmental process	11	0.028314277
GO:0006468~protein amino acid phosphorylation	21	0.028893477
GO:0048545~response to steroid hormone stimulus	9	0.030354731
GO:0007167~enzyme linked receptor protein signaling pathway	13	0.030451206
GO:0048565~gut development	4	0.03051738
GO:0043407~negative regulation of MAP kinase activity	4	0.03051738
GO:0016310~phosphorylation	24	0.030890604
GO:0051270~regulation of cell motion	9	0.031228716
GO:0001893~maternal placenta development	3	0.032076557
GO:0042325~regulation of phosphorylation	16	0.03277587
GO:0045934~negative regulation of nucleobase, nucleoside, nucleotide and nucleic acid metabolic process	17	0.035341015
GO:0007090~regulation of S phase of mitotic cell cycle	3	0.036207534
GO:0007398~ectoderm development	9	0.036435924
GO:0042471~ear morphogenesis	5	0.036665433
GO:0043066~negative regulation of apoptosis	13	0.038284051
GO:0008283~cell proliferation	15	0.039144981
GO:0051172~negative regulation of nitrogen compound metabolic process	17	0.039248832
GO:0001841~neural tube formation	4	0.039973844
GO:0043069~negative regulation of programmed cell death	13	0.041564695
GO:0006917~induction of apoptosis	12	0.042136077
GO:0010035~response to inorganic substance	9	0.042158107
GO:0060548~negative regulation of cell death	13	0.042766221
GO:0012502~induction of programmed cell death	12	0.043017406
GO:0012501~programmed cell death	19	0.043551309
GO:0048732~gland development	7	0.043969141
GO:0022405~hair cycle process	4	0.045194271
GO:0001942~hair follicle development	4	0.045194271
GO:0007368~determination of left/right symmetry	4	0.045194271
GO:0022404~molting cycle process	4	0.045194271
GO:0042303~molting cycle	4	0.047925051
GO:0007162~negative regulation of cell adhesion	4	0.047925051
GO:0045667~regulation of osteoblast differentiation	4	0.047925051
GO:0001838~embryonic epithelial tube formation	4	0.047925051
GO:0042633~hair cycle	4	0.047925051
GO:0030198~extracellular matrix organization	6	0.048104005
GO:0007166~cell surface receptor linked signal transduction	46	0.048768893
GO:0006796~phosphate metabolic process	27	0.048780288
GO:0006793~phosphorus metabolic process	27	0.048780288
GO:0021587~cerebellum morphogenesis	3	0.049719237
GO:0031128~developmental induction	3	0.049719237

GO:0035115~embryonic forelimb morphogenesis	3	0.049719237
GO:0001502~cartilage condensation	3	0.049719237
GO:0051492~regulation of stress fiber formation	3	0.049719237
GO:0045168~cell-cell signaling involved in cell fate specification	3	0.049719237
GO:0043627~response to estrogen stimulus	6	0.049761407
GO:0003007~heart morphogenesis	5	0.050048384
GO:0007243~protein kinase cascade	13	0.050540179
GO:0006720~isoprenoid metabolic process	4	0.050735094
GO:0035148~tube lumen formation	4	0.050735094
GO:0001701~in utero embryonic development	8	0.051147881
GO:0006766~vitamin metabolic process	5	0.054303387
GO:0044092~negative regulation of molecular function	12	0.054485982
GO:0001825~blastocyst formation	3	0.05456781
GO:0008299~isoprenoid biosynthetic process	3	0.05456781
GO:0033261~regulation of S phase	3	0.05456781
GO:0046149~pigment catabolic process	2	0.055921085
GO:0040037~negative regulation of fibroblast growth factor receptor signaling pathway	2	0.055921085
GO:0032536~regulation of cell projection size	2	0.055921085
GO:0031133~regulation of axon diameter	2	0.055921085
GO:0042167~heme catabolic process	2	0.055921085
GO:0008219~cell death	21	0.056076417
GO:0030111~regulation of Wnt receptor signaling pathway	4	0.056589295
GO:0010558~negative regulation of macromolecule biosynthetic process	17	0.05772314
GO:0016265~death	21	0.058148938
GO:0032231~regulation of actin filament bundle formation	3	0.059575223
GO:0009746~response to hexose stimulus	4	0.05963149
GO:0034284~response to monosaccharide stimulus	4	0.05963149
GO:0040007~growth	8	0.060379206
GO:0048534~hemopoietic or lymphoid organ development	10	0.060923059
GO:0000165~MAPKKK cascade	8	0.061876376
GO:0008544~epidermis development	8	0.061876376
GO:0001525~angiogenesis	7	0.063230158
GO:0043547~positive regulation of GTPase activity	3	0.064733745
GO:0008633~activation of pro-apoptotic gene products	3	0.064733745
GO:0010564~regulation of cell cycle process	6	0.06617626
GO:0006915~apoptosis	18	0.067397024
GO:0000122~negative regulation of transcription from RNA polymerase II promoter	10	0.067789829
GO:0007548~sex differentiation	7	0.068282648
GO:0010817~regulation of hormone levels	7	0.068282648
GO:0031327~negative regulation of cellular biosynthetic process	17	0.068700964
GO:0007346~regulation of mitotic cell cycle	7	0.070017571
GO:0048806~genitalia development	3	0.070035878
GO:0021575~hindbrain morphogenesis	3	0.070035878
GO:0001523~retinoid metabolic process	3	0.070035878
GO:0006776~vitamin A metabolic process	3	0.070035878

GO:0016101~diterpenoid metabolic process	3	0.070035878
GO:0001755~neural crest cell migration	3	0.070035878
GO:0044057~regulation of system process	11	0.070928679
GO:0002683~negative regulation of immune system process	5	0.073205344
GO:0010746~regulation of plasma membrane long-chain fatty acid transport	2	0.073860329
GO:0051497~negative regulation of stress fiber formation	2	0.073860329
GO:0060441~branching involved in lung morphogenesis	2	0.073860329
GO:0045110~intermediate filament bundle assembly	2	0.073860329
GO:0042904~9-cis-retinoic acid biosynthetic process	2	0.073860329
GO:0010748~negative regulation of plasma membrane long-chain fatty acid transport	2	0.073860329
GO:0042905~9-cis-retinoic acid metabolic process	2	0.073860329
GO:0031558~induction of apoptosis in response to chemical stimulus	2	0.073860329
GO:0060438~trachea development	2	0.073860329
GO:0035238~vitamin A biosynthetic process	2	0.073860329
GO:0033674~positive regulation of kinase activity	9	0.074038316
GO:0045778~positive regulation of ossification	3	0.075474351
GO:0001892~embryonic placenta development	3	0.075474351
GO:0046777~protein amino acid autophosphorylation	5	0.078390786
GO:0007242~intracellular signaling cascade	32	0.078534519
GO:0001889~liver development	4	0.079427237
GO:0009890~negative regulation of biosynthetic process	17	0.080132165
GO:0006721~terpenoid metabolic process	3	0.081042119
GO:0006606~protein import into nucleus	5	0.081050684
GO:0002520~immune system development	10	0.081103167
GO:0048609~reproductive process in a multicellular organism	15	0.081411812
GO:0032504~multicellular organism reproduction	15	0.081411812
GO:0030097~hemopoiesis	9	0.081471717
GO:0042476~odontogenesis	4	0.082972575
GO:0051170~nuclear import	5	0.086502872
GO:0018149~peptide cross-linking	3	0.08673235
GO:0051347~positive regulation of transferase activity	9	0.087711566
GO:0043623~cellular protein complex assembly	7	0.088754002
GO:0030335~positive regulation of cell migration	5	0.089294329
GO:0042472~inner ear morphogenesis	4	0.090262802
GO:0043062~extracellular structure organization	7	0.090765091
GO:0031557~induction of programmed cell death in response to chemical stimulus	2	0.091459996
GO:0045683~negative regulation of epidermis development	2	0.091459996
GO:0006787~porphyrin catabolic process	2	0.091459996
GO:0042362~fat-soluble vitamin biosynthetic process	2	0.091459996
GO:0033015~tetrapyrrole catabolic process	2	0.091459996
GO:0032232~negative regulation of actin filament bundle formation	2	0.091459996
GO:0002695~negative regulation of leukocyte activation	4	0.094005045
GO:0045787~positive regulation of cell cycle	4	0.094005045
GO:0051240~positive regulation of multicellular organismal process	9	0.094221975
GO:0010647~positive regulation of cell communication	11	0.097158063

6.2.2 GO analysis of candidate genes downregulated at stage 14

Given is the biological process, the number of genes and the P-value. Biological processes were sorted according to the P-value from lowest to highest.

Table 6.4 Summary of GO analysis of genes downregulated at stage 14

Biological Process	Count	P-Value
GO:0007017~microtubule-based process	25	2.09E-10
GO:0007018~microtubule-based movement	16	6.13E-09
GO:0030030~cell projection organization	25	3.15E-07
GO:0006928~cell motion	25	2.56E-05
GO:0035295~tube development	16	3.30E-05
GO:0030031~cell projection assembly	10	3.76E-05
GO:0001539~ciliary or flagellar motility	5	1.29E-04
GO:0060271~cilium morphogenesis	6	4.43E-04
GO:0030324~lung development	9	7.72E-04
GO:0030323~respiratory tube development	9	9.40E-04
GO:0007507~heart development	13	1.22E-03
GO:0051674~localization of cell	16	1.23E-03
GO:0048870~cell motility	16	1.23E-03
GO:0060541~respiratory system development	9	1.36E-03
GO:0000902~cell morphogenesis	17	1.99E-03
GO:0042384~cilium assembly	5	2.12E-03
GO:0032989~cellular component morphogenesis	18	2.43E-03
GO:0048729~tissue morphogenesis	11	3.17E-03
GO:0048858~cell projection morphogenesis	13	3.64E-03
GO:0002009~morphogenesis of an epithelium	8	3.91E-03
GO:0032990~cell part morphogenesis	13	5.13E-03
GO:0007423~sensory organ development	12	6.04E-03
GO:0046777~protein amino acid autophosphorylation	7	6.77E-03
GO:0048232~male gamete generation	14	8.57E-03
GO:0007283~spermatogenesis	14	8.57E-03
GO:0048286~lung alveolus development	4	8.96E-03
GO:0007242~intracellular signaling cascade	38	9.30E-03
GO:0019953~sexual reproduction	18	9.96E-03
GO:0007276~gamete generation	16	1.23E-02
GO:0003007~heart morphogenesis	6	1.48E-02
GO:0048609~reproductive process in a multicellular organism	18	1.72E-02
GO:0032504~multicellular organism reproduction	18	1.72E-02
GO:0008360~regulation of cell shape	5	2.20E-02

GO:0051350~negative regulation of lyase activity	5	2.33E-02
GO:0031280~negative regulation of cyclase activity	5	2.33E-02
GO:0007194~negative regulation of adenylate cyclase activity	5	2.33E-02
GO:0001701~in utero embryonic development	9	2.42E-02
GO:0001568~blood vessel development	11	2.47E-02
GO:0000226~microtubule cytoskeleton organization	8	2.71E-02
GO:0007588~excretion	5	2.77E-02
GO:0016331~morphogenesis of embryonic epithelium	5	2.77E-02
GO:0045893~positive regulation of transcription, DNA-dependent	17	2.83E-02
GO:0001944~vasculature development	11	2.84E-02
GO:0051056~regulation of small GTPase mediated signal transduction	11	2.91E-02
GO:0043193~positive regulation of gene-specific transcription	6	2.92E-02
GO:0017157~regulation of exocytosis	4	2.93E-02
GO:0051254~positive regulation of RNA metabolic process	17	3.06E-02
GO:0001890~placenta development	5	3.09E-02
GO:0022037~metencephalon development	4	3.16E-02
GO:0051173~positive regulation of nitrogen compound metabolic process	21	3.16E-02
GO:0031328~positive regulation of cellular biosynthetic process	22	3.16E-02
GO:0043009~chordate embryonic development	13	3.27E-02
GO:0009792~embryonic development ending in birth or egg hatching	13	3.44E-02
GO:0035088~establishment or maintenance of apical/basal cell polarity	3	3.46E-02
GO:0007169~transmembrane receptor protein tyrosine kinase signaling pathway	10	3.49E-02
GO:0009891~positive regulation of biosynthetic process	22	3.60E-02
GO:0046903~secretion	12	3.70E-02
GO:0048545~response to steroid hormone stimulus	9	3.78E-02
GO:0048639~positive regulation of developmental growth	3	3.91E-02
GO:0010628~positive regulation of gene expression	19	4.08E-02
GO:0007264~small GTPase mediated signal transduction	12	4.09E-02
GO:0042475~odontogenesis of dentine-containing tooth	4	4.16E-02
GO:0045761~regulation of adenylate cyclase activity	6	4.19E-02
GO:0006468~protein amino acid phosphorylation	21	4.25E-02
GO:0048598~embryonic morphogenesis	12	4.31E-02
GO:0050796~regulation of insulin secretion	4	4.44E-02
GO:0007193~inhibition of adenylate cyclase activity by G-protein signaling	4	4.44E-02
GO:0021915~neural tube development	5	4.58E-02
GO:0016310~phosphorylation	24	4.61E-02
GO:0031279~regulation of cyclase activity	6	4.68E-02
GO:0006796~phosphate metabolic process	28	4.75E-02
GO:0006793~phosphorus metabolic process	28	4.75E-02
GO:0001654~eye development	7	4.75E-02
GO:0051046~regulation of secretion	9	4.85E-02
GO:0016055~Wnt receptor signaling pathway	7	4.90E-02
GO:0030817~regulation of cAMP biosynthetic process	6	5.03E-02

GO:0051339~regulation of lyase activity	6	5.03E-02
GO:0032583~regulation of gene-specific transcription	7	5.05E-02
GO:0048732~gland development	7	5.20E-02
GO:0007010~cytoskeleton organization	15	5.23E-02
GO:0030814~regulation of cAMP metabolic process	6	5.38E-02
GO:0045941~positive regulation of transcription	18	5.67E-02
GO:0046034~ATP metabolic process	6	5.76E-02
GO:0043627~response to estrogen stimulus	6	5.76E-02
GO:0046599~regulation of centriole replication	2	5.83E-02
GO:0007498~mesoderm development	5	5.91E-02
GO:0010557~positive regulation of macromolecule biosynthetic process	20	6.20E-02
GO:0002791~regulation of peptide secretion	4	6.26E-02
GO:0046928~regulation of neurotransmitter secretion	3	6.41E-02
GO:0051017~actin filament bundle formation	3	6.41E-02
GO:0045944~positive regulation of transcription from RNA polymerase II promoter	13	6.50E-02
GO:0030808~regulation of nucleotide biosynthetic process	6	6.75E-02
GO:0030802~regulation of cyclic nucleotide biosynthetic process	6	6.75E-02
GO:0001947~heart looping	3	6.97E-02
GO:0045935~positive regulation of nucleobase, nucleoside, nucleotide and nucleic acid metabolic process	19	7.11E-02
GO:0048839~inner ear development	5	7.16E-02
GO:0019216~regulation of lipid metabolic process	6	7.18E-02
GO:0030799~regulation of cyclic nucleotide metabolic process	6	7.39E-02
GO:0007044~cell-substrate junction assembly	3	7.53E-02
GO:0002088~lens development in camera-type eye	3	7.53E-02
GO:0006140~regulation of nucleotide metabolic process	6	8.07E-02
GO:0009205~purine ribonucleoside triphosphate metabolic process	6	8.30E-02
GO:0060429~epithelium development	9	8.33E-02
GO:0009199~ribonucleoside triphosphate metabolic process	6	8.53E-02
GO:0006357~regulation of transcription from RNA polymerase II promoter	21	8.55E-02
GO:0010604~positive regulation of macromolecule metabolic process	24	8.55E-02
GO:0042733~embryonic digit morphogenesis	3	8.71E-02
GO:0042476~odontogenesis	4	9.14E-02
GO:0042692~muscle cell differentiation	6	9.26E-02
GO:0051588~regulation of neurotransmitter transport	3	9.31E-02
GO:0009144~purine nucleoside triphosphate metabolic process	6	9.51E-02
GO:0060411~heart septum morphogenesis	2	9.52E-02
GO:0030182~neuron differentiation	14	9.64E-02
GO:0009612~response to mechanical stimulus	4	9.93E-02

6.2.3 GO analysis of candidate genes upregulated at stage 27

Given is the biological process, the number of genes and the P-value. Biological processes were sorted according to the P-value from lowest to highest.

Table 6.5 Summary of GO analysis of genes upregulated at stage 27

Biological Process	Count	P-value
GO:0030182~neuron differentiation	41	1.16E-16
GO:0031175~neuron projection development	29	8.25E-14
GO:0048666~neuron development	32	4.71E-13
GO:0048667~cell morphogenesis involved in neuron differentiation	25	1.88E-12
GO:0048812~neuron projection morphogenesis	25	2.84E-12
GO:0000904~cell morphogenesis involved in differentiation	26	8.19E-12
GO:0007409~axonogenesis	23	1.90E-11
GO:0030030~cell projection organization	31	2.15E-11
GO:0048858~cell projection morphogenesis	25	5.67E-11
GO:0032990~cell part morphogenesis	25	1.42E-10
GO:0000902~cell morphogenesis	29	2.41E-10
GO:0032989~cellular component morphogenesis	30	6.46E-10
GO:0007389~pattern specification process	24	1.85E-09
GO:0007155~cell adhesion	39	6.09E-09
GO:0022610~biological adhesion	39	6.21E-09
GO:0048706~embryonic skeletal system development	13	2.39E-08
GO:0043009~chordate embryonic development	25	2.43E-08
GO:0009792~embryonic development ending in birth or egg hatching	25	2.89E-08
GO:0045664~regulation of neuron differentiation	16	3.87E-08
GO:0009952~anterior/posterior pattern formation	16	7.73E-08
GO:0010975~regulation of neuron projection development	12	8.50E-08
GO:0050767~regulation of neurogenesis	17	1.26E-07
GO:0007411~axon guidance	14	1.31E-07
GO:0051960~regulation of nervous system development	18	1.74E-07
GO:0001501~skeletal system development	23	2.27E-07
GO:0003002~regionalization	18	2.52E-07
GO:0007268~synaptic transmission	22	3.05E-07
GO:0006928~cell motion	28	4.70E-07
GO:0006836~neurotransmitter transport	12	5.09E-07
GO:0031344~regulation of cell projection organization	12	1.04E-06
GO:0019226~transmission of nerve impulse	23	1.11E-06
GO:0050770~regulation of axonogenesis	10	1.25E-06
GO:0007267~cell-cell signaling	31	1.57E-06
GO:0048598~embryonic morphogenesis	21	2.02E-06
GO:0060284~regulation of cell development	17	2.18E-06

GO:0016337~cell-cell adhesion	19	6.52E-06
GO:0048066~pigmentation during development	7	7.93E-06
GO:0048705~skeletal system morphogenesis	12	1.01E-05
GO:0006813~potassium ion transport	14	1.29E-05
GO:0010769~regulation of cell morphogenesis involved in differentiation	10	1.61E-05
GO:0051969~regulation of transmission of nerve impulse	13	2.65E-05
GO:0048568~embryonic organ development	14	2.79E-05
GO:0030001~metal ion transport	24	3.29E-05
GO:0031644~regulation of neurological system process	13	3.95E-05
GO:0022604~regulation of cell morphogenesis	12	4.44E-05
GO:0043062~extracellular structure organization	13	7.32E-05
GO:0044057~regulation of system process	18	1.01E-04
GO:0048704~embryonic skeletal system morphogenesis	8	1.04E-04
GO:0007610~behavior	23	1.07E-04
GO:0015672~monovalent inorganic cation transport	18	1.43E-04
GO:0030814~regulation of cAMP metabolic process	10	1.62E-04
GO:0048562~embryonic organ morphogenesis	11	2.46E-04
GO:0001505~regulation of neurotransmitter levels	8	2.91E-04
GO:0050804~regulation of synaptic transmission	11	2.94E-04
GO:0030799~regulation of cyclic nucleotide metabolic process	10	3.26E-04
GO:0042438~melanin biosynthetic process	4	3.66E-04
GO:0006140~regulation of nucleotide metabolic process	10	3.97E-04
GO:0006812~cation transport	24	4.26E-04
GO:0016358~dendrite development	6	5.11E-04
GO:0051046~regulation of secretion	13	5.39E-04
GO:0006582~melanin metabolic process	4	5.41E-04
GO:0032940~secretion by cell	13	6.70E-04
GO:0030817~regulation of cAMP biosynthetic process	9	7.24E-04
GO:0007626~locomotory behavior	15	8.59E-04
GO:0043473~pigmentation	7	9.14E-04
GO:0016477~cell migration	15	9.23E-04
GO:0003001~generation of a signal involved in cell-cell signaling	8	0.001231481
GO:0030802~regulation of cyclic nucleotide biosynthetic process	9	0.001265542
GO:0030808~regulation of nucleotide biosynthetic process	9	0.001265542
GO:0006811~ion transport	28	0.001768227
GO:0048870~cell motility	15	0.0025172
GO:0051674~localization of cell	15	0.0025172
GO:0001568~blood vessel development	13	0.002811991
GO:0035108~limb morphogenesis	8	0.002961616
GO:0035107~appendage morphogenesis	8	0.002961616
GO:0060341~regulation of cellular localization	13	0.003114642
GO:0035239~tube morphogenesis	9	0.003134576
GO:0021700~developmental maturation	8	0.00331301
GO:0001944~vasculature development	13	0.003419115
GO:0048489~synaptic vesicle transport	5	0.003519358
GO:0035295~tube development	12	0.003569016

GO:0048736~appendage development	8	0.003695362
GO:0060173~limb development	8	0.003695362
GO:0007156~homophilic cell adhesion	9	0.003789648
GO:0030198~extracellular matrix organization	8	0.00389868
GO:0017157~regulation of exocytosis	5	0.003929277
GO:0007269~neurotransmitter secretion	5	0.003929277
GO:0046903~secretion	14	0.005404261
GO:0032535~regulation of cellular component size	13	0.006246604
GO:0055085~transmembrane transport	21	0.006911794
GO:0046928~regulation of neurotransmitter secretion	4	0.007224663
GO:0030815~negative regulation of cAMP metabolic process	3	0.007250275
GO:0034109~homotypic cell-cell adhesion	3	0.007250275
GO:0060425~lung morphogenesis	3	0.007250275
GO:0060216~definitive hemopoiesis	3	0.007250275
GO:0030818~negative regulation of cAMP biosynthetic process	3	0.007250275
GO:0048754~branching morphogenesis of a tube	6	0.008159968
GO:0007157~heterophilic cell adhesion	4	0.008248185
GO:0045596~negative regulation of cell differentiation	11	0.009099984
GO:0060562~epithelial tube morphogenesis	6	0.009251241
GO:0030800~negative regulation of cyclic nucleotide metabolic process	3	0.009545066
GO:0030803~negative regulation of cyclic nucleotide biosynthetic process	3	0.009545066
GO:0030809~negative regulation of nucleotide biosynthetic process	3	0.009545066
GO:0045761~regulation of adenylate cyclase activity	7	0.010452748
GO:0007605~sensory perception of sound	7	0.010967908
GO:0031279~regulation of cyclase activity	7	0.012051707
GO:0051588~regulation of neurotransmitter transport	4	0.013163109
GO:0002009~morphogenesis of an epithelium	7	0.013208821
GO:0051339~regulation of lyase activity	7	0.013208821
GO:0001763~morphogenesis of a branching structure	6	0.013856403
GO:0051216~cartilage development	6	0.013856403
GO:0050954~sensory perception of mechanical stimulus	7	0.014441604
GO:0031103~axon regeneration	3	0.014956548
GO:0007413~axonal fasciculation	3	0.014956548
GO:0045980~negative regulation of nucleotide metabolic process	3	0.014956548
GO:0050877~neurological system process	35	0.015730745
GO:0060485~mesenchyme development	5	0.017544866
GO:0019748~secondary metabolic process	6	0.017956203
GO:0008344~adult locomotory behavior	5	0.019898081
GO:0001701~in utero embryonic development	9	0.020509356
GO:0031102~neuron projection regeneration	3	0.021389283
GO:0000768~syncytium formation by plasma membrane fusion	3	0.021389283
GO:0007416~synaptogenesis	4	0.023087282
GO:0048729~tissue morphogenesis	9	0.023132422
GO:0006887~exocytosis	7	0.02355024
GO:0030534~adult behavior	6	0.024933099
GO:0014032~neural crest cell development	4	0.025044074

GO:0014033~neural crest cell differentiation	4	0.025044074
GO:0000165~MAPKKK cascade	9	0.02591496
GO:0030326~embryonic limb morphogenesis	6	0.026053265
GO:0035113~embryonic appendage morphogenesis	6	0.026053265
GO:0006949~syncytium formation	3	0.028758271
GO:0030318~melanocyte differentiation	3	0.028758271
GO:0048488~synaptic vesicle endocytosis	3	0.028758271
GO:0050808~synapse organization	5	0.029616122
GO:0031290~retinal ganglion cell axon guidance	3	0.032768659
GO:0050931~pigment cell differentiation	3	0.032768659
GO:0001667~ameboidal cell migration	4	0.03373438
GO:0001764~neuron migration	5	0.034504837
GO:0048167~regulation of synaptic plasticity	5	0.034504837
GO:0060627~regulation of vesicle-mediated transport	6	0.037588508
GO:0048791~calcium ion-dependent exocytosis of neurotransmitter	2	0.038070802
GO:0006583~melanin biosynthetic process from tyrosine	2	0.038070802
GO:0046148~pigment biosynthetic process	4	0.038592163
GO:0033555~multicellular organismal response to stress	4	0.038592163
GO:0007229~integrin-mediated signaling pathway	5	0.045608009
GO:0008361~regulation of cell size	9	0.045875901
GO:0006029~proteoglycan metabolic process	4	0.049308912
GO:0021545~cranial nerve development	3	0.050763034
GO:0016192~vesicle-mediated transport	18	0.052921235
GO:0042440~pigment metabolic process	4	0.05515485
GO:0048678~response to axon injury	3	0.05570552
GO:0030516~regulation of axon extension	3	0.05570552
GO:0008038~neuron recognition	3	0.060808768
GO:0040007~growth	8	0.063432166
GO:0007628~adult walking behavior	3	0.066064826
GO:0045103~intermediate filament-based process	3	0.066064826
GO:0035136~forelimb morphogenesis	3	0.066064826
GO:0007167~enzyme linked receptor protein signaling pathway	12	0.06630625
GO:0007018~microtubule-based movement	6	0.066795171
GO:0010817~regulation of hormone levels	7	0.071348392
GO:0009954~proximal/distal pattern formation	3	0.071465987
GO:0001755~neural crest cell migration	3	0.071465987
GO:0014031~mesenchymal cell development	4	0.074545726
GO:0048762~mesenchymal cell differentiation	4	0.074545726
GO:0060441~branching involved in lung morphogenesis	2	0.07469758
GO:0060438~trachea development	2	0.07469758
GO:0006904~vesicle docking during exocytosis	3	0.077004782
GO:0016050~vesicle organization	4	0.078035575
GO:0001558~regulation of cell growth	8	0.080849044
GO:0050771~negative regulation of axonogenesis	3	0.082673971
GO:0050772~positive regulation of axonogenesis	3	0.082673971
GO:0051970~negative regulation of transmission of nerve impulse	3	0.082673971

GO:0021675~nerve development	3	0.082673971
GO:0009611~response to wounding	16	0.083449246
GO:0042476~odontogenesis	4	0.085225078
GO:0048589~developmental growth	5	0.086531155
GO:0006355~regulation of transcription, DNA-dependent	43	0.086826183
GO:0007242~intracellular signaling cascade	32	0.088261636
GO:0018149~peptide cross-linking	3	0.088466543
GO:0048278~vesicle docking	3	0.088466543
GO:0008037~cell recognition	4	0.088922057
GO:0031280~negative regulation of cyclase activity	4	0.088922057
GO:0051350~negative regulation of lyase activity	4	0.088922057
GO:0007194~negative regulation of adenylate cyclase activity	4	0.088922057
GO:0007160~cell-matrix adhesion	5	0.09222525
GO:0032229~negative regulation of synaptic transmission, GABAergic	2	0.092486595
GO:0016188~synaptic vesicle maturation	2	0.092486595

6.2.4 GO analysis of candidate genes downregulated at stage 27

Given is the biological process, the number of genes and the P-value. Biological processes were sorted according to the P-value from lowest to highest.

Table 6.6 Summary of GO analysis of genes downregulated at stage 27

Biological Process	Count	P-value
GO:0042398~cellular amino acid derivative biosynthetic process	3	0.004423821
GO:0009309~amine biosynthetic process	3	0.009715815
GO:0042423~catecholamine biosynthetic process	2	0.020148791
GO:0006575~cellular amino acid derivative metabolic process	3	0.037332173
GO:0007595~lactation	2	0.050523221
GO:0042401~biogenic amine biosynthetic process	2	0.054036675
GO:0007610~behavior	4	0.054132144
GO:0006584~catecholamine metabolic process	2	0.061026178
GO:0009712~catechol metabolic process	2	0.061026178
GO:0034311~diol metabolic process	2	0.061026178
GO:0018958~phenol metabolic process	2	0.062765791
GO:0051591~response to cAMP	2	0.074856742
GO:0032102~negative regulation of response to external stimulus	2	0.088491623
GO:0007626~locomotory behavior	3	0.090424381